

The effect of **monopile-induced turbulence** on local **suspended sediment pattern** around UK wind farms

# The effect of **monopile-induced turbulence** on local **suspended sediment pattern** around UK wind farms

Prepared for The Crown Estate

Prepared by the Institute of Estuarine and Coastal Studies, University of Hull

12 November 2018

© Crown Copyright 2018

ISBN 978-1-906410-77-3



## **Institute of Estuarine & Coastal Studies (IECS)**

The University of Hull  
Cottingham Road  
Hull HU6 7RX, UK

Tel: +44 (0)1482 464120

Fax: +44 (0)1482 464130

Email: [iecs@hull.ac.uk](mailto:iecs@hull.ac.uk)

[www.hull.ac.uk/iecs](http://www.hull.ac.uk/iecs)



# Document control

*Title:* The effect of monopile-induced turbulence on local suspended sediment patterns around UK wind farms: field survey report

*Reference No:* IECS-YBB313-2017

*Version:* Final

*Submitted to:* The Crown Estate

*Submission date:* 12 November 2018

<b>Proposal QA</b>	<b>Name</b>	<b>Position</b>	<b>Date</b>
Prepared by	R Forster	IECS	07/04/2017
Prepared by	J Strong	IECS	07/04/2017
Prepared by	S Simmons	U HULL	07/04/2017
Reviewed by	D McKee	U Strathclyde	26/04/2017
Reviewed by	J Rees	Cefas	22/05/2017
Reviewed by	C Green	The Crown Estate	07/05/2017
Revised version	R Forster	IECS	12/02/2018
Reviewed by	C Green	The Crown Estate	09/08/2018
Revised version	R Forster	IECS	10/09/2018
Reviewed by	C Green	The Crown Estate	30/10/2018
Revised version	R Forster	IECS	12/11/2018

## Disclaimer

The opinions expressed in this report are entirely those of the authors and do not necessarily reflect the view of The Crown Estate. The Crown Estate is not liable for the accuracy of the information provided or responsible for any use of the content.

## Dissemination Statement

This publication (excluding the logos) may be re-used free of charge in any format or medium. It may only be used accurately and not in a misleading context. The material must be acknowledged as The Crown Estate copyright and use of it must give the title of the source publication. Where third party copyright material has been identified, further use of that material requires permission from the copyright holders concerned.

## Project Personnel

This report was written and researched by Dr. Rodney Forster (IECS Director).

Dr James Strong (IECS Senior Ecologist) designed the field survey programme, coordinated the logistics of the research cruises and was Scientist-in-command during the surveys. The field survey team consisted of Dr. David McKee (University of Strathclyde), with responsibility for optical measurements; Mr Jon Rees, Mr. Tom Hull and Mr Erik Fitton (Cefas), with responsibility for continuous surface logging; Prof Dan Parsons, Dr. Xuxu Wu, Prof Jack Hardisty and Dr Ross Jennings (University of Hull) with responsibility for design and operation of ADCP measurements. ADCP processing was done by Dr. Steve Simmons (University of Hull). Processing of optical measurements was done by Dr. Ina Lefering (University of Strathclyde). Dr James Strong, Dr. Steve Simmons, Dr. David McKee and Mr Jon Rees commented on draft versions of this report.

## Suggested citation

Forster, RM., 2018. The effect of monopile-induced turbulence on local suspended sediment patterns around UK wind farms: field survey report. An IECS report to The Crown Estate. ISBN 978-1-906410-77-3; November 2018.

## TABLE OF CONTENTS

LIST OF FIGURES.....	IV
LIST OF TABLES.....	VII
GLOSSARY.....	VIII
EXECUTIVE SUMMARY.....	10
1. PROJECT DESCRIPTION.....	13
Rationale.....	13
Aims of the project.....	21
Project workflow.....	22
2. PLUME DETECTION FROM SATELLITE OPTICAL IMAGERY.....	23
Methods.....	23
Medium resolution satellite imagery (hiroc processing).....	23
Low resolution satellite imagery (standard processing).....	25
Satellite validation at SmartBuoy observation sites.....	25
Selection of site for fieldwork.....	26
Within-site location of sampling routes to guide fieldwork.....	28
3. ENVIRONMENTAL CONDITIONS AT THANET OFFSHORE WIND FARM.....	30
Spatial and temporal variability in the climatological mean.....	30
Inter-annual variability at Thanet.....	33
Context for fieldwork in August 2016.....	35
4. PRELIMINARY FIELDWORK.....	39
Method development.....	39
Flow-through measurement of optical backscatter, temperature and salinity.....	39
Gravimetric determination of suspended particulate material.....	40
5. RESEARCH CRUISES TO INVESTIGATE PLUME FORMATION AND CONTENT.....	41
Additional methods used on Thanet survey.....	44
Results.....	48
Vertical structure of the water column.....	50
Variability in surface water quality across the OWF site.....	54
6. SYNTHESIS.....	67
7. REFERENCES.....	71
8. ACKNOWLEDGEMENTS.....	74
APPENDIX.....	75

## LIST OF FIGURES

Figure 1 Wake formation associated with individual monopiles of the Greater Gabbard wind farm .....	14
Figure 2 Examples of wake generation by offshore wind farms of the Thames approaches	15
Figure 3 Wake formation visible in a Landsat-8 scene of an offshore wind farm in the German Bight.....	16
Figure 4 Surface appearance of irregular water colour patterns possibly due to von Kármán vortex street formation in monopile wake. ....	20
Figure 5 Example of HIGHROC processing chain for Sentinel-2 developed at the Flemish Institute for Technological Research (VITO).....	23
Figure 6 Initial comparison of high-resolution satellite-derived turbidity (Landsat-8) versus CEFAS SmartBuoy data. ....	24
Figure 7 Validation of satellite-derived sediment concentration for North Sea and Irish Sea sites. ....	25
Figure 8 Determination of plume prevalence for the offshore wind farm sites around the UK. Presence of plumes was scored from analysis of a minimum of 25 clear-sky satellite scenes for each site, during the period of operation of Sentinel-2. (Source: H. Hall (2018), “Analysis of the distribution of sediment plumes associated with offshore wind farms around the UK”, Thesis, University of Hull). ....	26
Figure 9 (left) Diagram of monopile foundation and transition piece construction at Thanet offshore wind farm (right) transition piece of turbine E01 at the site. ....	27
Figure 10 Location of Thanet offshore wind farm in the outer Thames Estuary, showing positions of WaveNet waverider and SmartBuoys.....	28
Figure 11 Current speed (in knots) and current direction at tidal diamond ‘L’ on Admiralty chart 1610 ‘Approaches to the Thames Estuary’.....	29
Figure 12 Location of Thanet offshore wind farm (red box) showing four control areas used for analysis of regional variability in suspended sediment concentration. ....	30
Figure 13 Monthly mean SPM concentrations ( $\text{mg l}^{-1}$ ) for the outer Thames region including Thanet offshore wind farm. Daily satellite-derived maps of surface SPM were averaged for the period 2002-2010 by month. Images have a linear scaling between 0 and $40 \text{ mg l}^{-1}$ ; values above $40 \text{ mg l}^{-1}$ show as dark brown.....	31
Figure 14 Mean monthly SPM ( $\text{mg l}^{-1}$ ) for the Thanet site and four surrounding areas for comparison. Note: insufficient satellite images were available in December to allow calculation of the monthly mean.....	32
Figure 15 Time series of monthly mean surface suspended particulate material (black line, first y-axis; $\text{mg l}^{-1}$ ).....	33
Figure 16 Time series of annual mean suspended particulate material ( $\text{mg l}^{-1}$ ).....	34
Figure 17 Exceedance curves for satellite-derived surface suspended particulate material within the zone of the Thanet offshore wind farm. ....	35

Figure 18 Changes in the 8-day average of satellite-derived surface suspended particulate material. ....	37
Figure 19 Deck sampling rig for continuous measurement of suspended sediment load, temperature and salinity. ....	39
Figure 20 RV <i>Meriel</i> D at dock in Ramsgate during survey 2. ....	41
Figure 21 Example of Sentinel-2 ebb tide scene of Thanet used for detection of plume direction. ....	42
Figure 22 Map of RV <i>Meriel</i> D locations during survey days 2 and 3 of the first survey week. ....	43
Figure 23 Map of RV <i>Meriel</i> D locations during survey days 1, 2 and 3 of the second survey week. ....	43
Figure 24 Rosette sampler and optics CTD device for vertical profiling of the water column. ....	45
Figure 25 LISST particle size analyzer in deployment frame ....	46
Figure 26 An example of changing current flow direction during the flood tide at Thanet. ...	48
Figure 27 Location of sampling stations (green symbols) near turbine E01 during the mid-flood tide on 19 <sup>th</sup> August 2017. ....	49
Figure 28 Profiling of the upper 10 m of the water column for physical and optical measurements. Locations inside and outside of the plume from tower D03 on 5 <sup>th</sup> August 2016 for repeated profiling. ....	51
Figure 29 Profiling of the upper 10 m of the water column for physical and optical measurements. Locations inside and outside of the plume from tower E01 on 19 <sup>th</sup> August 2016. ....	52
Figure 30 Analysis of suspended particulate material at locations upstream and downstream of (left panel) turbine E01 during the flood tide on 19 <sup>th</sup> August 2016 and (right panel) turbine c15 during the ebb tide on 19 <sup>th</sup> August 2016 ....	53
Figure 31 Map of ‘Time section 3’ on 19 <sup>th</sup> August 2017, with an approach to turbine E01 in the plume, attachment to the tower, and subsequent release and drift (out of plume). ....	55
Figure 32 Optical backscatter measurements with deck and in-water (moon-pool) instruments during Time 3. ....	56
Figure 33 Map of events for ‘Time section 4’ on 19 <sup>th</sup> August 2017, with a period of drift between 10:28 and 10:41 (out of plume, then crossing plume of E01). ....	57
Figure 34 Optical backscatter measurements with deck and in-water (moon-pool) instruments during Time 4 on 19 <sup>th</sup> August 2017. Orange horizontal lines mark periods without the vessel’s engine engaged (drifting or tethered), bars at the higher level denote periods within plumes. ....	58
Figure 35 High-resolution record of entering the plume of turbine E01 with logging of surface temperature and back-scatter at 532 nm. ....	59

Figure 36 Estimation of suspended sediment concentration derived from acoustic backscatter at a frequency of 600 kHz (red line) for the near surface zone (3-5 m, upper panel), and near the sea-bed (17-20 m, lower panel). .....60

Figure 37 Estimation of suspended sediment concentration derived from acoustic backscatter at a frequency of 600 kHz (red line) for the near surface zone (3-5 m, upper panel), and near the sea-bed (17-20 m, lower panel). .....61

Figure 38 Measurement of the current magnitude through the water column. Upper panel: vertical profiles before (1), during (2) and after (3) passage through the visible plume. Lower panel: time series of surface- and bottom-averaged magnitudes during transect through the plume, marked by a spike in surface backscatter. ....63

Figure 39 Measurement of the northwards velocity component through the water column. Upper panel: vertical profiles before (1), during (2) and after (3) passage through the visible plume. Lower panel: time series of surface- and bottom-averaged N velocity during transect through the plume, marked by a spike in surface backscatter. ....64

Figure 40 Measurement of the eastwards velocity component through the water column. Upper panel: vertical profiles before (1), during (2) and after (3) passage through the visible plume. Lower panel: time series of surface- and bottom-averaged E velocity during transect through the plume, marked by a spike in surface backscatter. ....65

Figure 41 Measurement of the vertical velocity component through the water column. Upper panel: vertical profiles before (1), during (2) and after (3) passage through the visible plume. Lower panel: time series of surface- and bottom-averaged vertical velocity during transect through the plume, marked by a spike in surface backscatter. ....66

## LIST OF TABLES

Table 1 Observational studies of wake effects at offshore wind farm sites .....	17
Table 2 Satellite-derived water quality parameters produced by the HIGHROC Sentinel-2 processing chain .....	24
Table 3 Estimation of the annual mean SPM ( $\text{mg l}^{-1}$ ) and 50% exceedance point for Thanet offshore wind farm site before and after construction. ....	34
Table 4 Description of sampling methods used during Thanet surveys. ....	47
Table 5 Direction and speed of drifts during the flood tide phase of Day 3, Survey 2. ....	48
Table 6 Depth-averaged water column properties for vertical profiles upstream, in and outside of the plume from turbine D03 on 5 <sup>th</sup> August 2017. ....	50
Table 7 Depth-averaged water column properties for vertical profiles upstream, in and outside of the plume from turbine E01 on 19th August 2017. ....	50
Table 8 Comparison of surface suspended particulate material ( $\text{mg l}^{-1}$ ) for locations upstream or downstream (in visible plume). ....	53
Table 9 Comparison at depth 10 m of suspended particulate material ( $\text{mg l}^{-1}$ ) for locations upstream or downstream (in visible plume). ....	54
Table 10 Comparison just above the sea floor (20 m) of suspended particulate material ( $\text{mg l}^{-1}$ ) for locations upstream or downstream (in visible plume). ....	54



## GLOSSARY

ADCP	Acoustic Doppler Current Profiler
ARD	Analysis-ready data
CEFAS	Centre for Environment, Fisheries and Aquaculture Sciences, Lowestoft, UK
cDOM	Chromophoric dissolved organic matter
Copernicus	Flagship European Commission environmental monitoring programme
CTD	Instrument to measure conductivity (salinity), temperature and pressure (depth) of the water.
ESA	European Space Agency
Framework-7	Science funding programme of the European Commission for the period 2002-2013.
GFF	Glass Fibre Filters
GPS	Global Positioning System
HIGHROC	HIGH spatial and temporal Resolution Ocean Colour project, 2014-2017
IOP	Inherent Optical Properties
L2W	Level-2 water products derived from satellite images
Landsat-8	United States Geological Survey earth observing satellite with medium optical resolution, operating from 2013 to present.
MERIS	ESA low spatial-resolution optical spectrometer carried onboard the ENVISAT satellite and operational from 2003 to 2012
MODIS/AQUA	AQUA is a NASA low spatial-resolution optical spectrometer carried onboard the MODIS satellite and operational from 2002 to present.
NASA	National Aeronautics and Space Administration

---

OBS	Optical backscatter
OWF	Offshore wind farm
RTK dGPS	Real-Time Kinematic and Differential Global Positioning System
SeaWIFS	NASA-operated low spatial-resolution Sea-Viewing Wide Field-of-View Sensor operational from 1997 to 2010
Sentinel-2	ESA earth observing twin satellites with medium optical resolution, operating from 2015 to present
SmartBuoy	Remote marine environmental monitoring system operated by Cefas.
SPM	Suspended particulate matter (material).
VIIRS	NASA/NOAA-operated low spatial-resolution Visible Infrared Imaging Radiometer Suite on Suomi satellite, operational from 2011.

## EXECUTIVE SUMMARY

Energy generation from offshore wind in the seas around the British Isles is set to increase greatly over the next decade, with an ambitious target ambition of 30GW of installed capacity to be on-line by 2030. Offshore wind would then provide up to 20% of the UK's electricity, up from approximately 6% in 2017. Clean sources of low-carbon energy are essential, but consideration must also be given to any effects of energy generation on the environment. This report examines the interaction of monopile wind turbine foundations with flowing water, which results in the formation of visible downstream wakes.

Offshore wind farms (OWF), containing blades, turbines and their bases can interact with the atmosphere or with the surrounding water to form visually-observable features. In the atmosphere, clouds and fog may be formed or dispersed by the movement of spinning turbine blades. For the sea surface, decreases in surface roughness downwind of wind farms have been measured under certain conditions. This is due to a reduction in wind speeds in the lee of the farm. Also visible at the surface, elongated, optically-distinct plumes of turbid water have been observed close to monopiles and for some distance down-current of a wind farm. Turbid wakes can be seen at sea level, from aircraft, and from space and are most frequently observed around wind farms along the east coast of England. The increasing availability of high quality satellite images since 2013 has raised awareness of wind farm / environment interactions. Several scientific papers have been produced in recent years describing the interactions of monopiles with moving water, using numerical modelling and scaled-down flume tank experiments.

Understanding the nature of the monopile wakes, and whether they pose any disturbance to the marine environment, would help the OWF sector better gauge the necessity of monitoring activities. The formation and consequences of turbid wake formation is the subject of the investigations in this report. A combination of satellite remote sensing and fieldwork on the Thanet OWF were used to investigate the causes of turbid wakes. The concentration of suspended particulate matter (SPM) is the main control on water transparency in the southern North Sea, and it was hypothesised that changes in water colour due to monopile-current interactions would result in a higher concentration of sediments in the surface layer.

Remote sensing analysis used images from different satellites and sensors to quantify natural variability. Work in previous projects had established that turbidity and sediment load of the water can be accurately estimated from optical measurements e.g. water-leaving radiances viewed from space. Firstly, 10-meter resolution true-colour images from Sentinel-2 were used to screen for the presence of turbid wakes at all UK offshore wind farms. The cluster of sites in and around the Thames Estuary showed the highest prevalence. **Wake features were recorded in the majority of satellite images of the Thanet, London Array, Greater Gabbard, and Galloper Extension OWFs. In contrast, wakes were absent or rare in sites north of the Humber and in offshore Irish Sea areas.** Wake lengths of 1 km or more were regularly observed at Thanet and other Thames Estuary sites. The ratio of wake length to monopile diameter was larger than that predicted in the scientific literature from scale models and numerical models.

After selection of Thanet as the most suitable site for fieldwork, with the highest chances of encountering turbid wakes, further satellite time-series analysis was undertaken to establish the range of naturally-occurring variability in turbidity of the Thames Estuary region. The region showed a strong inter-annual, intra-annual and spatial variability in the concentration

of SPM at the sea surface. SPM was highest in the winter months, and was high close to shore in the inner areas of the estuary. Thanet OWF was shown to lie in a transition zone between the clearer offshore water, and turbid estuarine water. **The average sediment load at the Thanet wind farm site varied six-fold over the course of a year.**

The methods used to investigate the differences between water quality upstream of the OWF site, and water in the plumes, were profiling of the water column with optical and acoustic instrumentation, and direct sampling of the water at different depths. Profiling was carried out with the vessel drifting, or physically tethered to a monopile in order to remain within the plume during the sampling time. Samples were taken from visually-identified locations in and out of distinct plumes for laboratory analysis of optically-active components (sediment quantity and composition, plankton, and dissolved material).

Results of vertical profiling showed that even though the water column upstream of the OWF site was apparently well-mixed in terms of temperature, SPM concentration (and backscatter) were higher in midwater and particularly near the sea-bed. There was strong evidence that the existing vertical gradient in suspended load was altered during contact of flowing water with the monopile structure so that downstream of the monopile (e.g. within the wake), there was a more homogeneous vertical distribution of sediment. **Hence, the surface concentration of SPM in the wake was higher than that in surrounding waters and was therefore more visible from above.**

Sampling was undertaken continuously with a deck-mounted flow-through instrument package, and an in-water optical backscatter (OBS) instrument mounted in the ship's moon-pool. A greatly reduced signal-to-noise ratio was obtained when the ship was drifting passively as compared to underway with power, possibly due to interference by bubbles. Under these conditions, entry to a wake area resulted in increased surface turbidity readings, and slightly decreased temperature. Optical measurements showed a lack of difference between different spectral bands, indicated that the observed increase in attenuation (and scattering) within the wake was spectrally-neutral, and therefore unlikely to be caused by water constituents such as chlorophyll or chromophoric dissolved organic matter (cDOM), which have strong spectral characteristics.

**Together, the fieldwork results supported an original working hypothesis that the colour of turbid plumes was caused by increased suspended sediment concentrations in the surface water.**

Not only can it be said with high confidence that suspended sediment concentration was higher at the surface, but initial evidence was found from both direct measurements and acoustic back-scatter that the near-bed concentration of sediment was actually lower within the plume.

**This indicated that a re-distribution of suspended material from the lower water column to the surface was caused by the increased turbulence within the wake. Localised scour of the seabed was not the source of the surface-visible wakes.**

The final section of the report discussed the potential ecological consequences of turbid wake formation. Large offshore wind farms in areas of significant water column stratification may generate sufficient turbulent mixing in their wakes that changes the distribution of heat throughout the water. Limited evidence for thermal mixing was found here, as water upstream of the Thanet test site was well-mixed.

If sufficiently large in scale, the increase in surface sediment concentration observed here could lead to a decrease in local ecosystem productivity due to reduced underwater light availability.

Changes in sediment concentration and water clarity in the outer Thames area must be placed in a regional perspective. **Steep gradients in turbidity within a short distance of the OWF study site were observed in satellite images of the Thames area; these were caused by the river plume itself, and the interaction of waves and tides on the shallow seabed.** On the century time-scale, recent research has shown that the southern North Sea has changed from a clear-water system in which sunlight penetrated to the sea-bed over large areas to a system with 50% reduced water clarity.

Reductions in water clarity have been reported for many other coastal seas and are likely to be caused by multiple factors. These can be due to increased supply of light-attenuating materials from the land to the sea or decreased sinks for light-attenuating materials in the sea. Destruction of naturally-occurring sediment sinks such as filter-feeding oyster reefs or sublittoral seagrass beds will prevent marine sediments from settling. Changes in benthic habitats may occur naturally due to storm events, or may be caused by anthropogenic disturbance to the seabed. It is therefore likely that the benthic species and habitats existing at sites such as Thanet were already adapted to an environment in which rapid changes in sediment deposition and erosion are a common feature. Organisms in the water column would encounter periodically darker and more turbulent conditions on passage past a monopile, but these changes would be well within the range of variability encountered in any given two week period (e.g. neap-spring cycle). **Hence, the additional turbidity added locally by monopile wakes would have limited ecological effects.**

## 1. PROJECT DESCRIPTION

### Rationale

The UK leads the world in developing energy generation from offshore wind farms (OWF). Out of a global installed capacity of ~19.7 GW, UK shelf seas have 7.9 GW of capacity to date with a further 24 GW of offshore wind capacity planned or in development. This compares to 5.3 GW and 1.3 GW of offshore power for Germany and Denmark respectively. The potential impact of wind farms on the marine environment has been the subject of recent ecological research ((Wilson & Elliott 2009, Bailey et al. 2010, Wilson et al. 2010, Lindeboom et al. 2011)) particularly with respect to the EU Marine Strategy Framework Directive which aims to protect the natural functioning of the seas while working with the Maritime Spatial Planning Directive to achieve the sustainable economic development of the seas ('blue growth'). The Crown Estate grants leases to operators for the use of the seabed in England Wales and Northern Ireland to produce renewable energy, and has a commitment to maintaining the long-term wellbeing of its assets. In the case of the marine environment, this means pursuing good environmental practice through effective monitoring and management. An understanding of not only the influence of OWF on the marine environment, but also of the marine environment on OWF is central to the planning considerations for many sea areas which will be used for energy generation.

While there is an increasing body of evidence on the effects of OWF on the seabed and its organisms (e.g. Franco et al, 2015), an increasingly important aspect of OWF development is the interaction of sites with their surrounding air flows and water flows (hydrodynamics). Individual wind turbines and their monopile, or jacket and tripod bases can cause wake effects e.g. alterations in air flow, or wave height and current speeds (Christiansen & Hasager 2005), with the scale of effects being dependent upon the site depth and number of structures (van der Molen et al. 2014). A consequence is the formation of visually-observed features in the atmosphere or in the water associated with individual turbines or entire wind farms. Three general types of optical effect can be considered:

1. In the atmosphere, turbine-air flow interactions may (very rarely) cause localised fog or condensation trails, or cause dispersal of low-lying cloud in the lee of a wind farm.
2. For the sea, a decrease in surface roughness can be observed in optical and radar images at considerable distances down-wind of a wind farm under certain conditions.
3. For the sea, elongated, optically-distinct wakes at the sea surface which have been observed close to monopiles and for some distance down-current of a wind farm.

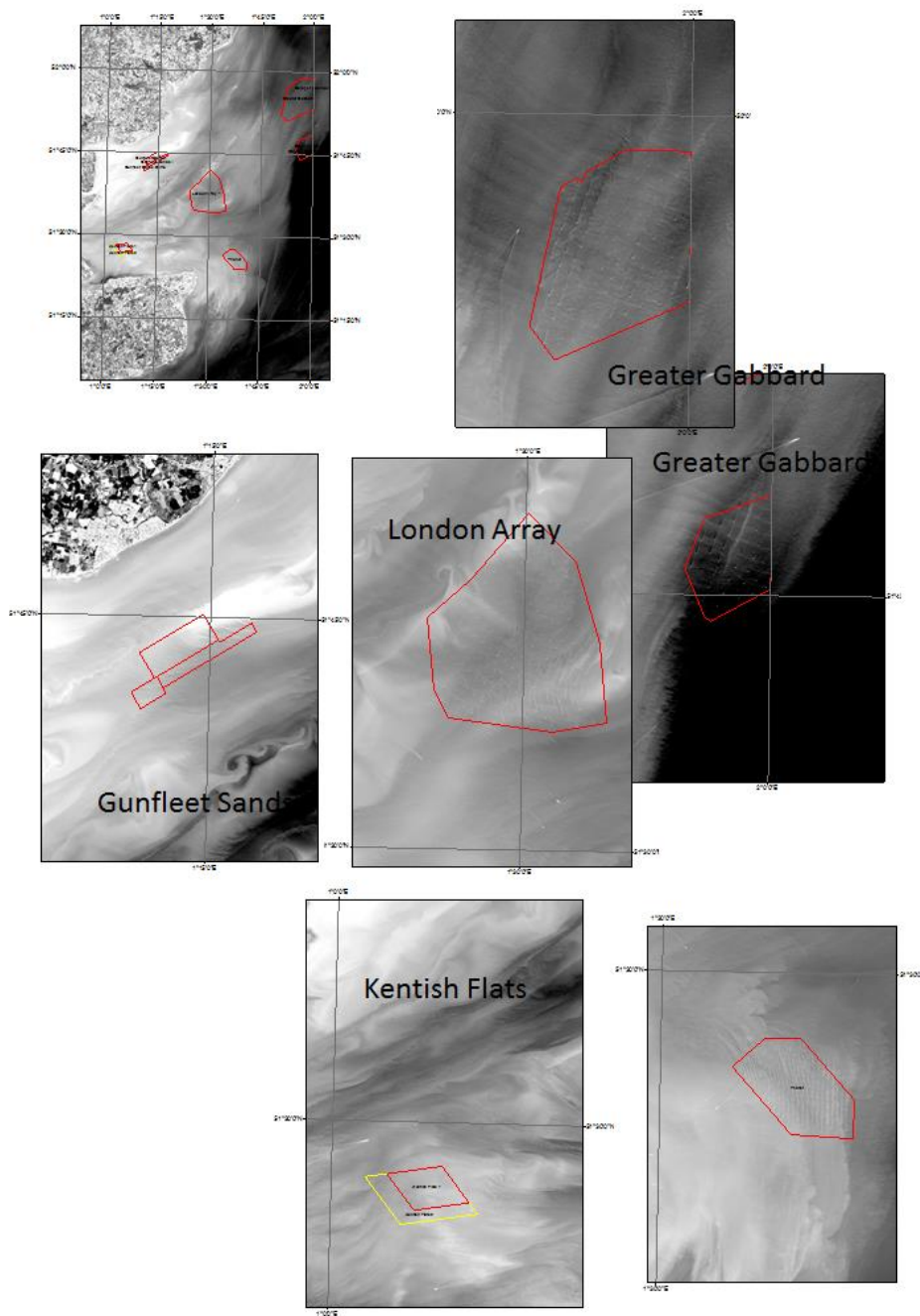
The topic of this report are the plumes at the sea surface which have been observed close to monopiles and appear to be associated with water flows rather than changes in wind speed. Such plumes can be seen clearly by operators within a site (Mander, pers. comm; Thanet wind farm), from commercial aircraft (Capuzzo, pers. comm; from research vessels (Baeye & Fettweis 2015)), or from space (Vanhellemont & Ruddick 2014). Figure 1 shows the Greater Gabbard wind farm on 30<sup>th</sup> June 2015 with wake formation associated with monopiles. Whilst the surface extent of plumes can be seen, their extent throughout the water column is at present unknown.



**Figure 1** Wake formation associated with individual monopiles of the Greater Gabbard wind farm

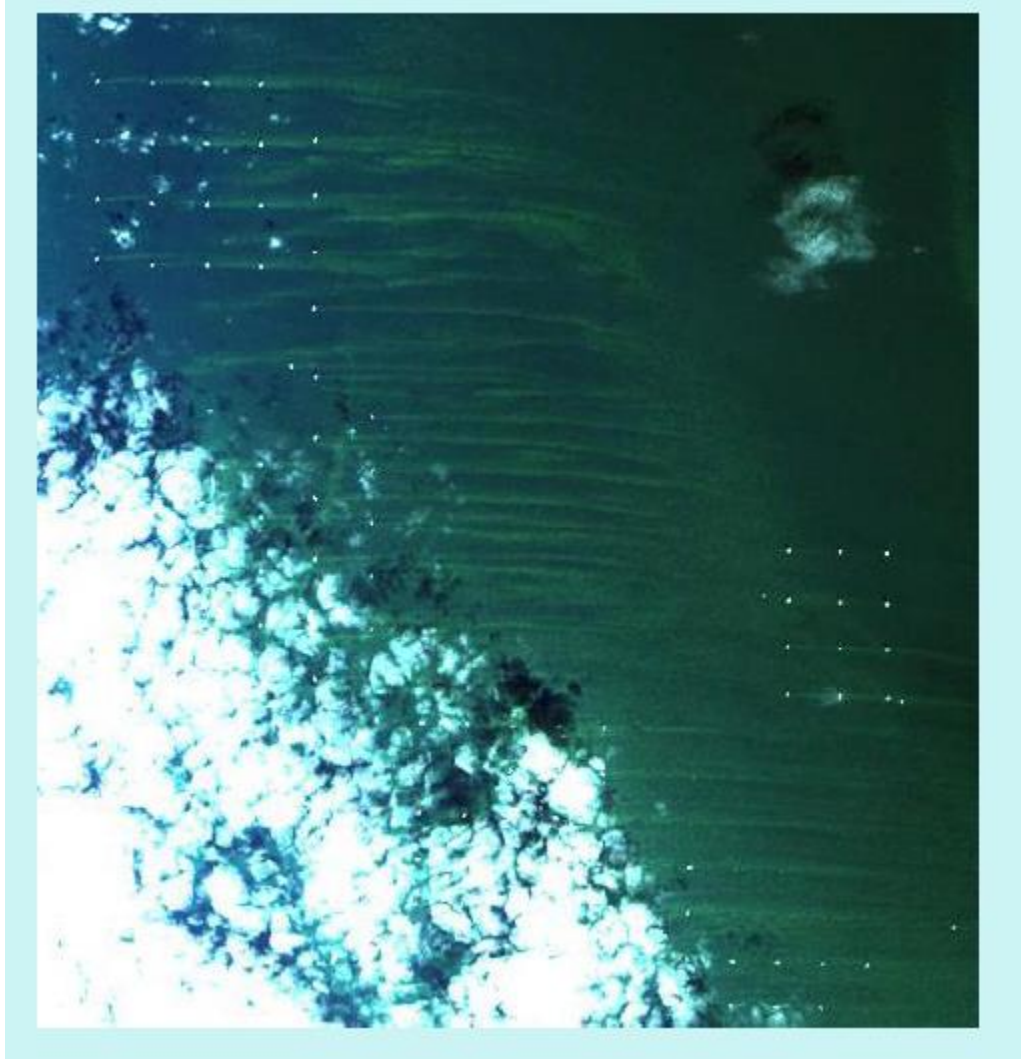
(Source: E. Capuzzo, Cefas; hand-held digital camera)

The first images of wind farm sediment wakes from a satellite optical sensor, Landsat-8, were reported by the report author at a meeting of the Optimising Array Form for Energy Extraction and Environmental Benefit project (September 2013, Edinburgh; **Figure 2**). Following calibration of Landsat images to surface reflectance, Vanhellemont and Ruddick (2014) published maps of surface sediment concentrations showing plumes associated with wind farms in the Thames estuary. Similar images have been noted for other OWFs in the waters of Germany (Figure 3), The Netherlands and Belgium, suggesting that this is a general phenomenon associated with the placement of these structures in the sea. As well as optical remote sensing, satellite Synthetic-Aperture-Radar has been used to detect the changes in surface roughness associated with wakes in a Chinese OWF (Table 1a; Li et al. 2014). *In situ* investigations of OWF wakes have only been reported in one paper to date (Baeye and Fettweis 2015).



**Figure 2** Examples of wake generation by offshore wind farms of the Thames approaches  
(Source: R. Forster; Landsat-8, panchromatic band).



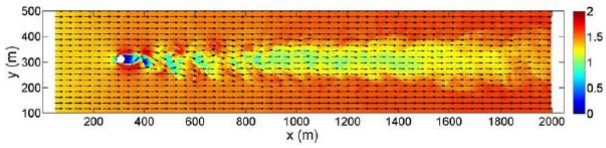


**Figure 3** Wake formation visible in a Landsat-8 scene of an offshore wind farm in the German Bight.

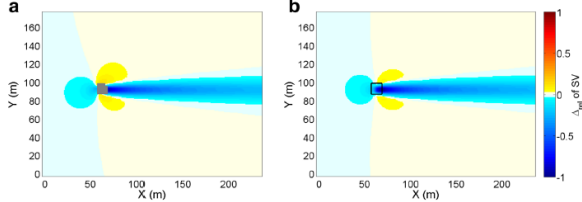
(Source: K Stelzer, Brockmann Consult).

In turn, the initial observations of wake effects have triggered a series of recent investigations using a range of hydrodynamic models and scaled-down flume tank experiments (Table 1b and 1c respectively). One plausible explanation of wake formation is due to turbulence generated by the monopile-current interaction, causing an unsteady, swirling (von Kármán-type) vortex which appears evident in near-surface photography (Figure 4).

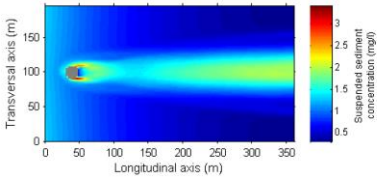
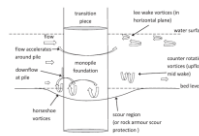
**Table 1** Observational studies of wake effects at offshore wind farm sites

Research article	Method	Outcome
van Hellemont & Ruddick (2014) first peer-reviewed report of turbid wakes associated with UK OWF	Landsat-8 images processed to obtain true-colour images and maps of SPM	Turbid wakes were clearly visible at Thanet and London Array OWFs. Monopile wakes were spectrally distinct from ship wakes with spectra resembling sediment-rich waters. Wakes were 30-150 wide and several km long.
Li et al (2014) SAR observation and numerical modelling of tidal current wakes at an East China Sea OWF.	Synthetic-aperture-radar images showed distinct wakes associated with individual monopiles. Numerical modelling to estimate flow speed reduction.	Tidal current wakes ranged from 1 to 2 km. Turbulent intensity decreased logarithmically with distance from the structure. 
Baeye and Fettweis (2015); Baeye et al. (2016). In situ analysis of OWF plumes	Measurements of acoustic back-scatter from surface and near-bed at Belwind 1 OWF.	Found five times higher SPM in wake. Hypothesised that suggested that the epifaunal communities growing on the monopile surface and the protective rock collar at the base filter and trap fine SPM from the water column, resulting in an accumulation of SPM. When turbulence exceed a certain velocity, fine particles in the fluff layer are re-suspended.

**Table 1b** Modelling studies of monopile wake dynamics

Research article	Method	Outcome
Cazenave et al 2016 Modelling of OWF impact on stratification	Unstructured grid (Finite Volume Community Ocean Model) used to model	Appearance of individual wakes consistent with previous studies, detectable in model up to 250 diameters downstream (5 % current reduction at 1 km).  Whole wind farm effects for a 240-turbine site are detectable across the UK shelf seas, potentially influencing tides and stratification.
Yin et al. (2017), report to The Crown Estate	Modelling investigation of turbid wakes around London Array Offshore Wind Farm using TELEMAC	Movement of fine sand around a simulated London Gateway showed clearly visible wakes due to turbulence-induced vertical transport from the near-bed.
van der Molen et al. 2014 "Predicting the large-scale consequences of offshore wind turbine array development on a North Sea ecosystem"	The impact on waves, sound and biogeochemistry of an offshore wind-turbine array were modelled with combined hydrodynamic and biogeochemical modelling.	All three models suggested relatively weak environmental changes due to OWF interaction with physical surroundings.
Rivier et al. (2016)	MARS-3D fine-scale numerical modelling of current-monopile-sediment interactions	<p>Showed details of a horseshoe vortex of enhanced current speed to the sides of the monopile structure, decreased velocity in wake.</p>  <p><b>No turbid wake</b> predicted as particle size in the model (sand) had too high a settling velocity. Suggests wakes only occur with fine sediments.</p>
Carpenter et al. 2016 potential OWF effects of North Sea stratification	Combination of modelling and in situ measurements in the German Bight to estimate regional scale impact of enhanced mixing.	Effects of current small OWF in German water is insufficient to significantly change stratification pattern, but authors state that further North Sea OWF development does have potential to alter water column physics at North Sea scale.
Grashorn & Stanev 2016 Kármán vortex and turbulent wake generation by wind park piles	High-resolution numerical modelling of monopile-current dynamics using Semi-implicit Cross-scale Hydroscience Integrated System Model (SCHISM)	Appearance of turbid wakes can be explained by formation of Karman vortices downstream of monopile. Close similarity between model output and satellite observations.

**Table 1c** Flume tank and scale-model studies of representative monopile structures.

Research article	Method	Outcome
Rogan et al. (2016)	1:50 scale physical model used to measure current velocities and turbulence in monopile wake with different current speeds.	Turbulence in the wake of the cylindrical model monopile was estimated to be detectable up to 400 pile-diameters downstream (~2000 m for a 5m monopile.)
Report of OPHELIA project	INTERREG regional project with three partners Plymouth University used an experimental basin to study wake structure downstream of the pile (Rogan et al. 16) University of Le Havre used wave flume to make detailed velocity measurements. Caen University used both numerical models MARS3d and physical experiments with sediments in flume.	<p>Numerous predictions and outcomes in the report <a href="https://interregofelia.files.wordpress.com/2015/05/1-2-report-en.pdf">https://interregofelia.files.wordpress.com/2015/05/1-2-report-en.pdf</a></p> <p>e.g. predicted shape of sediment plume with fine sand as substrate.</p>  <p>Figure VI.3: Suspended sediment concentration (mg/l) at the surface using a monopile with a diameter of 15 m, an input velocity of <math>0.5 \text{ m.s}^{-1}</math> and a sand diameter of <math>65 \mu\text{m}</math> using explicit resolution (dry cells are in gray).</p>
Miles et al (2017) Current and wave effects around wind farm monopile foundations	Scale model of monopile in flume tank subject to different current speeds and wave heights.	 <p>Fig. 1. Flow process near vertical monopile foundation.</p> <p>Velocity was reduced downstream of the pile, but returned to within 5% of background levels by 8 diameters (~40m for a 5 m monopile). Turbulence peaked at 1.5 diameters distance.</p>



**Figure 4** Surface appearance of irregular water colour patterns possibly due to von Kármán vortex street formation in monopile wake.

Source: Dimitry van der Zande, Royal Belgian Institute of Natural Sciences.

Images such as an iconic aerial photograph of cloud contrails forming in the wake of turbines at Horns Rev OWF (Hasager et al. 2013) have been used frequently in the popular media<sup>1</sup> and will no doubt continue to be used as installed capacity grows.

The increasing availability of high quality satellite images following the launch of Landsat-8 in 2012, Sentinel-2a in 2015 and Sentinel-2b in 2017 will lead to further enquiries<sup>2</sup> and perhaps concerns as to the nature of the easily-noticeable monopile wakes, and could put pressure on wind farm operators to increase their monitoring activities. As environmental studies before and during operations can be a significant element of operator costs<sup>3</sup>, any additional obligations on operators would be challenging, at a time when maximum effort is being made to reduce costs throughout the sector. It is therefore urgent to investigate the nature of the sediment plumes associated with monopiles.

### **Aims of the project**

The project was designed to test the following falsifiable hypotheses:

#### **Colour of plumes**

**H1)** Contrasts in colour between plumes and the surrounding water are due to differences in suspended sediment concentration and suspended sediment grain size.

Alternative: Other factors such as bubble formation or resuspended plankton cause the visual manifestation of plumes.

#### **Cause of plumes**

**H2a)** Plumes are caused by localised scouring of the seabed at the base of the monopile (as proposed by Vanhellemont & Ruddick (2014).

**H2b)** Plumes are caused by the release of mud and organic material associated with epifauna colonising the monopile as proposed by Baeye & Fettweis (2015).

**H2c)** Plumes are caused by re-distribution of suspended sediment in the water column due to increased vertical mixing in the monopile wake.

#### **Impact of plumes on OWF ecology**

**H3)** Formation of plumes may lead to changes in the ecology of waters around wind farms.

---

<sup>1</sup> E.g. <https://www.theguardian.com/environment/gallery/2014/may/02/the-beauty-of-windfarms-in-pictures>

<sup>2</sup> E.g. <https://gizmodo.com/satellite-captures-a-surprising-impact-of-offshore-wind-1788695549>

<sup>3</sup> the first Round 3 wind zones on the Dogger Bank have cost developers £60m (The Crown Estate 2010) <http://www.thecrownestate.co.uk/news-and-media/news/2015/largest-global-consent-for-offshore-wind-energy-granted-at-dogger-bank>

## **Project workflow**

The project was composed of several phases:

Work package 1 Project management

Work package 2 Analysis of satellite earth observation data

Work package 3 Construction of experimental techniques

Work package 4 Dedicated field sampling campaign

Work Package 5 Laboratory analysis of samples

Work package 6 Analysis and synthesis

## 2. PLUME DETECTION FROM SATELLITE OPTICAL IMAGERY

The availability of high-to-medium resolution satellite imagery has recently increased, and will continue to expand as the Copernicus programme<sup>4</sup> adds additional Sentinel satellites to its fleet. The different types of satellite imagery used in the project are explained below:

### Methods

#### MEDIUM RESOLUTION SATELLITE IMAGERY (HIROC PROCESSING)

The Framework-7 project 'HIGHROC' was funded in 2014 to develop the necessary technology for using satellite images in coastal waters, and to begin engaging with potential maritime users of the data. In the course of the project, validated maps of suspended sediments in the surface layer of the water were made available. A service chain was developed for bulk downloading and processing of optical images from Landsat-8 and Sentinel-2. Files containing image data were downloaded from the SciHub server of Copernicus ([scihub.copernicus.eu](http://scihub.copernicus.eu)) and stored on local servers. A series of steps shown in Figure 5 were programmed to reformat the images, identify water, land and cloud pixels (IDEPIX code<sup>5</sup>), correct for stray light effects due to bright pixels located alongside dark pixels (SIMEC code; Sterckx et al. 2015), and remove the effects of atmospheric absorption and scattering (ACOLITE code; van Hellemonst & Ruddick 2016). The final processing steps were to apply algorithms to convert optical data (reflectance of the water surface in discrete bands of the spectrum) into so-called 'Level 2 water' (L2W) products.



**Figure 5** Example of HIGHROC processing chain for Sentinel-2 developed at the Flemish Institute for Technological Research (VITO).

A range of L2W products was generated, depending on particular user requests (Table 2). For this project, the most relevant satellite-derived water quality parameters were: turbidity (measured in Formazin Nephelometric Units, FNU), chlorophyll a (measured in  $\text{mg m}^{-3}$ ), SPM (measured in  $\text{mg l}^{-1}$ ) and euphotic depth (the depth to which sunlight penetrates the water to 1% of its surface irradiance, measured in metres). A selection of sites in UK waters was used for the trialling of the HIGHROC water quality service: these encompass the east of England offshore wind farms from the Humber to the Thames.

<sup>4</sup> [www.copernicus.eu](http://www.copernicus.eu)

<sup>5</sup> <https://github.com/bcdev/beam-idepix>



**Table 2** Satellite-derived water quality parameters produced by the HIGHROC Sentinel-2 processing chain

Parameter (units)	Symbol	Type
Remote sensing reflectance spectrum ( $\text{sr}^{-1}$ ) at water level	Rrs	L2R
Aerosol reflectance spectrum	RHOa	L2R (aux)
Aerosol reflectance Angstrom exponent	ANG	L2R (aux)
Aerosol optical thickness	AOT	L2R (aux)
Suspended Particulate Matter ( $\text{g m}^{-3}$ )	SPM	L2W/S
Turbidity (FNU)	TUR	L2W/S
Particulate backscatter at 555nm ( $\text{m}^{-1}$ )	bbp555	L2W/S (aux)
Chlorophyll a ( $\text{mg m}^{-3}$ )	CHL	L2W/C
Algal pigment absorption coefficient at 443nm ( $\text{m}^{-1}$ )	apig443	L2W/C (aux)
Diffuse attenuation coefficient spectrum ( $\text{m}^{-1}$ )	Kd	L2W/K
Diffuse attenuation coefficient of PAR ( $\text{m}^{-1}$ )	KdPAR	L2W/K
Euphotic depth (m)	Ze	L2W/K
CDOM absorption coefficient at 443nm ( $\text{m}^{-1}$ )	aCDOM443	L2W
Secchi Depth (m)	SD	L2W
RGB Image (Rayleigh corrected)	RGB	L1

Validation of the HIGHROC high-resolution remote sensing products for UK and Belgian OWF sites for the southern North Sea (e.g. Figure 6) can be found in the final project report (Ruddick et al. 2018), and in a peer-reviewed publication in preparation (Doxaran et al 2018).

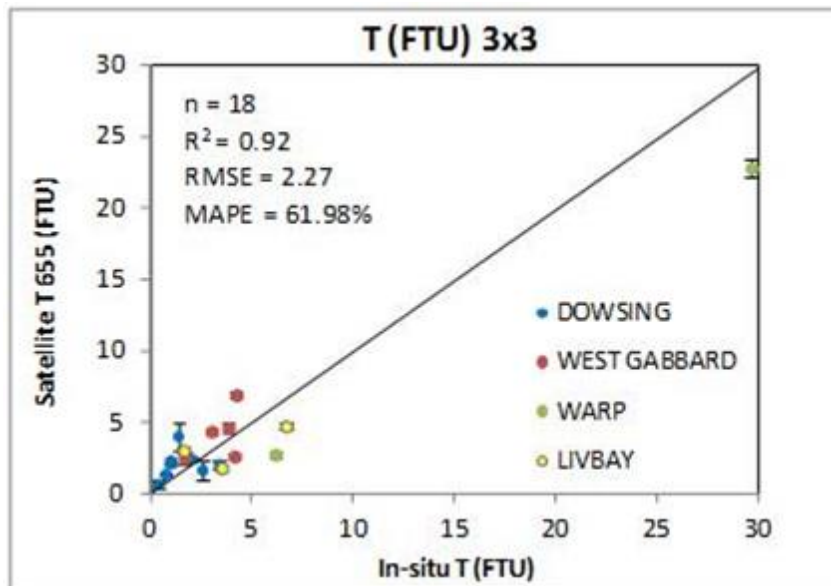


**Figure 6** Initial comparison of high-resolution satellite-derived turbidity (Landsat-8) versus CEFAS SmartBuoy data.

Source: David Doxaran, HIGHROC internal project report 'S2+ Validation report'.

## LOW RESOLUTION SATELLITE IMAGERY (STANDARD PROCESSING)

Satellite-derived water quality products at coarse resolution (1- 4 km pixel size) were selected from the Copernicus Marine Environmental Monitoring Service<sup>6</sup>, using a product which merges data from multiple ocean colour satellites over the time period 1997-2017. Individual files containing averages for each pixel at either 8-days or 30 days (monthly) time steps contain a merging of MERIS, MODIS/AQUA, VIIRS and SeaWiFS satellite data. An algorithm is applied to the optical data contained in each file to obtain the desired water quality product: in this case, an estimate of the surface Suspended Particulate Matter (Gohin et al. 2005).

## SATELLITE VALIDATION AT SMARTBUOY OBSERVATION SITES

SPM from satellite using this algorithm has been extensively tested at Cefas, and comparisons with in situ data show very strong correlations (Figure 7).

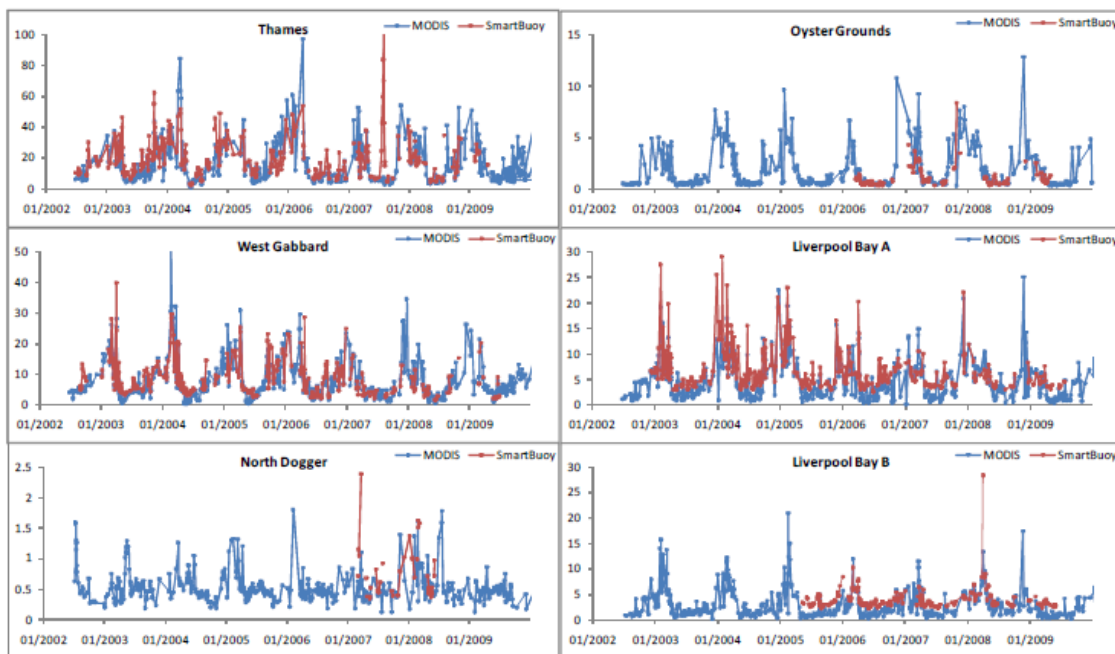


**Figure 7** Validation of satellite-derived sediment concentration for North Sea and Irish Sea sites.

Time series comparison between *in situ* (“SmartBuoy”) and satellite-based (“MODIS”) measurements of suspended particulate matter ( $\text{mg l}^{-1}$ ). Locations ‘Thames’ and ‘West Gabbard’ are located within 50 km of the Thanet study site.

From: Eggelton et al. 2011. Natural variability in EIA regions, ALST report. Figure 2.4

<sup>6</sup> Marine.copernicus.eu

## SELECTION OF SITE FOR FIELDWORK

Initial analysis of wake prevalence indicated that offshore wind sites with the most frequent presence of turbid wakes were London Array, Greater Gabbard, Galloper Extension and Thanet (Figure 8).

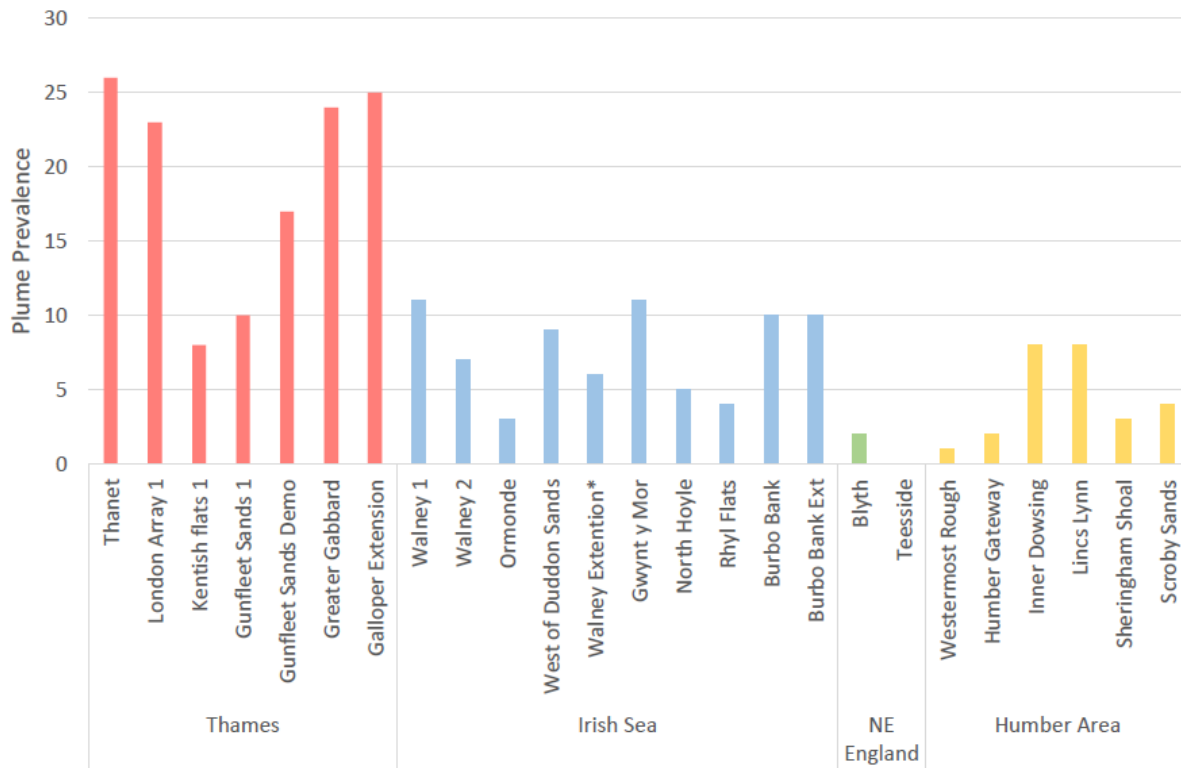


**Figure 8** Determination of plume prevalence for the offshore wind farm sites around the UK. Presence of plumes was scored from analysis of a minimum of 25 clear-sky satellite scenes for each site, during the period of operation of Sentinel-2. (Source: H. Hall (2018), “Analysis of the distribution of sediment plumes associated with offshore wind farms around the UK”, Thesis, University of Hull).

Of the high-prevalence sites, several factors determined the selection of Thanet OWF for research cruises. The availability of background knowledge of the site from previous projects in which IECS staff were involved in seabird surveys was important, as was a closer distance to the nearest non-tidal harbour (Ramsgate).

Thanet is a fully-operational Round 2 offshore wind farm site operated by Vattenfall AB. With a construction cost of £900 million, the farm has 100 turbines with a capacity of 300 MW. Each of the 3 MW turbines is supported by monopiles driven into the sea-bed (Figure 9). The depth of the water at the site ranges from 14 to 23 m above Chart Datum (Figure 10). Wave measurements used in this report were sourced from a Cefas wave buoy located at South Knock (Figure 10), and continuous *in situ* sediment measurements from SmartBuoys were downloaded from <http://wavenet.cefas.co.uk/Smartbuoy/Map>.

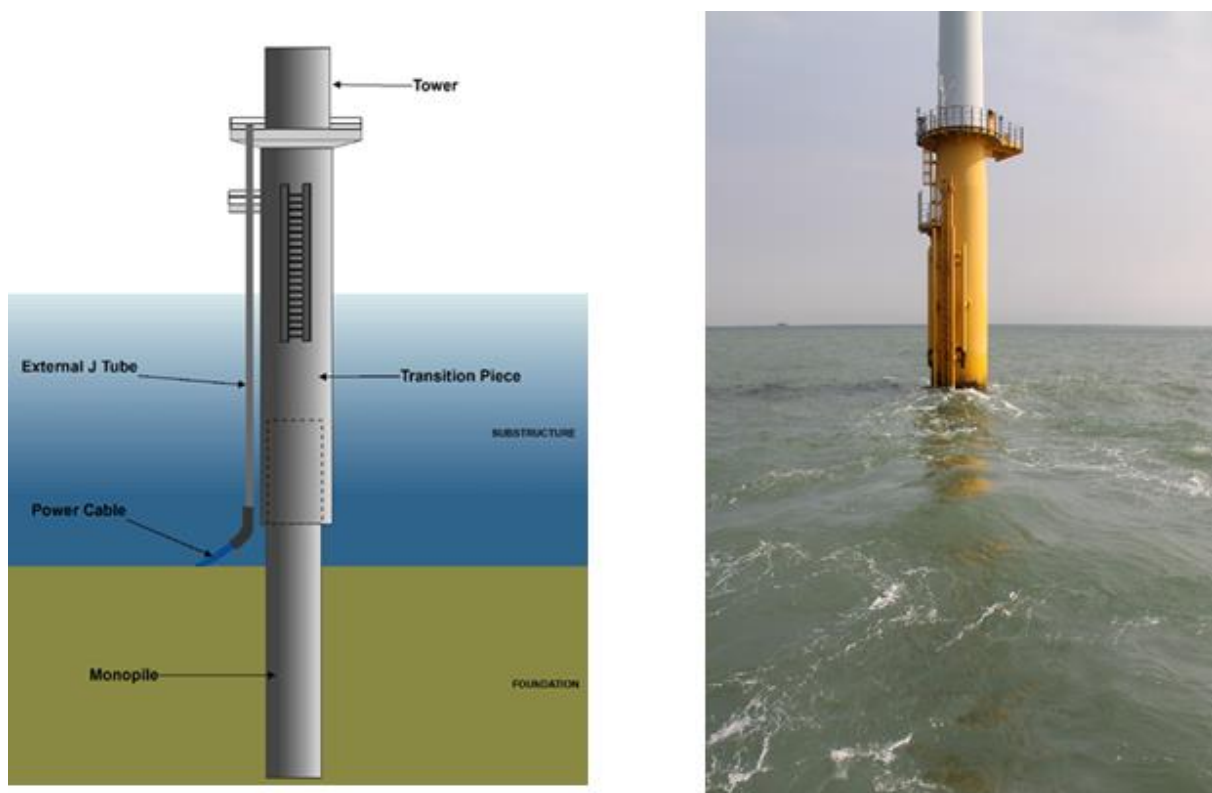


**Figure 9** (left) Diagram of monopile foundation and transition piece construction at Thanet offshore wind farm (right) transition piece of turbine E01 at the site.

The monopiles at Thanet OWF are 4.1 to 4.9 m in diameter and carry 3.0 MW Vestas V90 turbines.

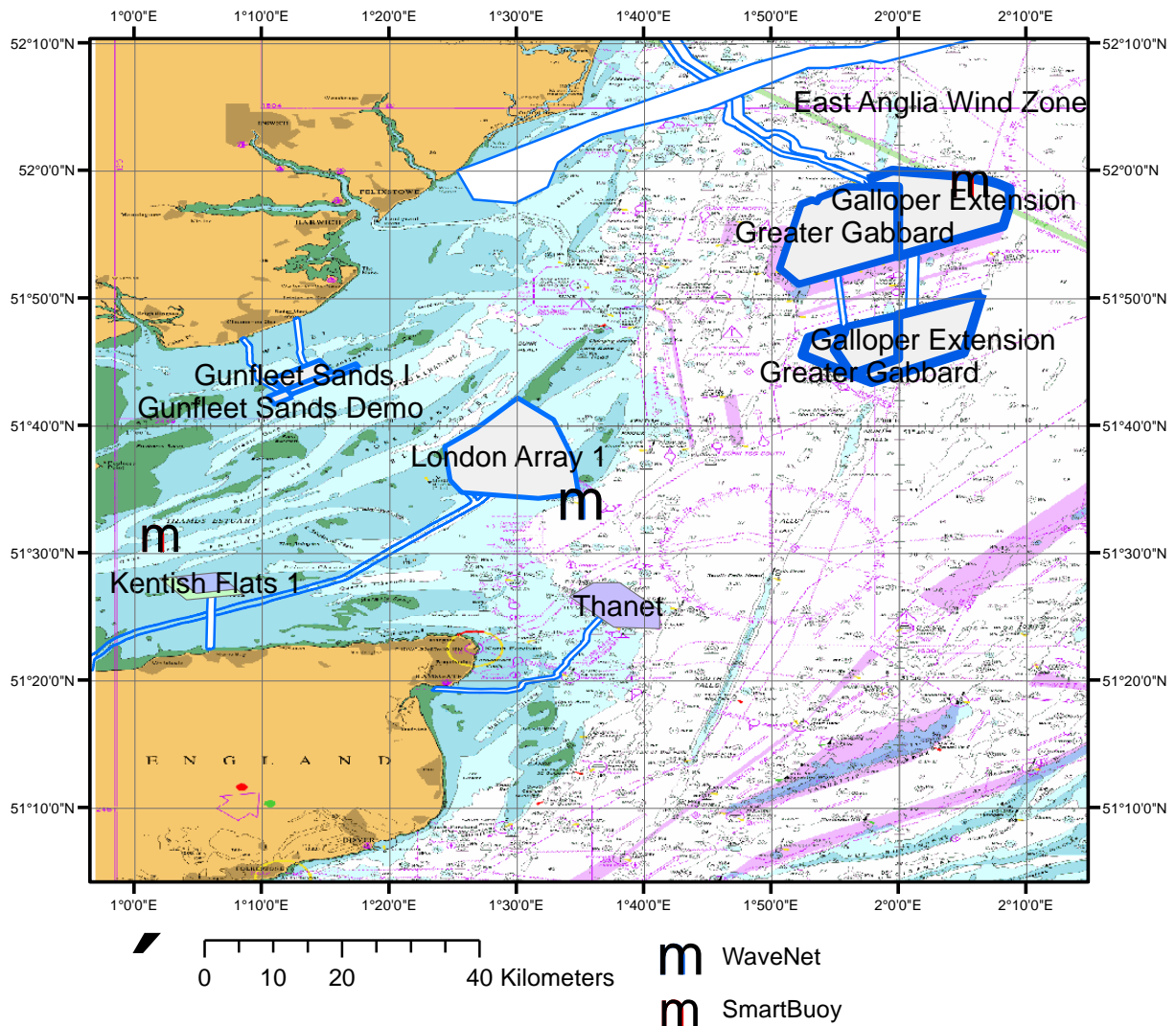


**Figure 10** Location of Thanet offshore wind farm in the outer Thames Estuary, showing positions of WaveNet waverider and SmartBuoys.

#### WITHIN-SITE LOCATION OF SAMPLING ROUTES TO GUIDE FIELDWORK

An initial analysis of 17 Landsat-8 images during the project start-up phase identified that plumes at Thanet were visible throughout most of the tidal cycle, and that the direction and length of the plumes could be predicted from tidal state. Sea-level data from the nearest tide gauge site at Sheerness was downloaded and used to compare satellite images to the tidal cycle. At low water, the tidal flow was from north to south and plumes across the site were strongly aligned in this direction. There was a clockwise rotation during the rising flood tide so that by mid-flood, plumes ran from north-east to south-west. Close to the peak of high tide at Sheerness there was a reversal in flow direction and plumes were seen to be aligned with the south-north current. A period of ‘no plume’ was observed in images acquired between 1 and 2 hours into the ebb tide: further satellite image analysis will be required to confirm this. During the peak ebb flow, plumes were aligned with the current leaving the Thames Estuary

from west to east. The timings of low and high tide will differ between the tide gauge at Sheerness and Thanet OWF itself. Statistics for a tidal diamond site within the wind farm show similar features to those described above with respect to the changes in direction of current flow (Figure 11).

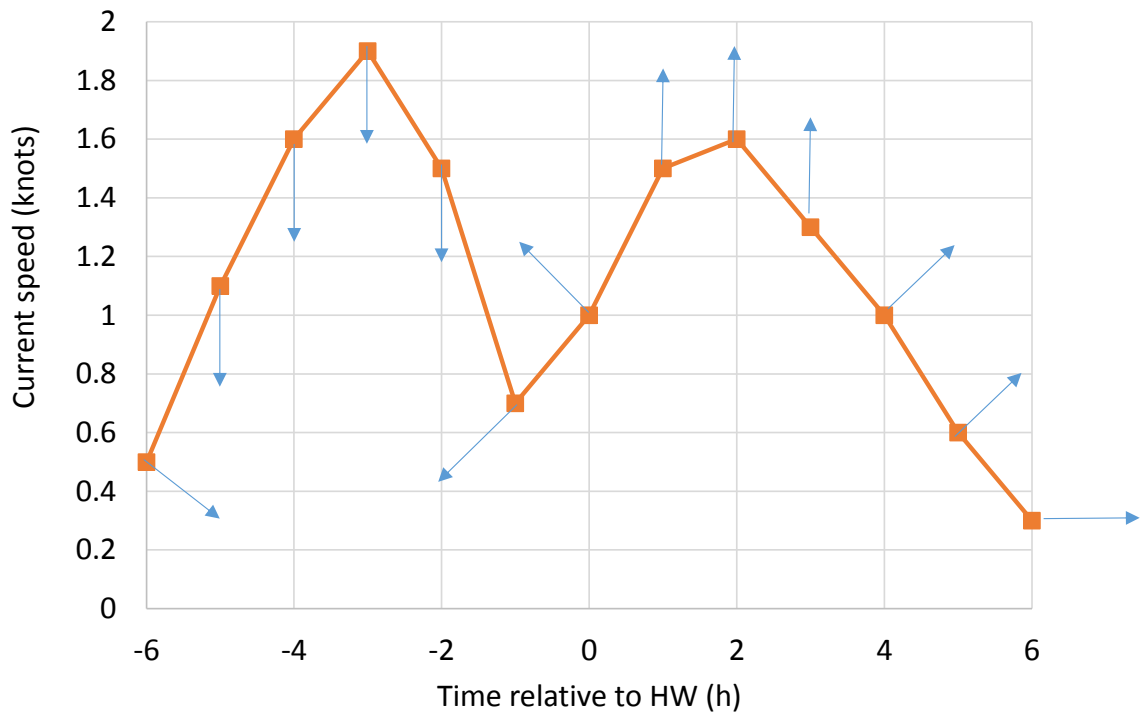


**Figure 11** Current speed (in knots) and current direction at tidal diamond 'L' on Admiralty chart 1610 'Approaches to the Thames Estuary'.

### 3. ENVIRONMENTAL CONDITIONS AT THANET OFFSHORE WIND FARM

The aim of this section is to provide context for the natural variability of conditions at the selected wind farm site. This is necessary to enable the wider project aims of estimating the scale of environmental effects for monopile-associated turbid wakes. Thanet OWF is located 11 km from the nearest point of the Kent coast at North Foreland (Figure 12). To the west of the site is the entrance to the Thames, with shallow water depths and sandbanks which fall dry on the lowest spring tides. Shallow water and sandbanks are also found to the south-west of the site. A large area of shallow ground known as Goodwin Sands lies 12 km to the south-west of Thanet OWF. The 20 m depth contour line runs north-south through the site, and waters to the east have depths of between 20 m to 30 m. Four control areas have been defined for the following analysis of variability in suspended sediment concentration within the Thanet region: North-West (NW\_ctrl), North-East (NE\_ctrl), South-East (SE\_ctrl) and South-West (SW\_ctrl) (Figure 12). These sites represent the variability in depth, proximity to sediment sources, and wave and tidal energy at Thanet OWF itself.

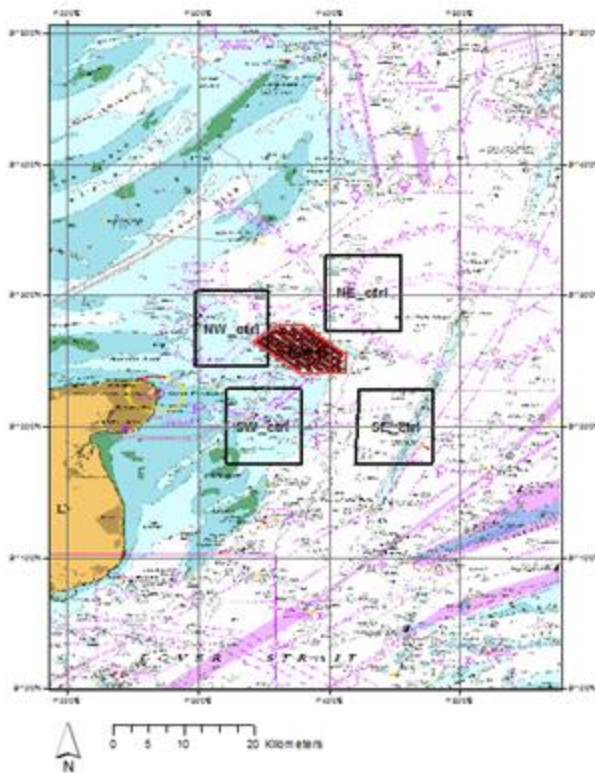


**Figure 12** Location of Thanet offshore wind farm (red box) showing four control areas used for analysis of regional variability in suspended sediment concentration.

#### **Spatial and temporal variability in the climatological mean**

A synoptic overview of turbidity or sediment concentrations at the regional scale can only be provided by analysis of aerial or satellite images. Here, an assessment was made of the mean monthly surface sediment concentration derived from a time series of MODIS satellite images available from the Copernicus Marine Environment Monitoring Service for the period 2002 to 2010 (Figure 13).

Maps of the surface sediment distribution showed that concentrations were highest in January and March with values of over  $40 \text{ mg l}^{-1}$ , and up to a maximum of  $100 \text{ mg l}^{-1}$ , in the outer Thames, between north Kent and Essex. The Thanet OWF site lies on the edge of this region of high turbidity, and winter SPM concentrations were lower to the open North Sea to the east. Sediment loading decreased greatly in the spring period: by May most of the Thames region showed values of SPM below  $20 \text{ mg l}^{-1}$  and the Thanet OWF site was indistinguishable from its surrounding waters. Sediment concentrations remained low throughout the summer until September, when zones of higher turbidity were apparent off the eastern Kent coast, and near the Essex coastline. By November, values had increased and the winter pattern of higher turbidity inshore could again be seen.

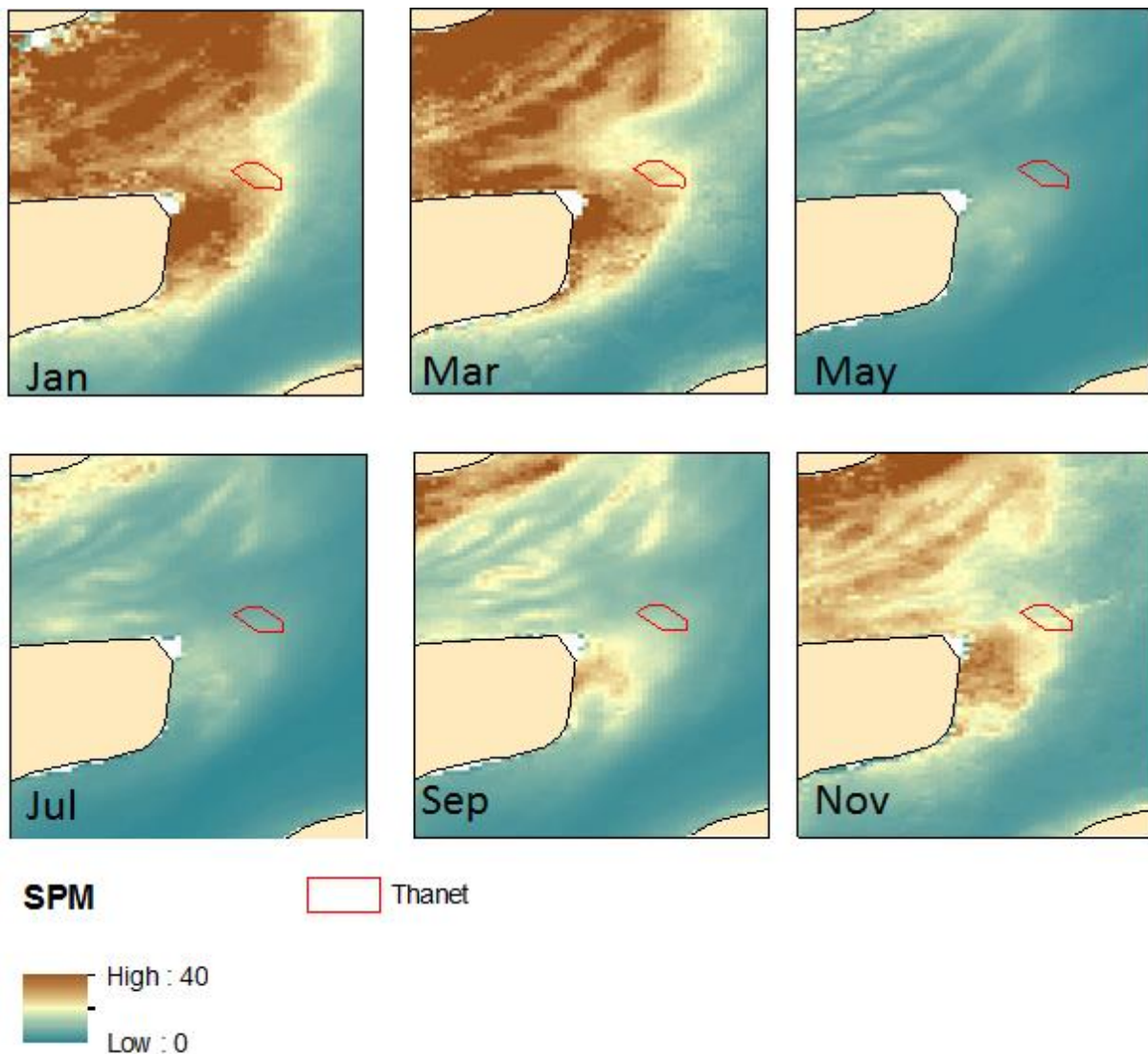


**Figure 13** Monthly mean SPM concentrations ( $\text{mg l}^{-1}$ ) for the outer Thames region including Thanet offshore wind farm. Daily satellite-derived maps of surface SPM were averaged for the period 2002-2010 by month. Images have a linear scaling between 0 and  $40 \text{ mg l}^{-1}$ ; values above  $40 \text{ mg l}^{-1}$  show as dark brown.



The predominant signal within the Thanet OWF, and at the four surrounding control sites, was a strong annual cycle (Figure 14). Monthly mean SPM values from the climatology were highest in late winter within the wind farm zone (mean values of 50-60 mg l<sup>-1</sup>) and decreased through the spring to a minimum of 6 mg l<sup>-1</sup> in June. Concentrations then increased slowly through the remaining summer months, and increased more rapidly towards the end of the calendar year.

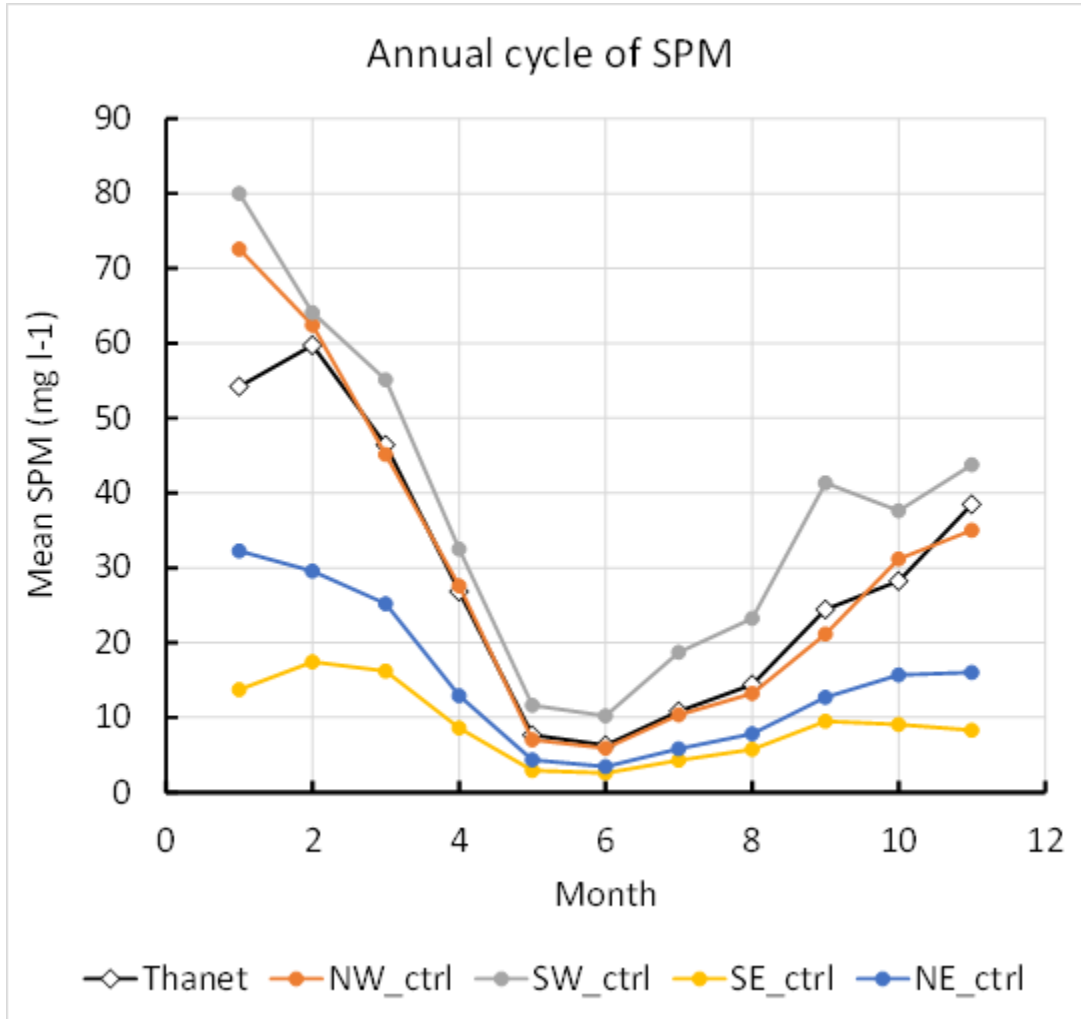


**Figure 14** Mean monthly SPM (mg l<sup>-1</sup>) for the Thanet site and four surrounding areas for comparison. Note: insufficient satellite images were available in December to allow calculation of the monthly mean.

All of the selected control zones showed similar annual cycles of SPM, but the amplitude varied between sites. The 'NW' control zone had greatest similarity to conditions within Thanet OWF, with SPM values differing only in January (a month for which a low number of satellite images resulted in a less reliable monthly mean). Compared to Thanet OWF, consistently higher SPM concentrations were detected at the 'SW' control area. This can be explained by the presence of shallow water within the zone. To the east, the deeper 'NE' and particularly 'SE' zones had lower SPM throughout the year. Values at 'SE' of 18 mg l<sup>-1</sup> in late Winter and 4 mg l<sup>-1</sup> in May and June are representative of the offshore southern North Sea.

## Inter-annual variability at Thanet

The availability of a continuous satellite earth observation dataset from 1997 to present allowed a first investigation to be made of any changes in the local sedimentary regime due to construction of the wind farm at Thanet. Placement of the 100 monopiles supporting wind turbines at the site started in January 2008 and was complete by June 2010.

The time series of monthly mean SPM before, during, and after construction show considerable intra- and inter-annual variability (Figure 15). It can be seen in the time series of annually-averaged mean SPM (Figure 16) that the year with highest mean concentration, 2010, with  $42 \text{ mg l}^{-1}$ , was 2.3 times higher than the year with lowest concentration (2001,  $17 \text{ mg l}^{-1}$ ). It is likely that the intra-annual and inter-annual variability were both driven by physical forces external to the region, as Thanet OWF and the neighbouring zone 'NW' show coupled changes in time (Figure 16). A calculation of percentage difference in sediment concentration between NW and Thanet (Figure 15) showed that Thanet had 2% lower SPM than NW before construction, with a 4% lower difference post-construction.

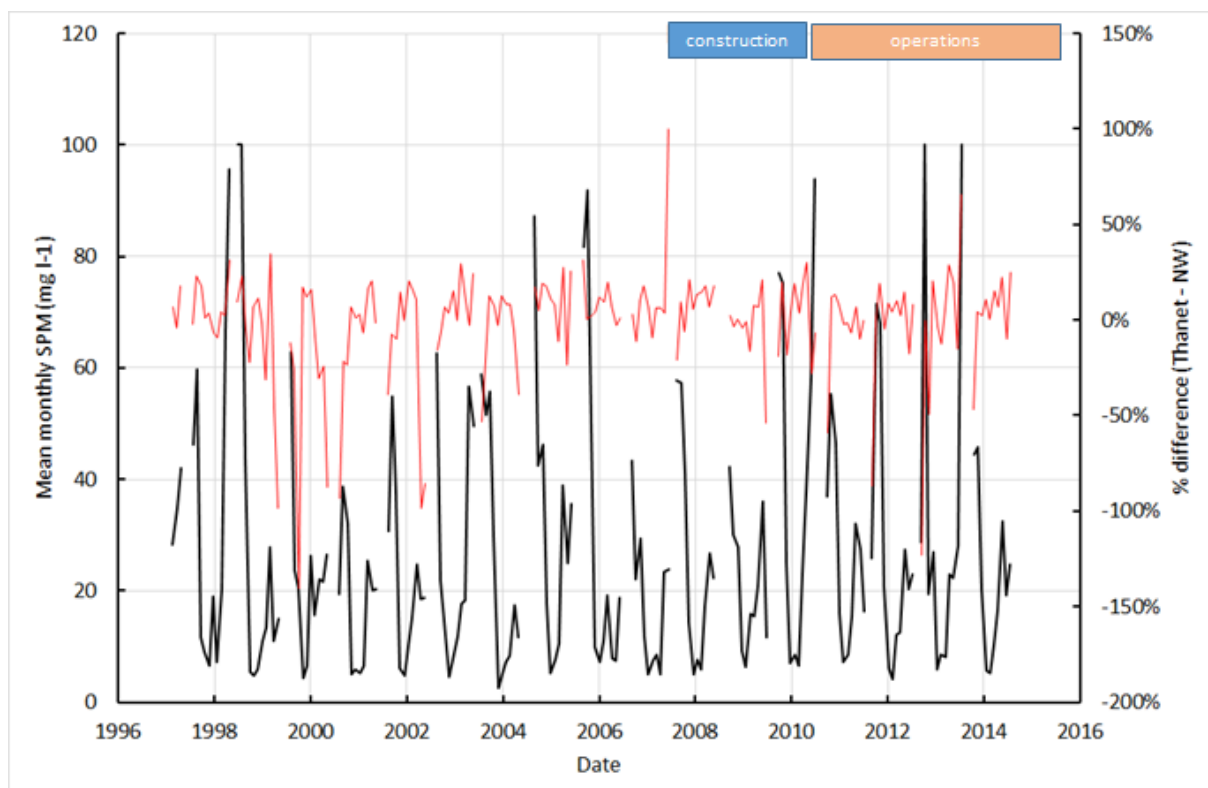


**Figure 15** Time series of monthly mean surface suspended particulate material (black line, first y-axis;  $\text{mg l}^{-1}$ )

Source: Time series of CMEMS MODIS SPM for the period before and after construction of the Thanet offshore wind farm. The relative difference between sediment concentrations within the wind farm versus the NW control site is shown as a percentage by the red line on the secondary y-axis.

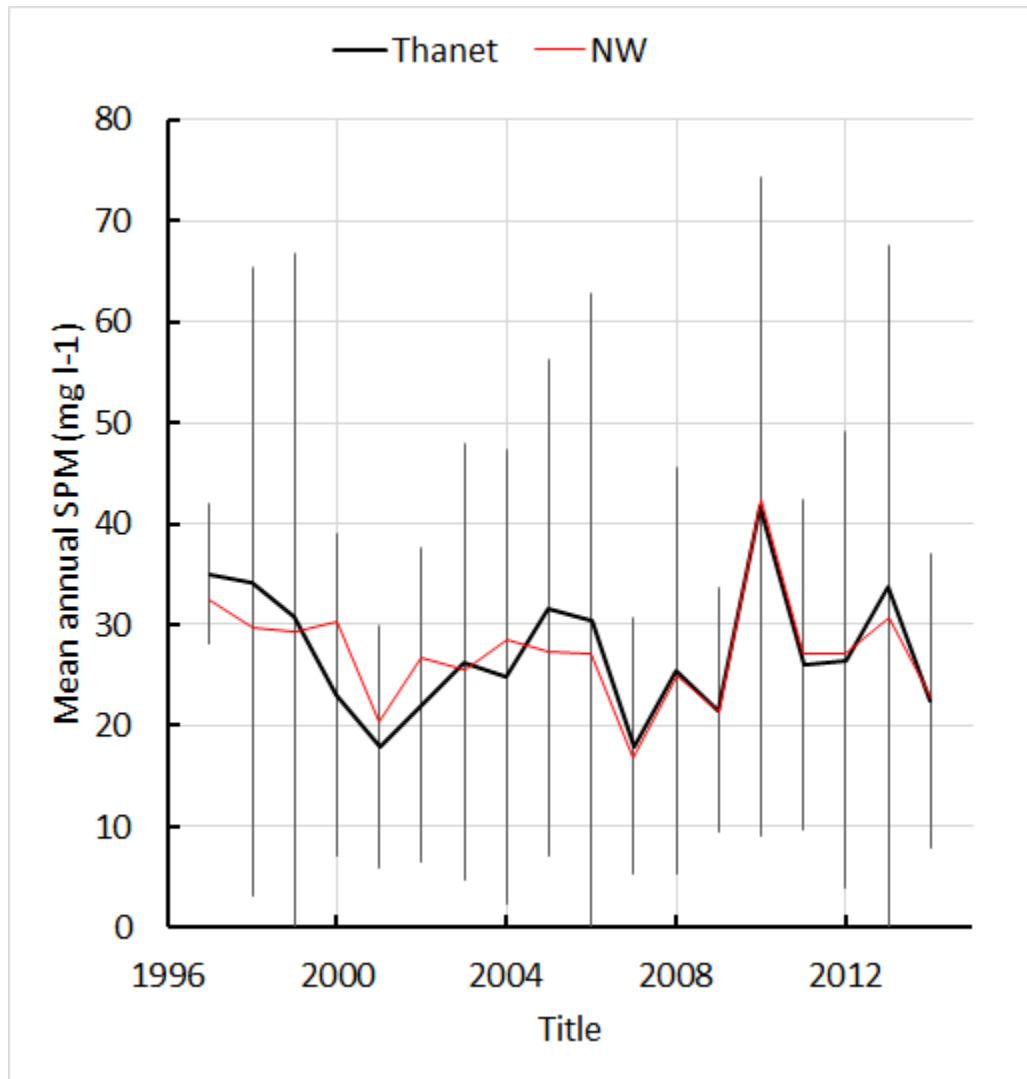


**Figure 16** Time series of annual mean suspended particulate material (mg l<sup>-1</sup>).

Source: derived from monthly mean satellite images for the surface area within the bounds of Thanet OWF (black line, with standard deviations), and NW control zone (red line).

Exceedance curve analysis was the method chosen for detection of any wind farm-induced changes to the local turbidity regime. This provides a means of capturing variability in parameters such as turbidity or sediment loading, which display a very high dynamic range (e.g., Figure 17).

**Table 3** Estimation of the annual mean SPM (mg l<sup>-1</sup>) and 50% exceedance point for Thanet offshore wind farm site before and after construction.

Condition	Annual mean	50% exceedance
pre-build	26.7	19.2
post-build	30.1	22.2

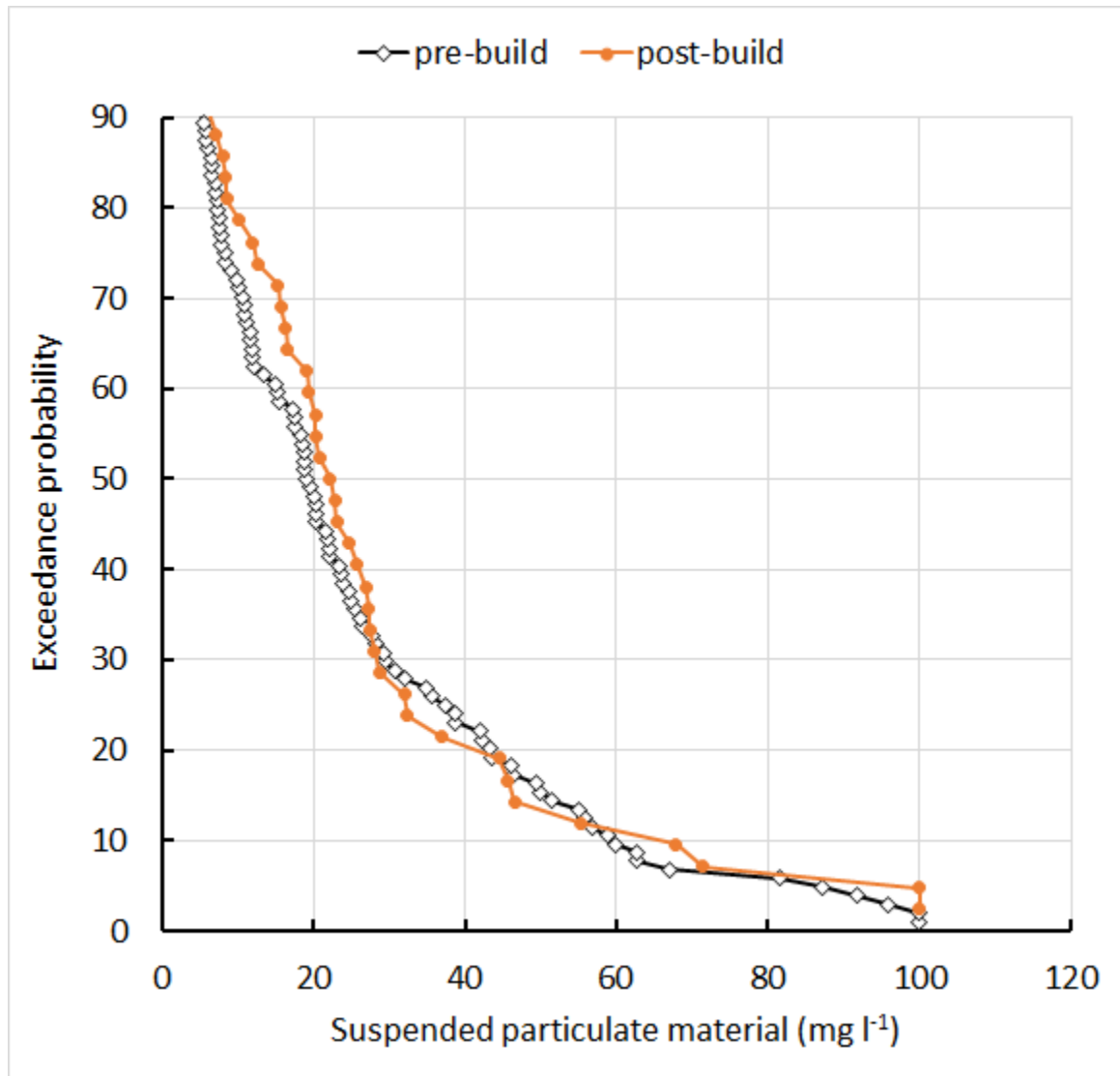


**Figure 17** Exceedance curves for satellite-derived surface suspended particulate material within the zone of the Thanet offshore wind farm.

Source: Curves were produced from monthly-mean SPM data for the periods before and after construction at the site (sampling is unequal in time: 104 months pre-build and 42 months post-build).

The statistical analysis described here has been carried out with low-resolution satellite images with a pixel resolution of 4 km. At this spatial scale, 70% of the OWF site is covered by only two pixels. When a sufficiently long time series of high resolution Sentinel-2, Sentinel-3 and Landsat-8 images (with pixel resolution of 10m, 30m and 300m) is available, it would be advisable to use this data to locate individual target polygons within the wind farm site and analyse changes in greater detail.

### Context for fieldwork in August 2016

Analysis of the satellite-derived surface sediment concentration for 2016 has been carried out at a higher temporal resolution to set the context for the conditions occurring at Thanet during the summer field surveys in WP4. Due to cloud cover, satellite images were available

on approximately 20% of days. To compensate, eight-day averaged SPM and wave height were compared throughout the year (Figure 18). The annual cycle of SPM concentration, with high values in the winter and a long period of low values from late April to early November can clearly be seen. Wave heights also showed, as expected, higher values during winter. However, the seasonal amplitude in wave heights is lower than that for SPM concentration.

A striking feature of the time series is the degree to which SPM can change within a short period of time. For example, a decrease in SPM of  $53 \text{ mg l}^{-1}$  could be seen between the 5<sup>th</sup> and 13<sup>th</sup> March. As wave height was still at the typical winter level of  $> 1.5\text{m}$ , the decrease in suspended material was not due mainly to changes in local physical forcing (resuspension from the seabed), but to other factors. A decreased supply of sediments from riverine run-off could be important, as could altered particle-particle interactions caused by increasing biological activity in the planktonic ecosystem as spring advances (causing increased stickiness, particle aggregation and sinking).

The sharp increase in SPM in the autumn e.g. an increase of  $45 \text{ mg l}^{-1}$  between 8<sup>th</sup> and 16<sup>th</sup> November was preceded by, and explained by, the passage of the first storm (highest wave heights of the year on 3<sup>rd</sup> November). Sampling for the project took place in August 2016. Mean significant wave height varied between 1 and 2 m during the two sampling weeks, and SPM concentration increased throughout the month from  $7 \text{ mg l}^{-1}$  in late July to  $14 \text{ mg l}^{-1}$  in early September.

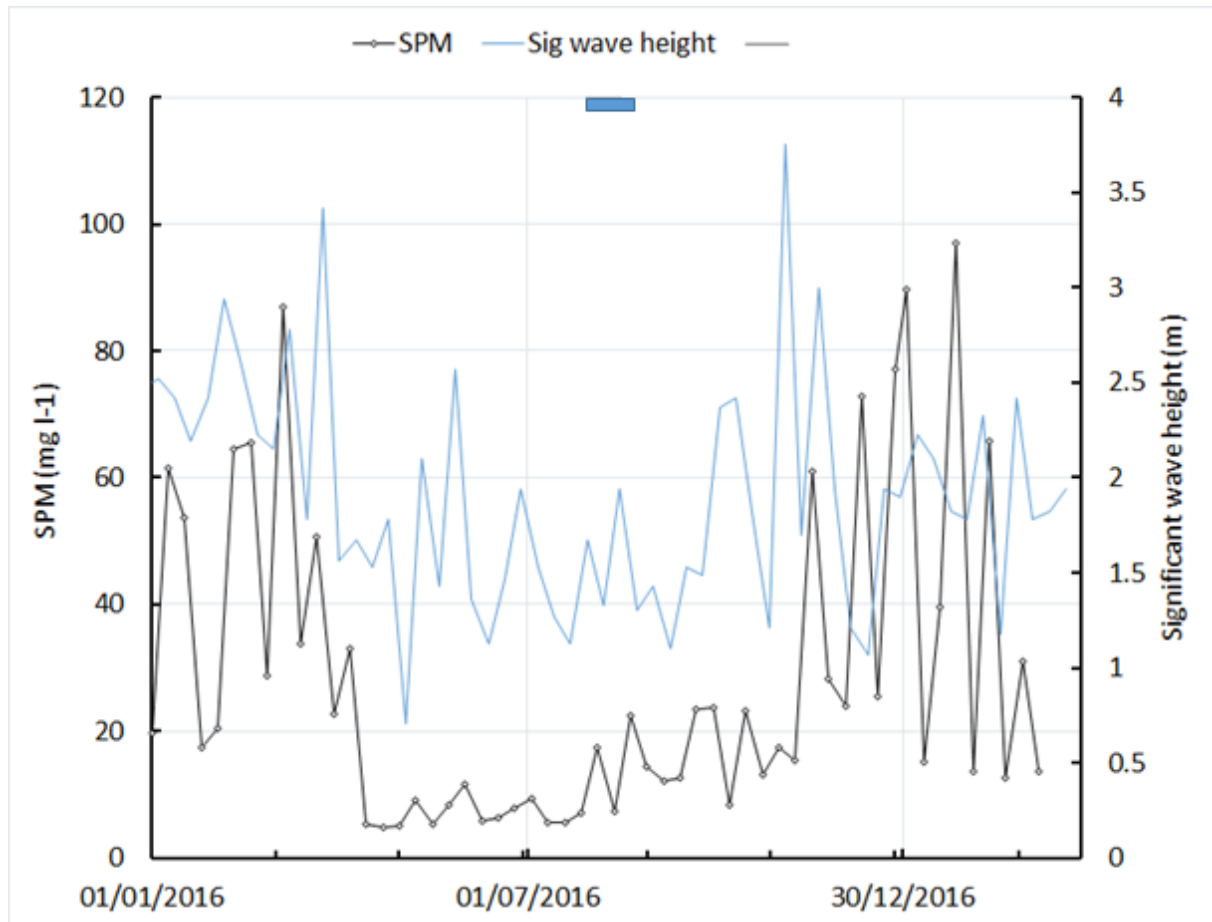


**Figure 18** Changes in the 8-day average of satellite-derived surface suspended particulate material.

SPM concentration within the zone of the Thanet offshore wind farm throughout 2016 (black line with symbols), is compared to the 8-day average of significant wave height (blue line). The sampling period for field surveys is shown by the blue bar at the top of the graph.

Conclusions on natural environmental variability :

Satellite optical imaging has been used as a means of ascertaining spatial and temporal variability in sediment concentrations of the outer Thames. Whilst this provides excellent coverage, it should be noted that measurements relate only to the upper meters of the water column, and that deeper layers are not quantified by this means. Satellite coverage requires clear-sky conditions, and this can create a bias towards calmer versus stormier conditions.

The concentration of SPM is the main control on water transparency in the southern North Sea, and it was hypothesised that changes in water colour due to monopile-current interactions result in a higher concentration of sediments in the surface layer. To give context for any local changes associated with plumes, natural variability must be taken into account.

The Thanet OWF lies at the boundary between turbid, outer Thames water masses to the west, and clearer North Sea / English Channel water to the east. Shallow water to the south west increases local turbidity. Adding to the complex spatial patterns are pronounced seasonal changes in suspended particulate matter. Turbidity can be over 6 times higher between the late winter maximum and the June minimum. Large changes in suspended material were also observed over short periods of time, possibly as a result of biological-physical interactions (algal blooms), storms, or run-off of the Thames and other rivers.

A further element of variability at Thanet is the difference in sediment load throughout the water column. As this data cannot be measured from satellites or from surface buoys, or ships-of-opportunities, the variability in the vertical dimension for this region is unknown.

## 4. PRELIMINARY FIELDWORK

### Method development

Methods required for the main field campaign were developed and tested during trial cruises-of-opportunity to Humber Gateway OWF in May and June of 2016.

#### FLOW-THROUGH MEASUREMENT OF OPTICAL BACKSCATTER, TEMPERATURE AND SALINITY

Sampling of the surface water composition from a moving vessel is an efficient means of rapidly gathering high-resolution spatial data for use in mapping the presence of turbid wakes. A commercial 'Pocket FerryBox' device has been used by the author in previous North Sea cruises for mapping plankton, but such a device could not be sourced within the time frame of the work programme in 2016. A simple deck-mounted flow-through system was developed in which seawater from the research vessel's clean seawater supply was routed through a series of de-bubbling tubes, the last of which contained instruments to measure optical backscatter, temperature and salinity (Figure 19). Readings were recorded automatically to a data logger.



**Figure 19** Deck sampling rig for continuous measurement of suspended sediment load, temperature and salinity.



### **GRAVIMETRIC DETERMINATION OF SUSPENDED PARTICULATE MATERIAL**

Optical measurements of backscatter give a reading of turbidity, which can be calibrated using seawater of known concentrations of suspended particulate matter. Direct measurements of SPM were carried out with a relatively low frequency, as the process involves sampling of the water followed by filtration. Water samples were taken either at the surface, or underwater using a Niskin bottle of volume 10 litres. Typically, three depths are selected corresponding to below surface, mid-water and just above the seabed. Water samples from the Niskin bottle were filtered on dried and pre-weighed Glass Fibre Filters (GFF), stored in dry conditions and taken back to the laboratory for gravimetric analysis. Weighing using an accurate balance was done and the amount of SPM found by difference. A further heating of the filter in an oven was done to remove organic material, thus giving the ash content and organic content. A relationship was then derived between the directly measured SPM, and indirect measurements from the optical and acoustic backscattering instruments.

## 5. RESEARCH CRUISES TO INVESTIGATE PLUME FORMATION AND CONTENT

Dedicated cruises within the project were planned to investigate the composition and causes of turbid wakes. Field campaigns took place during the summer period to ensure the highest chances of co-location of *in situ* and satellite measurements. Plume surveys were for 3 consecutive days duration during spring tides (maximum current velocity), with a low (early morning) - high (midday) - low (afternoon) tidal sequence followed on each day.

The charter vessel selected was the RV *Meriel D* (Figure 20).



**Figure 20** RV *Meriel D* at dock in Ramsgate during survey 2.

The survey team used methods developed in WP3 for continuous underway sampling of the water surface. The vessel was directed to take transects through known plume locations (pre-selected from satellite images, Figure 21).

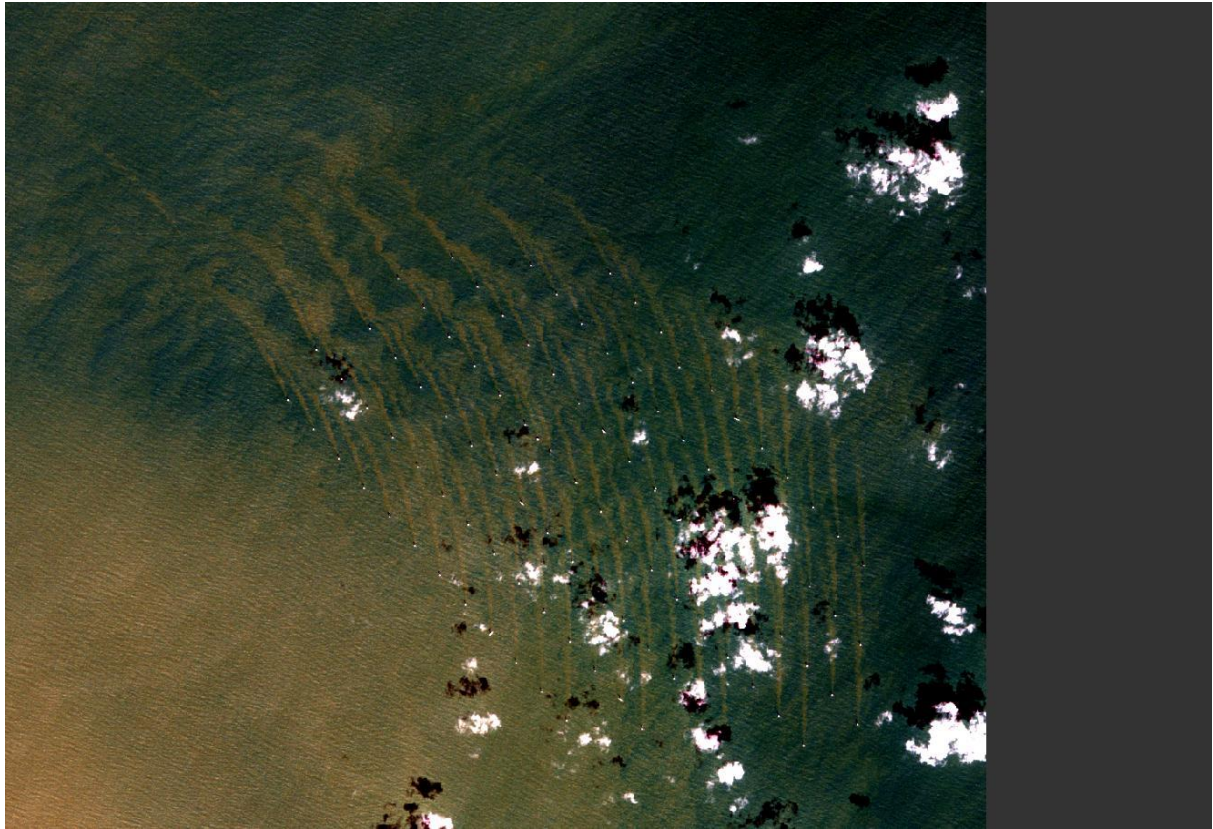


**Figure 21** Example of Sentinel-2 ebb tide scene of Thanet used for detection of plume direction.

Plots of vessel location with respect to the Thanet OWF for all days of the surveys are provided in Figure 22 and Figure 23. Full details of all actions during the surveys are given in Appendix 1. During the flood tide, sampling started to the north (e.g. upstream) of the OWF site. Plumes on the northern edge of the farm were targeted. During the ebb tide, the vessel was directed to the southern edge of the wind farm.

Details of all sampling events are given in the Appendix.

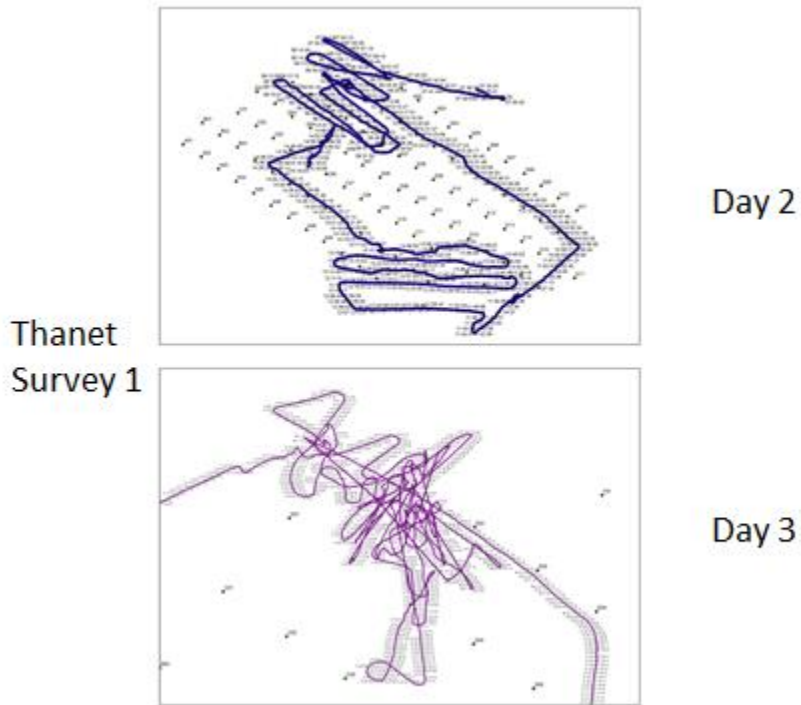


**Figure 22** Map of RV *Meriel D* locations during survey days 2 and 3 of the first survey week.

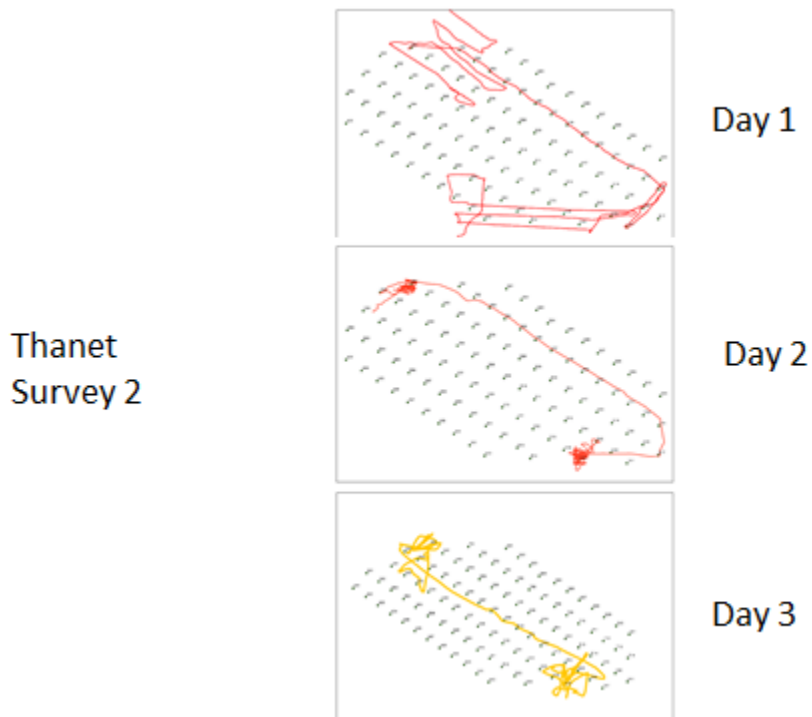


**Figure 23** Map of RV *Meriel D* locations during survey days 1, 2 and 3 of the second survey week.

## **ADDITIONAL METHODS USED ON THANET SURVEY**

Optical and acoustic profiling of the water column from surface to seabed was done at locations in and out of distinct plumes, together with discrete sampling of the water for laboratory analysis of optically-active components (sediment quantity and composition, plankton, dissolved material).

Parameters to be measured at vertical-profile stations included:

- Current profiles via Acoustic Doppler Current Profiler (ADCP) measurements across plumes to detect changes in flow velocity, and possibly sediment concentrations at depth via back-scatter
- Optical measurement of underwater light, back-scatter, attenuation and fluorescence (Figure 24; Figure 25)
- Bottle sampling of discrete depths for calibration purposes
- Site depth and sediment 'hardness' to estimate potential sediment sources to the water

## **Inherent Optical Properties of the water**

Inherent Optical Properties (IOP) *in situ* profiles were collected with a 25 cm pathlength AC-9 attenuation and absorption meter alongside a BB9 backscattering meter (both WETLabs Inc.). Both instruments were attached to a steel 'rosette' sampling frame with a central attachment point. The frame plus instruments could be lowered with the ship's winch to a maximum operating depth of 10 m.

Absorption and attenuation coefficients were determined for 9 different wavebands (10 nm FWHM) centred on 412, 440, 488, 510, 532, 555, 650, 676 and 715 nm while backscattering coefficients were calculated based on measurements of the volume scattering function at an effective scattering angle of 117°, measured at 412, 440, 488, 510, 532, 595, 650, 676 and 715 nm which were subsequently interpolated to AC-9 wavelengths. Both AC-9 and BB9 data were scaled to depth recorded using an SBE50 (SeaBird Electronics, Inc.) depth sensor.

An SBE19plus (SeaBird Electronics, Inc.) sensor and a BBFL2 sensor (WETLabs, Inc.) were mounted on the IOP frame collecting data on depth, temperature, conductivity, fluorescence and turbidity. All time stamps were synchronized and interpolated to match the frequency of the AC-9 instrument. All depth data were calibrated against the SBE50 depth sensor, the most sensitive in this configuration, using linear regression.

The AC-9 was calibrated in the lab before the survey using ultrapure water (Milli-Q, Millipore), while the BB9 data was subject to manufacturer's calibration. Data were corrected for the temperature and salinity dependence of pure seawater (Pegau et al., 1997) and for scattering errors using the semi-empirical correction by Röttgers et al. (2013). BB9 measurements were corrected according to the BB-9 manual (WETLabs, Inc., 2013) and  $\beta_p(117^\circ, \lambda)$  was converted to particulate backscattering coefficient,  $bbp(\lambda)$  using  $\chi = 0.9$  in accordance with Sullivan et al. (2005).

Detailed flow velocity fields and estimated suspended sediment concentrations were obtained using two ADCP deployed on a scaffold pole through the moon-pool of the vessel.

The RDI Teledyne 600 kHz and RDI Teledyne 1200 kHz units were coupled to the same Real-Time Kinematic and Differential Global Positioning System (RTK dGPS) to provide both position and velocity of the survey vessel. Positional data for all other instruments was linked to the primary Global Positioning System (GPS) using time-stamps. The clocks of all PCs and data-loggers were synchronised at the start of surveys. WinADCP proprietary software from the manufacturer was used to process primary acoustic data into text files with four outputs for each series of acoustic transect: magnitude, north velocity, east velocity and vertical velocity. Further processing in MatLab and Excel produced time-averaged files in which the velocities (in  $\text{m s}^{-1}$ ) were combined over 20 successive profiles corresponding to periods of  $\sim 30$  s. For each depth profile, the last valid depth bin before the seabed was located manually.



**Figure 24** Rosette sampler and optics CTD device for vertical profiling of the water column.



**Figure 25** LISST particle size analyzer in deployment frame

**Table 4** Description of sampling methods used during Thanet surveys.

Method	Depth range	Limits to use	Status
Physico-chemical properties of water: surface	Nominally 1m (from vessel water intake)	Time-stamped data requires geo-correction.	Data collected from two independent instruments, complete and used in this report.
Physico-chemical properties of water: sub-surface	0-10 m	Lower limit of CTD array limited by cable length.	Data complete and used in this report.
Bottle sampling of water	Surface to ~1 m above seabed	Infrequent, limited number of samples due to high processing time.	Data complete and used in this report.
Optical measurement of backscatter: on deck	Nominally 1m (from vessel water intake)	Bubbles entering the seawater supply whilst underway interfere with backscatter measurements.	Data complete and used in this report.
Optical measurement of inherent optical properties: subsurface	0-10 m	Lower limit of CTD+optical rig array limited by cable length.	Data complete and used in this report.
Laser sizing of particle size (LISST)	0-10 m	Lower limit of CTD+optical rig array limited by cable length.	Data set incomplete and not used.
Acoustic back-scatter (ADCP)	Surface to seabed	Decreases in back-scatter near the seabed can be due either to a lower load of suspended particles, or to there being a reduction in beam strength due to attenuated by the higher near-surface suspended sediment or the near-surface bubble plumes.	Data obtained whilst the vessel was drifting with engines stopped are complete and used in this report.  (The signal-to-noise ratio in underway measurements was too high to allow analysis).
Acoustic current velocity (ADCP)	Surface to seabed	Noise in measurements generated by pitch, roll and yaw of vessel may mask changes due to plume formation.	Data obtained whilst the vessel was drifting with engines stopped are complete and used in this report.



## Results

The ship-based surveys at Thanet provided direct confirmation of the clockwise rotation of plume direction observed from satellite images. By stopping the research vessel and allowing drift to proceed under the influence of the tidal current (and wind), it was possible from GPS positions to estimate the speed and direction of each drift (Table 5, Figure 26). The plume direction at the onset of the flood tide (measured at Sheerness; local tidal data was not available) was 187°. With a rotation rate of between 15° and 30° per hour, the plume direction shifted in a predictable manner and gradually increased speed during the mid-part of the flood tide.

**Table 5** Direction and speed of drifts during the flood tide phase of Day 3, Survey 2.

Drift	start	direction	speed (km h <sup>-1</sup> )
1	07:35:23	186°	2.3
2	08:28:05	200°	2.8
3	08:58:37	216°	3.3
4	10:03:03	241°	2.6

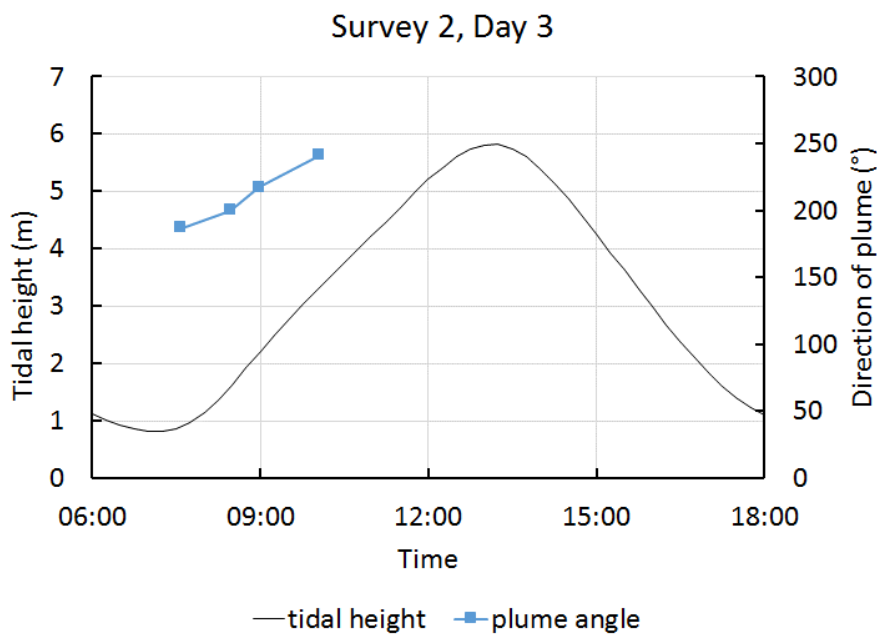


**Figure 26** An example of changing current flow direction during the flood tide at Thanet.

Understanding the nature of the optical differences between the water column within a plume, and that of the surrounding water, was the first research question to be approached. The methods used to investigate the differences between water quality upstream of the OWF site, and water in the plumes, were profiling of the water column with the optical instrumentation, and direct sampling of the water at different depths. Profiling was done with

the vessel drifting, or physically tethered to a monopile in order to remain within the plume during the sampling time.

Although clear sky conditions did not coincide with satellite overpasses during August 2016, the predictable relationship between plume direction and length with respect to tidal state allowed satellite images from other dates to be used as background reference during the preparation of results. In general, a good agreement was found between visual observations of plume position from researchers on the vessel and measurements with the various instruments. These in turn agreed well with the predicted position of plumes from the archive of satellite imagery (Figure 27).

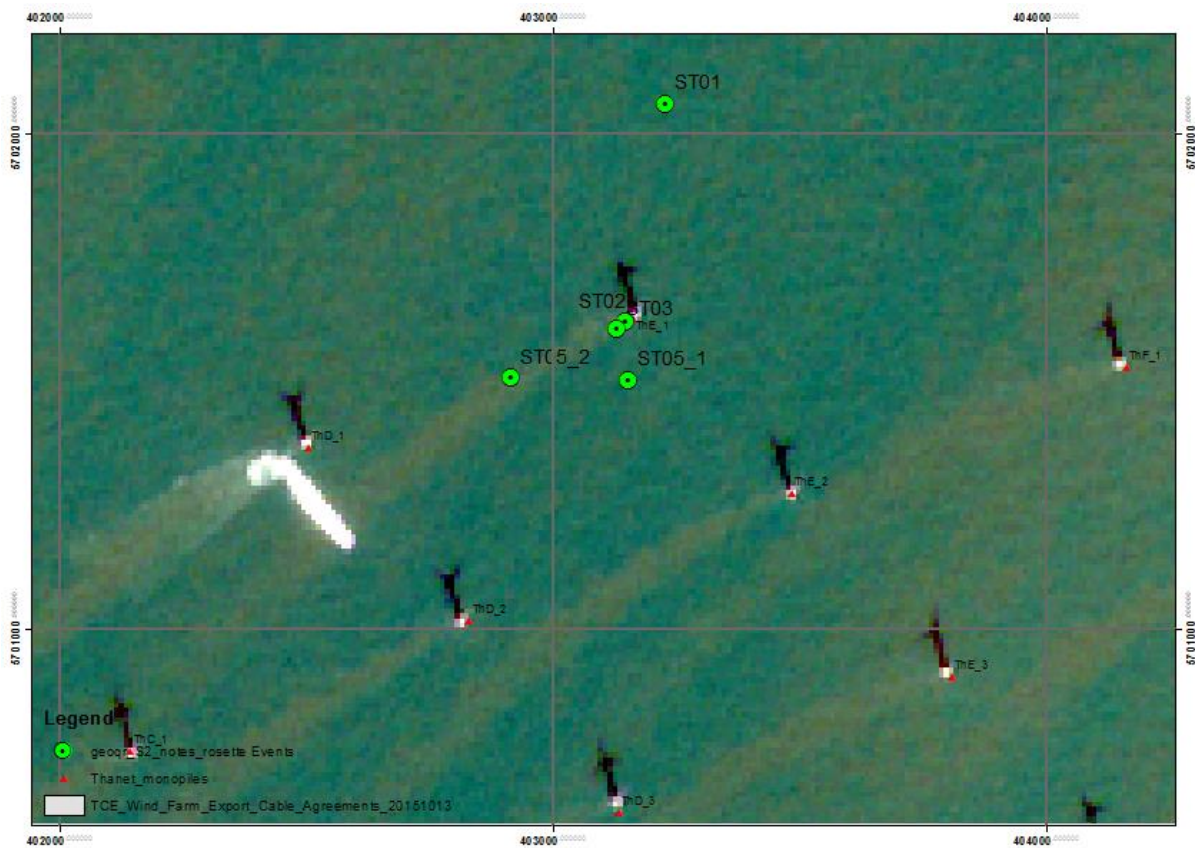


**Figure 27** Location of sampling stations (green symbols) near turbine E01 during the mid-flood tide on 19th August 2017.

Station ST01 is an upstream control site for water which has not interacted with the monopile array. A satellite image taken on a different date, but with the same tidal height, was used to approximate the plume position. The white patch close to turbine D\_1 is the wake of a crew transfer vessel near the monopile base. The image also shows the capability of Sentinel-2 at resolving fine resolution features such as the shadow of monopiles and blades.

## VERTICAL STRUCTURE OF THE WATER COLUMN

The upper 10 m of vertical structure of the water column near and within the Thanet OWF was measured three times on the first week of survey (two profiles outside of plume, one within), and four times during the second survey week (two profiles each). The upper half of the 19 to 23 m deep water column was measurable using the cable and winch available. Sampling of the full depth of the water was only achieved with the Niskin bottles for water collection (see later). The plume associated with turbine D03 was investigated during survey 1 (Figure 28). Temperature and salinity profiles within and outside of the plume did not differ, and were within the range of variability observed at the surface during the flood tide measuring period. Of the optically-active water column constituents, chlorophyll and cDOM were higher within the upper 10 m of the plume (Table 6), but chlorophyll was not higher than measurements made upstream of the OWF. This suggested that local horizontal variability in this parameter was high. Backscatter at 532 nm was distinctly higher at a depth of 6 to 10 m within the water column of the plume compared to outside of the plume.

An additional profile was generated on the 19<sup>th</sup> August by tethering the vessel to turbine E01, releasing the tether with immediate collection of a depth profile whilst in the plume. Shortly afterwards, as the vessel drifted out of the plume, a second profile was taken for comparison (Figure 29, Table 7). The results showed no significant differences in either the physical properties or the optical properties of the water between locations.

**Table 6** Depth-averaged water column properties for vertical profiles upstream, in and outside of the plume from turbine D03 on 5<sup>th</sup> August 2017.

		temperature [deg C]	salinity [psu]	chl f	cDOM fl	b_b(532 nm) [m <sup>-1</sup> ]
	upstream	18.60	34.67	1.41	3.51	0.027
D03	in plume	18.45	34.71	1.44	3.82	0.031
	out of plume	18.42	34.72	1.28	3.14	0.023

**Table 7** Depth-averaged water column properties for vertical profiles upstream, in and outside of the plume from turbine E01 on 19<sup>th</sup> August 2017.

		temperature [deg C]	Salinity [psu]	chl f	cDOM	_b(532 nm) [m <sup>-1</sup> ]
	in plume	18.87	34.70	1.30	3.12	0.023
	out of plume	18.88	34.70	1.29	3.05	0.022

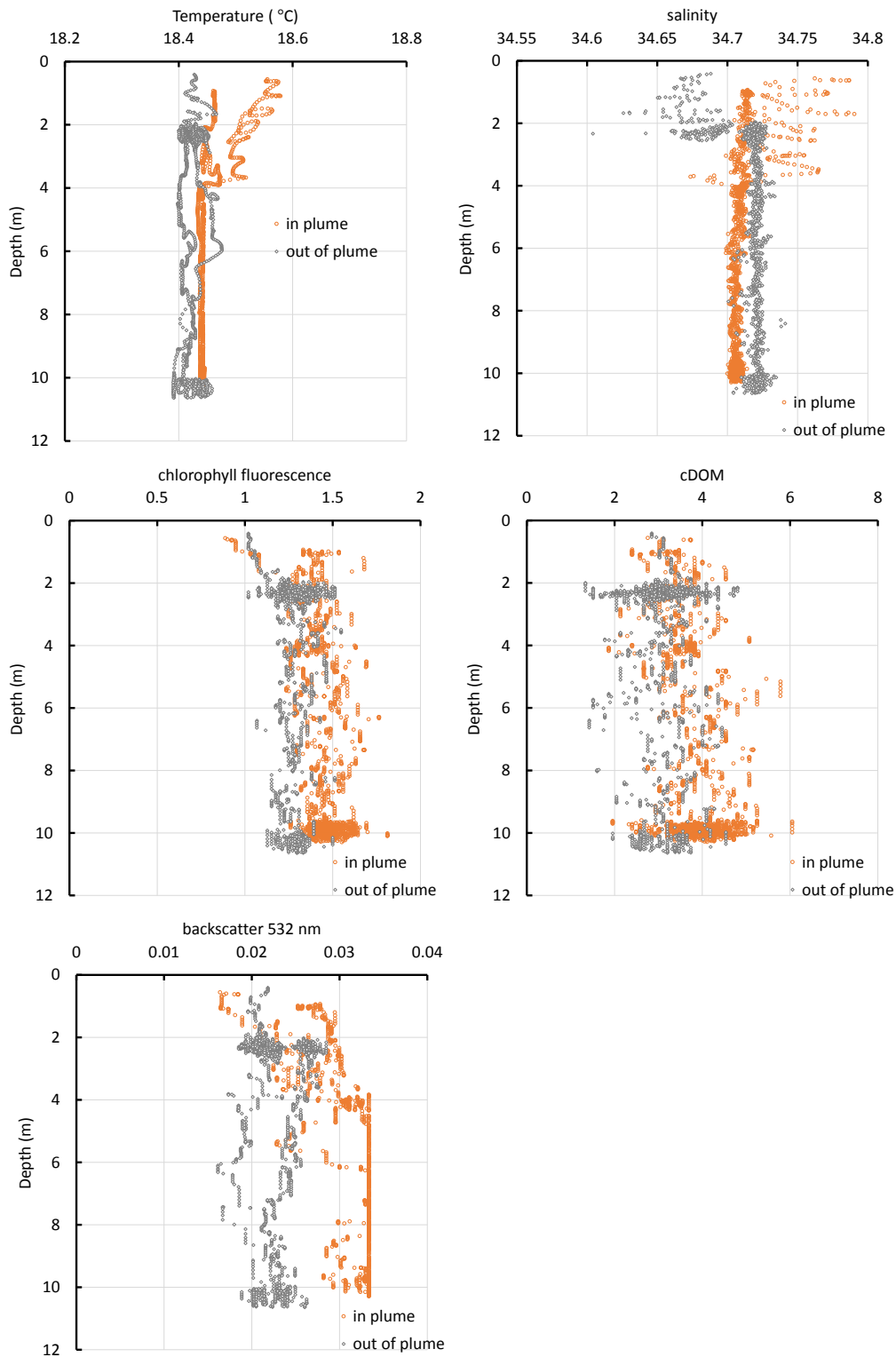


**Figure 28** Profiling of the upper 10 m of the water column for physical and optical measurements. Locations inside and outside of the plume from tower D03 on 5<sup>th</sup> August 2016 for repeated profiling.

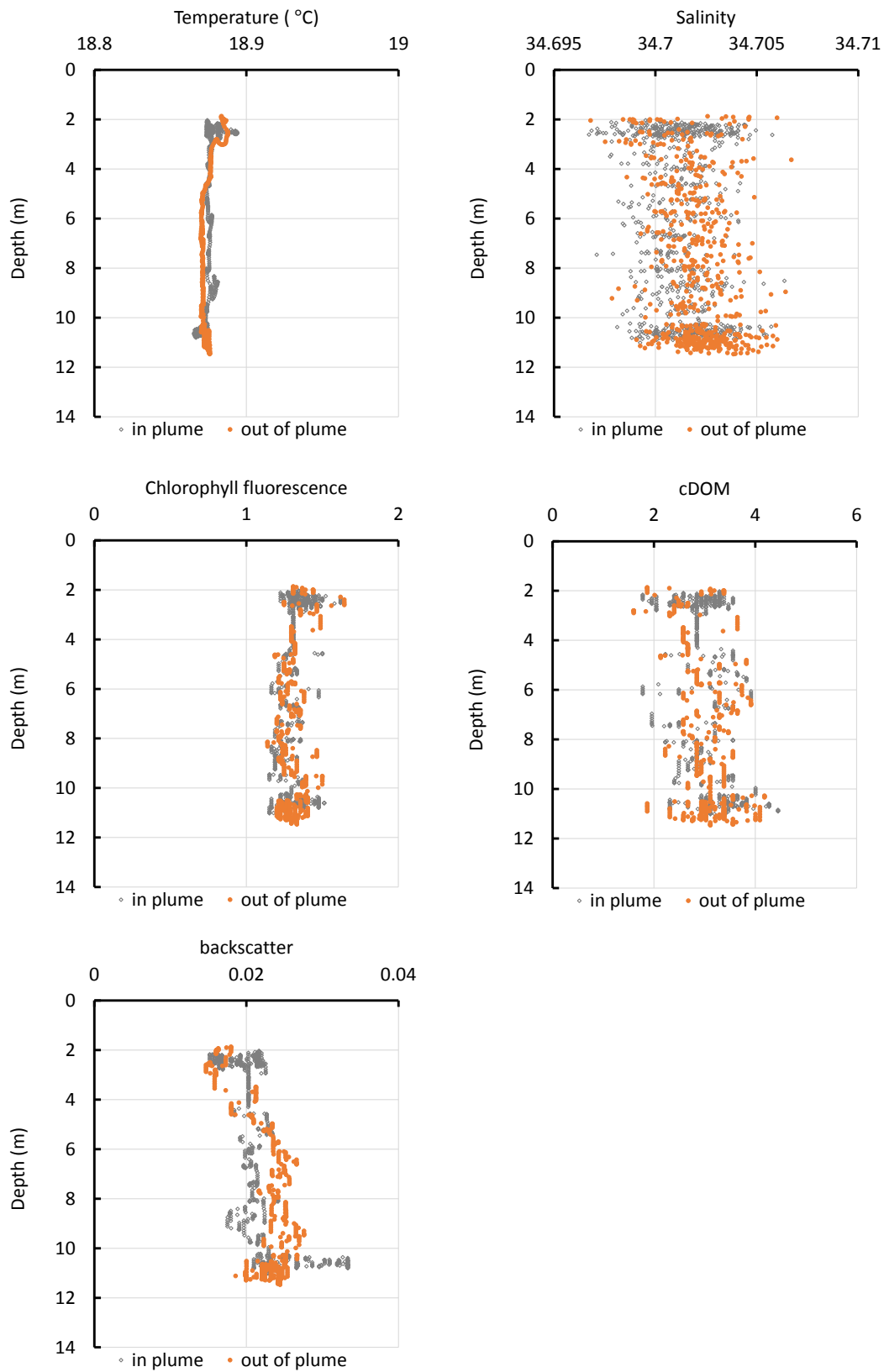


**Figure 29** Profiling of the upper 10 m of the water column for physical and optical measurements. Locations inside and outside of the plume from tower E01 on 19<sup>th</sup> August 2016.

Sampling of the water itself for gravimetric analysis was possible to a depth of over 20m, enabling the near-bed conditions to be measured (Figure 30). The deepest samples were collected at 20 m, within 3-5 m of the sea-bed. The measured SPM at the surface was higher for four out of five of the paired upstream-downstream comparisons (Table 8), with a mean difference within the plume of a 42% higher sediment load. The difference between the upstream and the in-plume water column was less at the mid-water position (plume 10% higher, Table 9), and close to the sea-bed (plume 20% higher, based on 2 samples, Table 10).

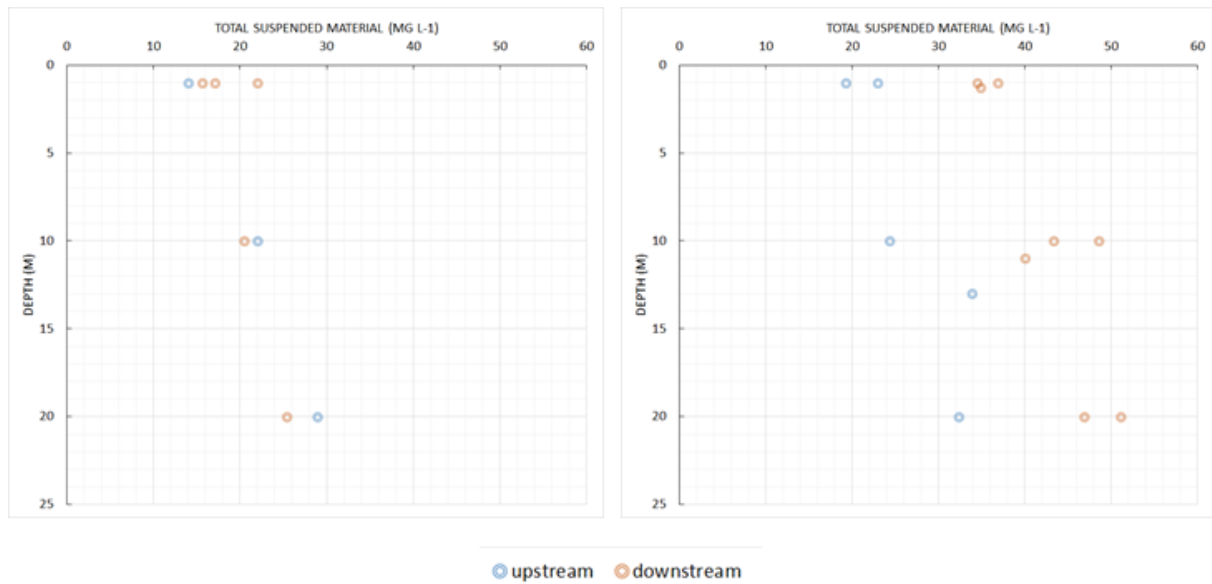


**Figure 30** Analysis of suspended particulate material at locations upstream and downstream of (left panel) turbine E01 during the flood tide on 19<sup>th</sup> August 2016 and (right panel) turbine c15 during the ebb tide on 19<sup>th</sup> August 2016

**Table 8** Comparison of surface suspended particulate material ( $\text{mg l}^{-1}$ ) for locations upstream or downstream (in visible plume).

Monopile	Condition	time	SPM		% difference
			upstream	downstream	
D02	flood	09:39	9.7	14.0	45%
		12:00	25.8	18.8	-27%
		13:08	9.9	19.5	97%
E01	flood	08:25	14.0	18.3	30%
E15	ebb	12:54	21.1	35.4	68%
					<b>42%</b>

**Table 9** Comparison at depth 10 m of suspended particulate material ( $\text{mg l}^{-1}$ ) for locations upstream or downstream (in visible plume).

Monopile	Condition	time	SPM	SPM	% difference
			upstream	downstream	
D02	Flood	11:26	25.8	28.2	9%
		12:52	24.2	20.8	-14%
E01	Flood	09:06	22.0	20.4	-7%
E15	Ebb	12:56	29.1	44.0	51%
					<b>10%</b>

**Table 10** Comparison just above the sea floor (20 m) of suspended particulate material ( $\text{mg l}^{-1}$ ) for locations upstream or downstream (in visible plume).

Monopile	Condition	time	SPM	SPM	% difference
			upstream	downstream	
E01	Flood	08:30:39	28.9	25.4	-12%
E15	Ebb	13:48:10	32.3	49.0	52%
					<b>20%</b>

Results of vertical profiling showed that even though the water column upstream of the OWF site was apparently well-mixed in terms of temperature, SPM concentration (and backscatter) were higher in midwater and particularly near the sea-bed. There is strong evidence that the existing vertical gradient in suspended load was altered during contact of the flowing water with the monopile structure so that downstream of the monopile (e.g. within the wake), there was a more homogeneous vertical distribution of sediment. Hence, the surface concentration of SPM in the wake was higher than that in surrounding waters.

#### VARIABILITY IN SURFACE WATER QUALITY ACROSS THE OWF SITE

Sampling was conducted continuously with the deck-mounted flow-through instrument package, and an in-water optical backscatter instrument mounted in the ship's moon-pool. A greatly reduced signal-to-noise ratio was obtained when the ship was drifting passively as compared to underway with power, possibly due to interference by bubbles. Hence, interpretation of results obtained underway require further filtering before useful plume maps can be made.

An example is shown in which a clear increase in optical backscatter within a plume was measured (Figure 31, Figure 32). The vessel approached the plume of turbine E01 from the south-west, entering the plume at 09:08. OBS measurements even at slow speed showed high variability between 09:08 and 09:15 (**Error! Reference source not found.**), some of

hich may be attributable to higher suspended sediment within the plume. After tethering to the tower at 09:20, measurements were made in the turbulent wake in close proximity (~30m). After release and drift, the vessel left the plume zone at 10:04. A small decrease in turbidity readings for both instruments was recorded at this point.

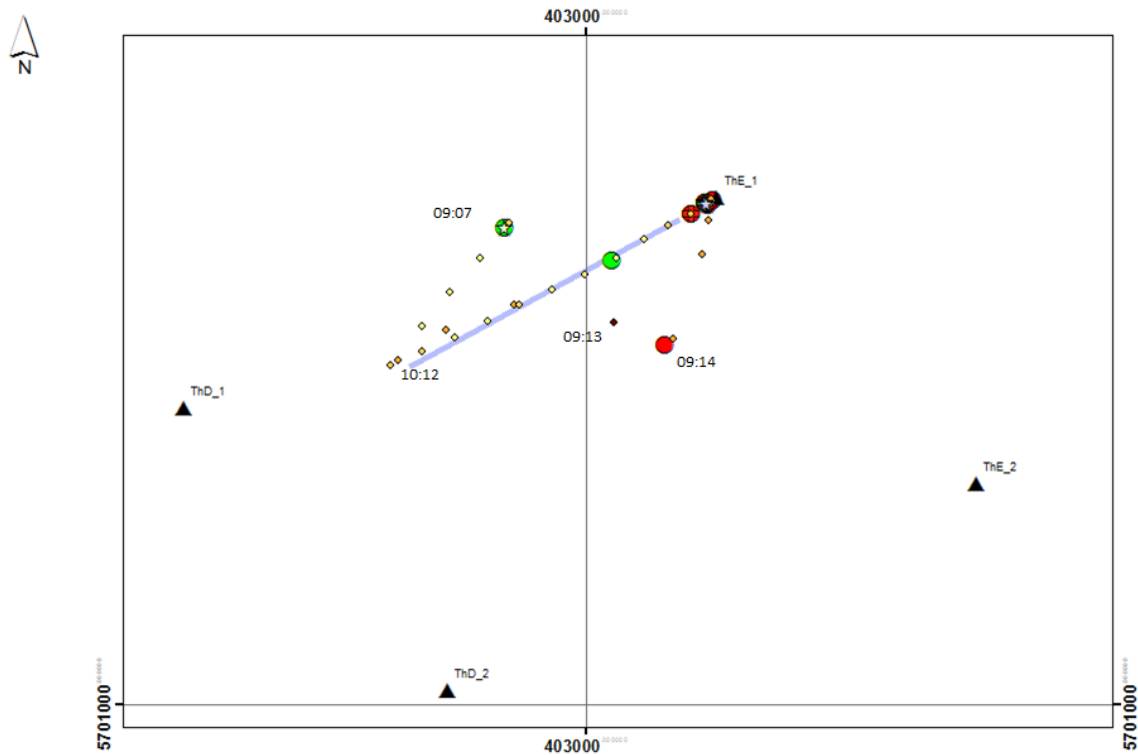


**Figure 31** Map of 'Time section 3' on 19<sup>th</sup> August 2017, with an approach to turbine E01 in the plume, attachment to the tower, and subsequent release and drift (out of plume).

Black triangles: positions of monopiles (labelled with Vattenfall numbering system; Circles: Red – visual observation of in plume, green out of plume. Coloured diamonds: vessel position with colour intensity indicating SPM concentration (shown as time series in Figure 32).



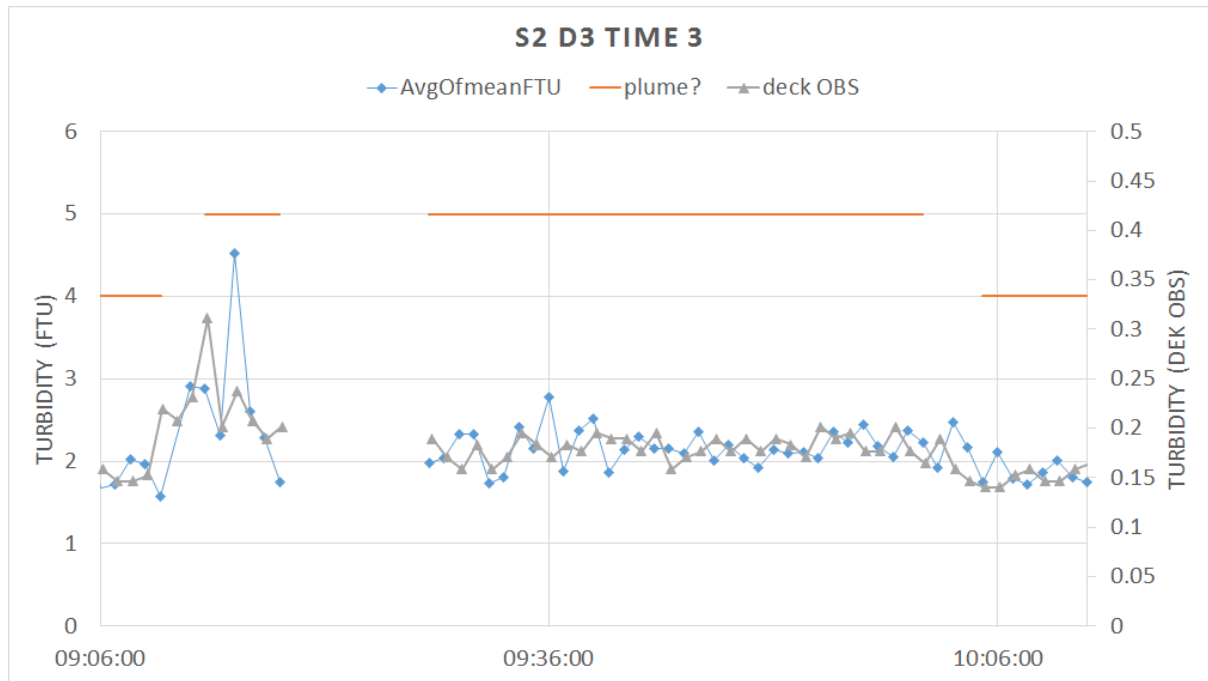


**Figure 32** Optical backscatter measurements with deck and in-water (moon-pool) instruments during Time 3.

The deck sensor was supplied with continuous seawater from the vessel's cooling water line, whereas the in-water was located directly in the water. Differences in position and in instrument logging frequency (deck – 0.016 Hz; moon-pool 1 Hz) may cause time delays between the measured values. Orange horizontal lines mark periods without the vessel's engine engaged (drifting or tethered), bars at the higher level denote periods within plumes.

The following period of drift (Time section 4 on 19<sup>th</sup> August 2017) also detected differences upon entering the plume of turbine E01. In this instance, later in the flood tide, with current flowing from east to west, the vessel was manoeuvred to a starting position which allowed a drift first through non-plume water, then a crossing of the plume (Figure 33). Entering the plume at 10:36 was marked by a small increase in optical backscatter.

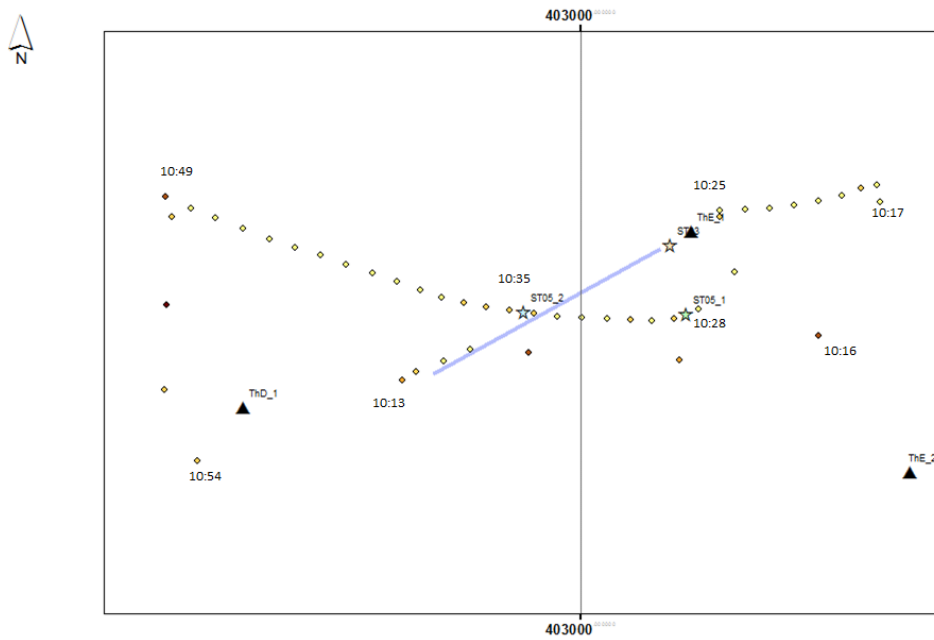


**Figure 33** Map of events for 'Time section 4' on 19<sup>th</sup> August 2017, with a period of drift between 10:28 and 10:41 (out of plume, then crossing plume of E01).

Black triangles: positions of monopiles (labelled with Vattenfall numbering system), blue stars: positions of water sampling events, coloured diamonds: vessel position with colour intensity indicating SPM concentration (shown as time series in Figure 34). Effects of wind on the vessel caused the drift direction to take a different trajectory to that of the tidal flow.

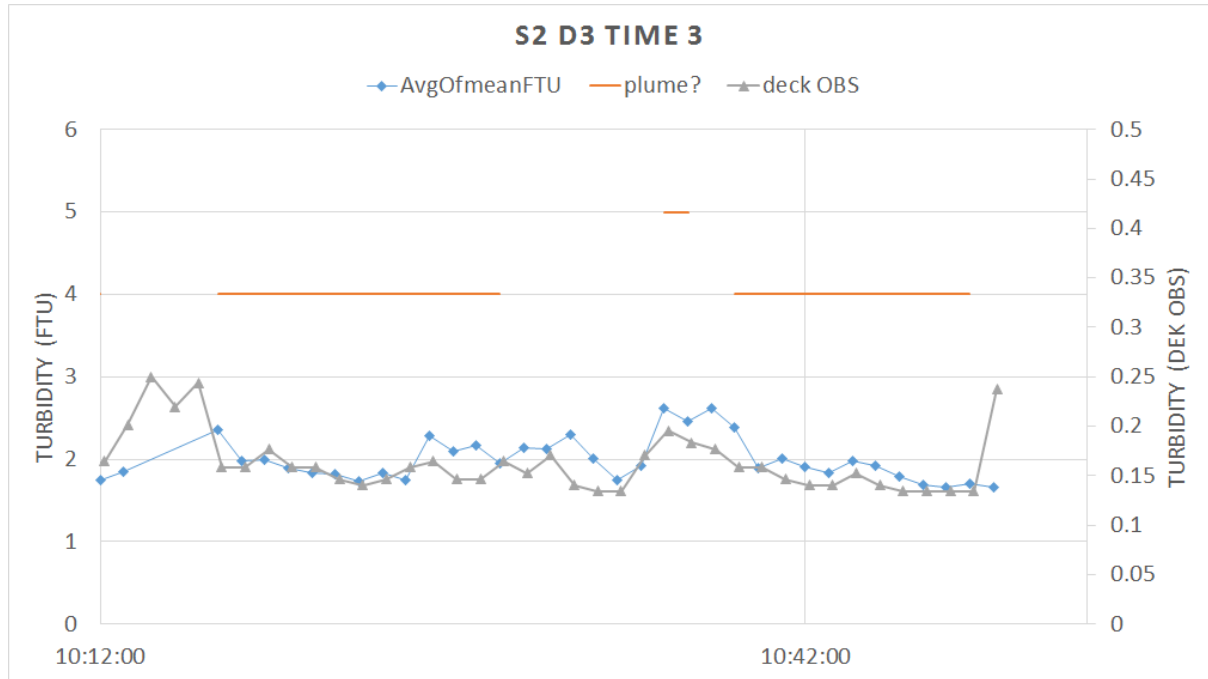


**Figure 34** Optical backscatter measurements with deck and in-water (moon-pool) instruments during Time 4 on 19<sup>th</sup> August 2017. Orange horizontal lines mark periods without the vessel's engine engaged (drifting or tethered), bars at the higher level denote periods within plumes.

A higher-resolution record of this event was captured by the optical instruments on the CTD rosette, which were logging in the surface water at a depth of 2m during the drift. The instrument data capture rates were higher than the other OBS instruments (10 Hz versus 0.016 Hz). Movement of the vessel into the plume resulted in a clear decrease in surface temperature of 0.03°C, accompanied by a 40% increase in scattering at 532 nm. Exiting the plume resulted in a gradual increase in temperature with a fall in back-scatter (Figure 35).

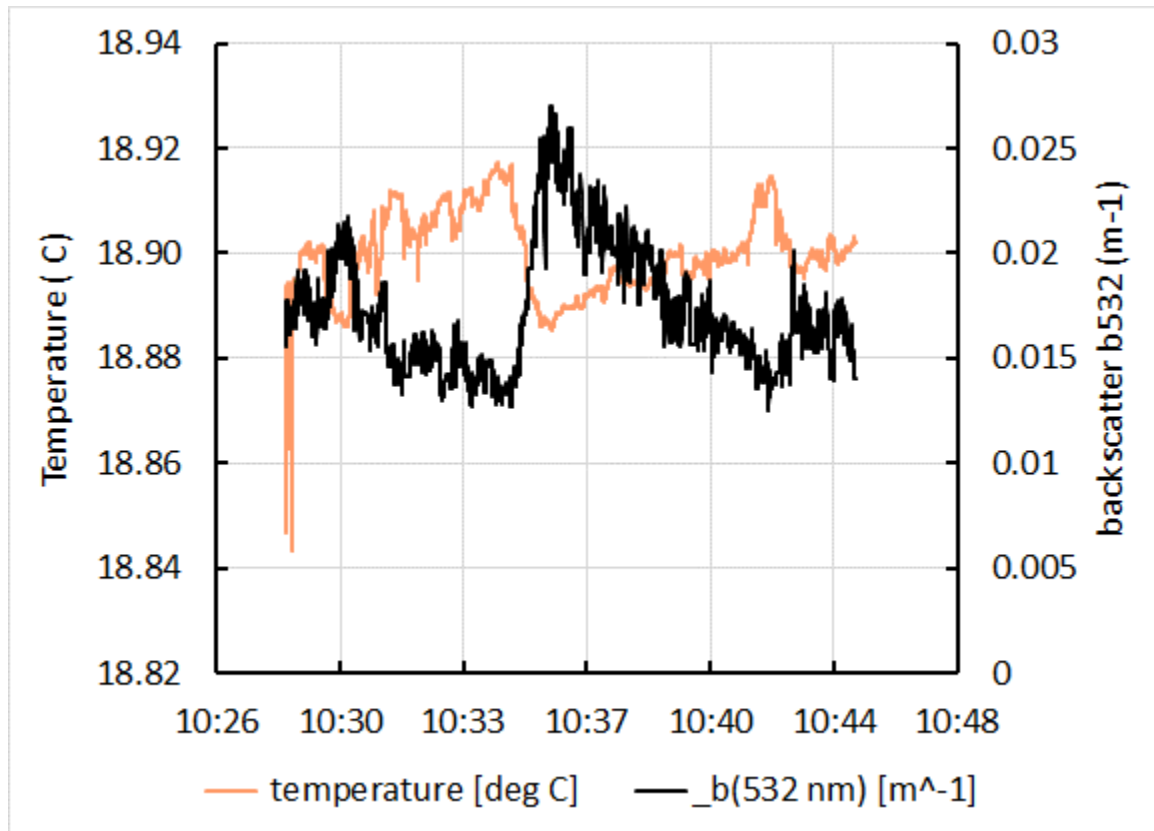


**Figure 35** High-resolution record of entering the plume of turbine E01 with logging of surface temperature and back-scatter at 532 nm.

Similar results were obtained with all channels on all optical instruments during this period (e.g. AC-9). A lack of difference between different spectral bands indicated that the observed increase in attenuation (and scattering) was spectrally-neutral, and therefore unlikely to be caused by water constituents such as chlorophyll or cDOM, which have strong spectral characteristics.

Although the optical instrument package was limited to a depth range of 10 m, and could not sample the near-bed water, it was possible to obtain continuous estimates of suspended sediment concentration throughout the entire water column from acoustic back-scatter. ADCP readings in the near-surface zone were influenced by vessel motion whilst underway, therefore sections of passive drift were examined. The previously-described results using optical backscatter were confirmed with the use of acoustics (Figure 36). Departure of the vessel from the observed surface plume zone of turbine E01 resulted in an approximately 20% decrease in acoustic back-scatter. Conversely, near-bed acoustic readings were lower within the plume and increased as the vessel drifted out of the plume. Two caveats should be added with respect to the use of acoustics: the 'footprint' of the acoustic beam at depth has not been calculated here, and it is possible that a higher surface sediment load will mask the back-scatter from deeper layers.

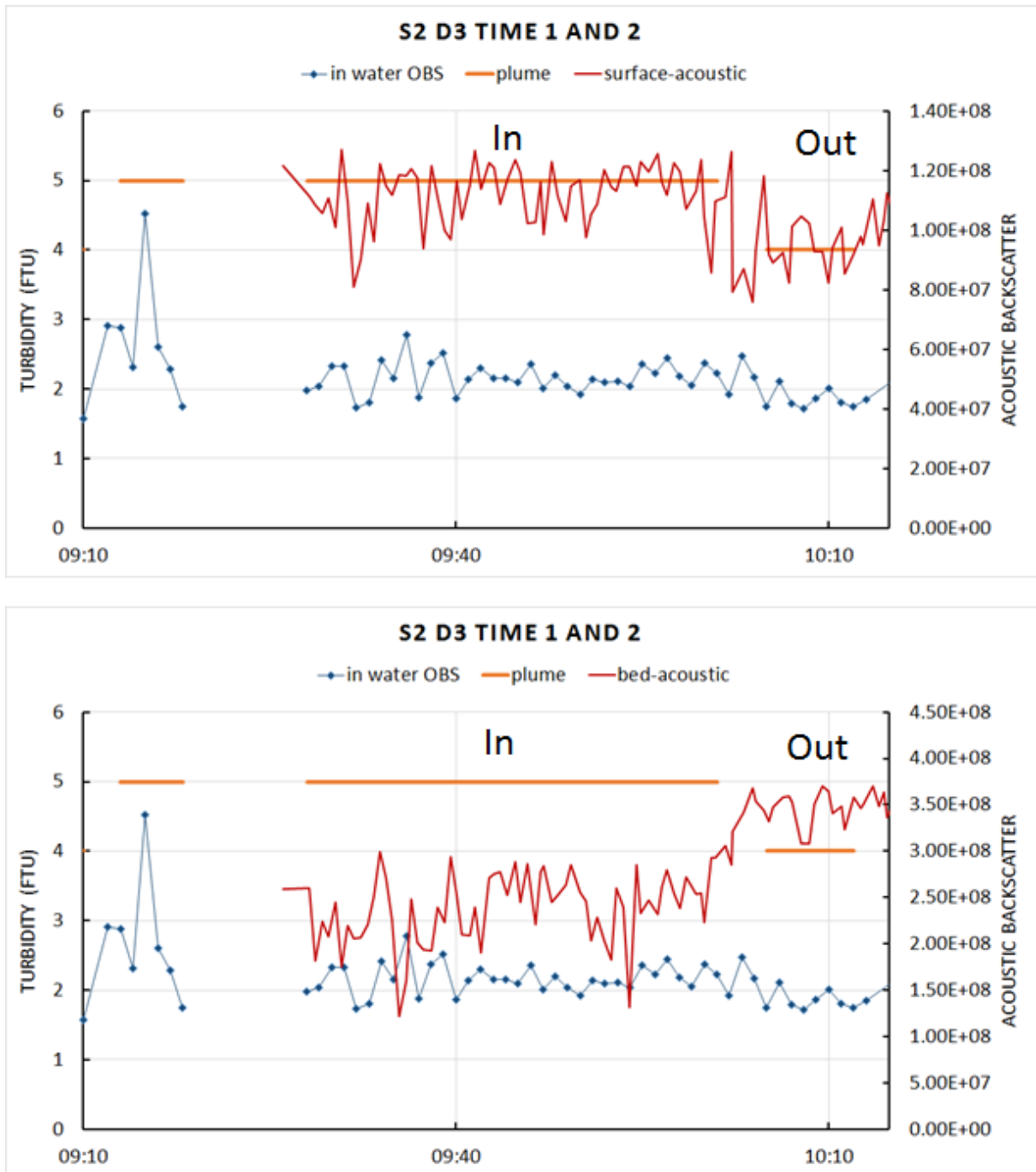


**Figure 36** Estimation of suspended sediment concentration derived from acoustic backscatter at a frequency of 600 kHz (red line) for the near surface zone (3-5 m, upper panel), and near the sea-bed (17-20 m, lower panel).

An additional example is shown for the plume-crossing drift described with high-resolution optical data logging in Figure 35. The near-surface acoustic signal did not respond to the period of drift within the plume (Figure 37), but near-bed acoustic back-scatter showed a marked decrease one minute before the vessel entered the plume. Near-bed back-scatter remained at a low level until after the plume was cleared, before returning to the level

recorded before the plume. The acoustic profile recorded suggested that the underwater shape of the plume was complex. Changes in particle size due to faster settling of larger, heavier particles will also influence the acoustic response.

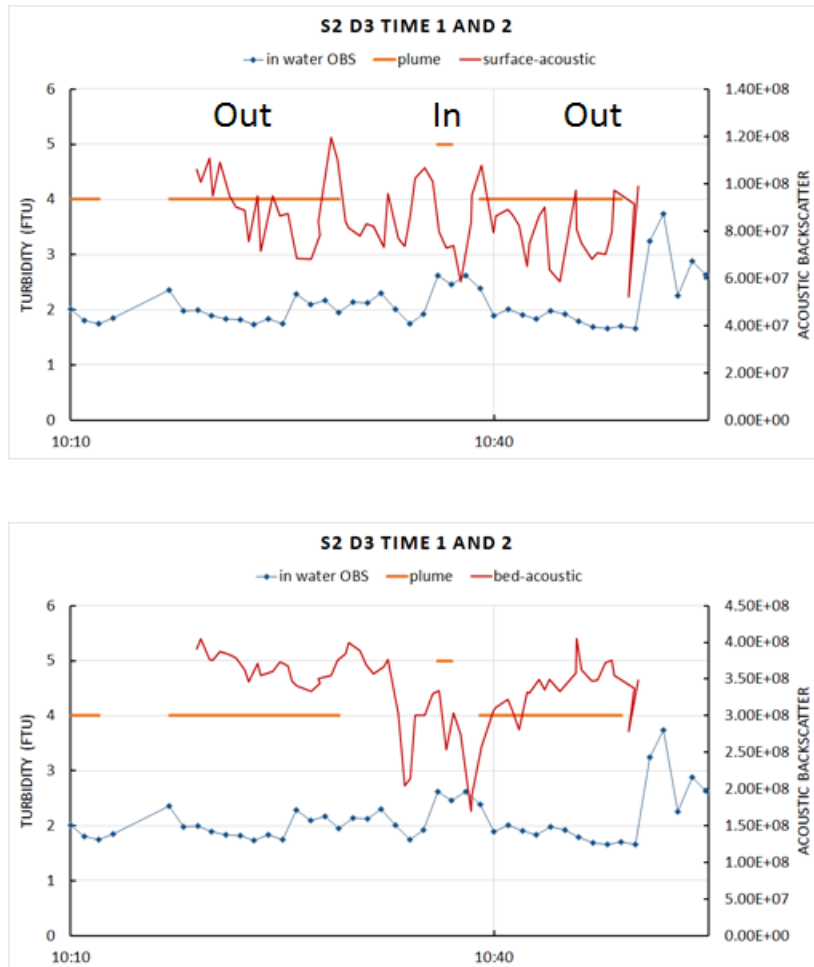


**Figure 37** Estimation of suspended sediment concentration derived from acoustic backscatter at a frequency of 600 kHz (red line) for the near surface zone (3-5 m, upper panel), and near the sea-bed (17-20 m, lower panel).

ADCP current measurements during the drift period shown in Figures 33, 34 and 36 were used to examine changes in the vertical structure of the water column. Figures were constructed to show the difference in current magnitude before, during and after the passive drift of the vessel into the plume of turbine E01 on 19<sup>th</sup> August (vertical profiles in upper panel of Figure 38). Differences in this parameter were insufficiently resolved due to noise introduced by wave-induced motions of the vessel (note standard deviations in Figure 38 upper panel). Depth averaging of the upper and lower 5 m of the water column to produce a time series showed a gradual increase in magnitude from 0.3 to 0.4 m s<sup>-1</sup> during the drift. Passage through the plume area did not result in a noticeable change (Figure 38, lower panel).

In contrast, the northwards component of water motion appeared to show changes coherent with the plume indicator (surface backscatter). The time series of northwards velocity at the

surface in Figure 39 (lower panel) showed a period of more negative velocity within the plume. The near-bed northward velocity did not show the same change.

The horizontal (eastward) component of water motion showed a shift from positive to negative values during the period of the drift (Figure 40, lower panel). The change started before plume entry and continued during and after exiting the plume. The vertical component of water movement was of lower magnitude than the horizontal components, with a higher variability between successive acoustic profiles (Figure 41, upper panel), and did not show clear patterns in time (Figure 41, lower panel).

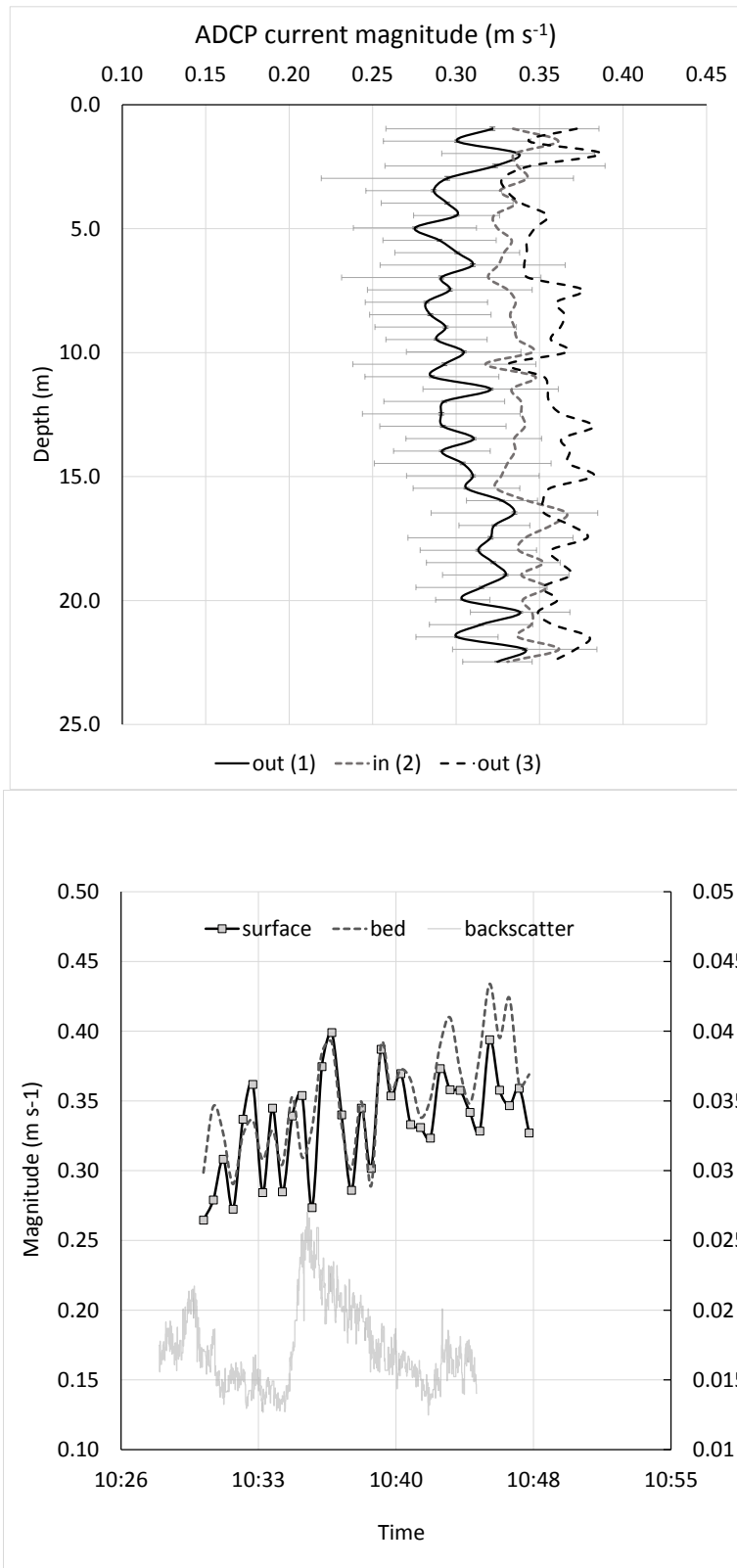


**Figure 38** Measurement of the current magnitude through the water column. Upper panel: vertical profiles before (1), during (2) and after (3) passage through the visible plume. Lower panel: time series of surface- and bottom-averaged magnitudes during transect through the plume, marked by a spike in surface backscatter.



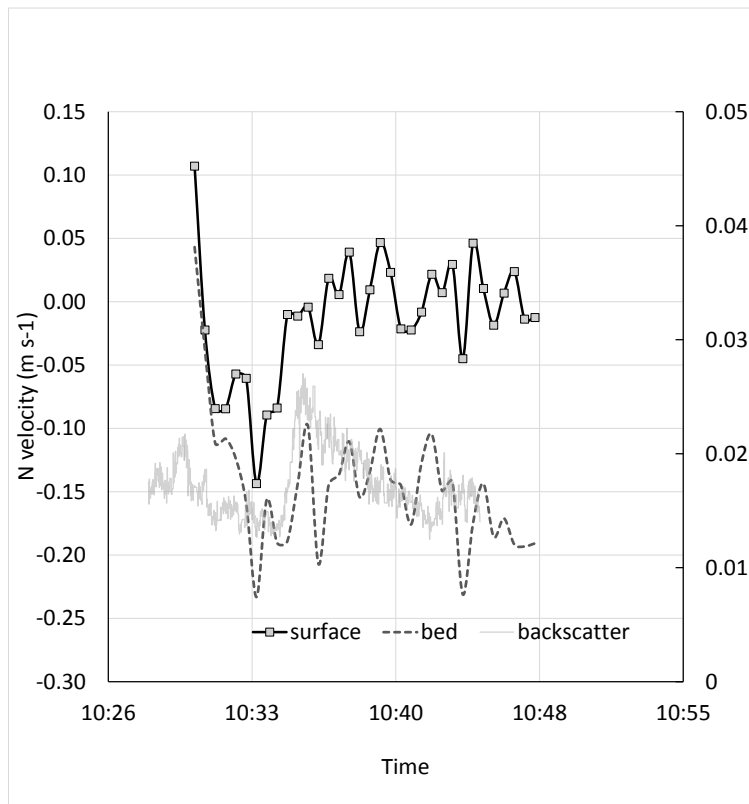
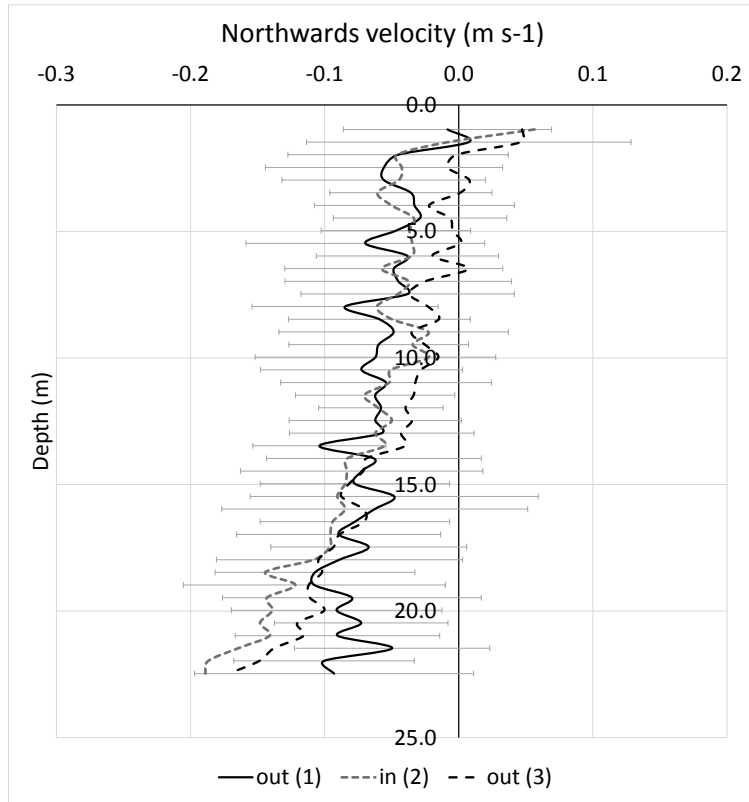


**Figure 39** Measurement of the northwards velocity component through the water column. Upper panel: vertical profiles before (1), during (2) and after (3) passage through the visible plume. Lower panel: time series of surface- and bottom-averaged N velocity during transect through the plume, marked by a spike in surface backscatter.

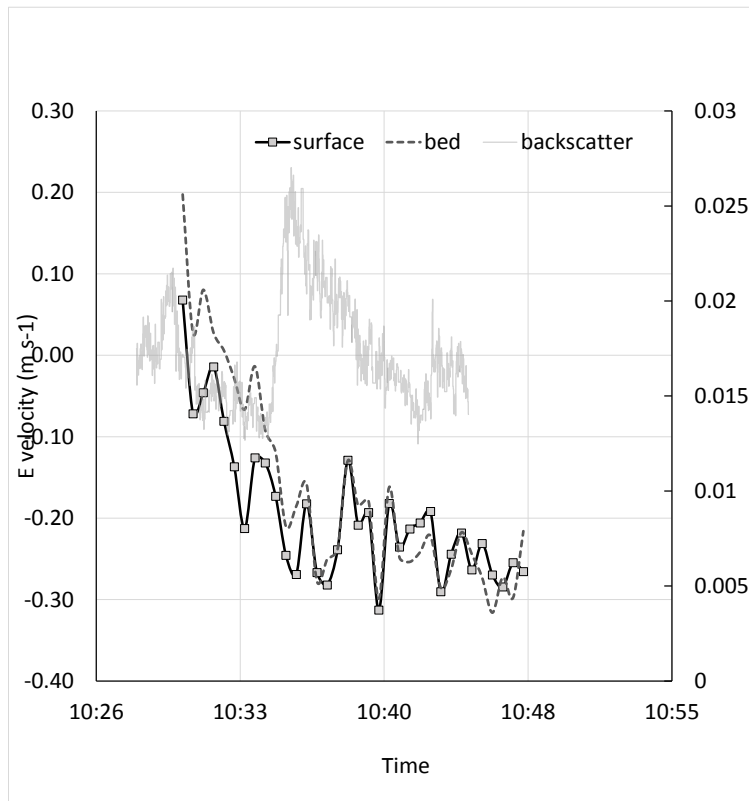
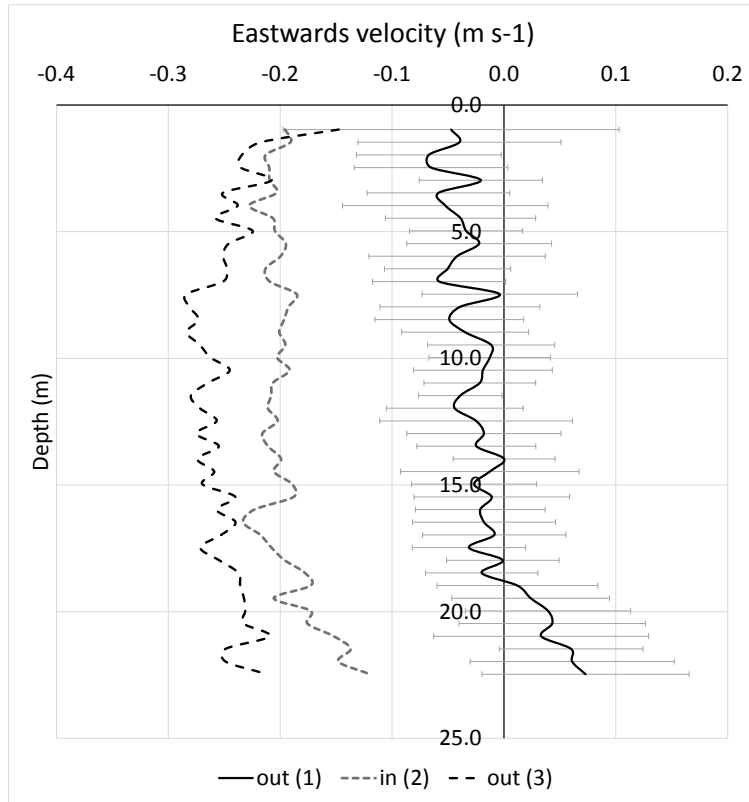


**Figure 40** Measurement of the eastwards velocity component through the water column. Upper panel: vertical profiles before (1), during (2) and after (3) passage through the visible plume. Lower panel: time series of surface- and bottom-averaged E velocity during transect through the plume, marked by a spike in surface backscatter.

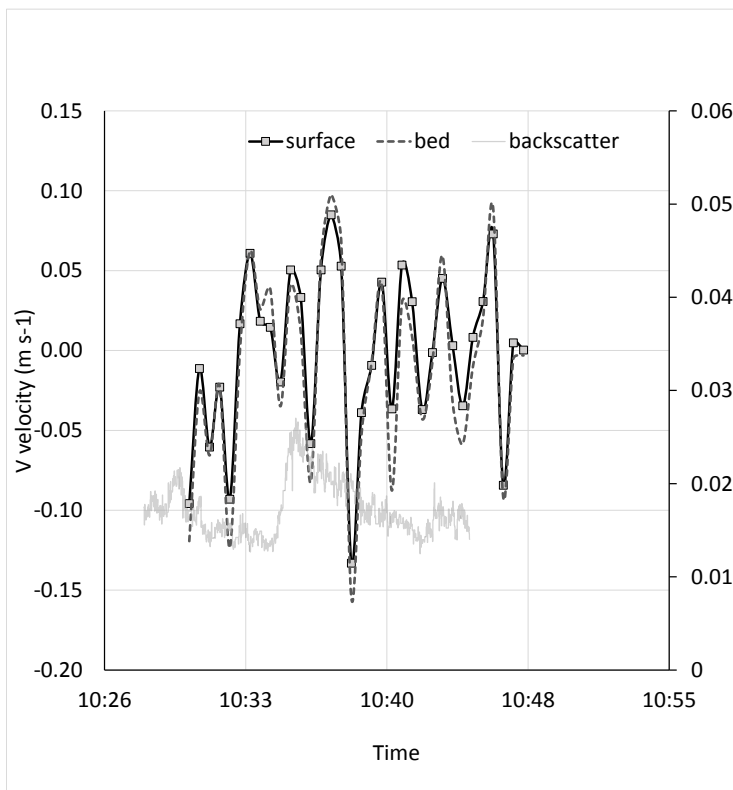
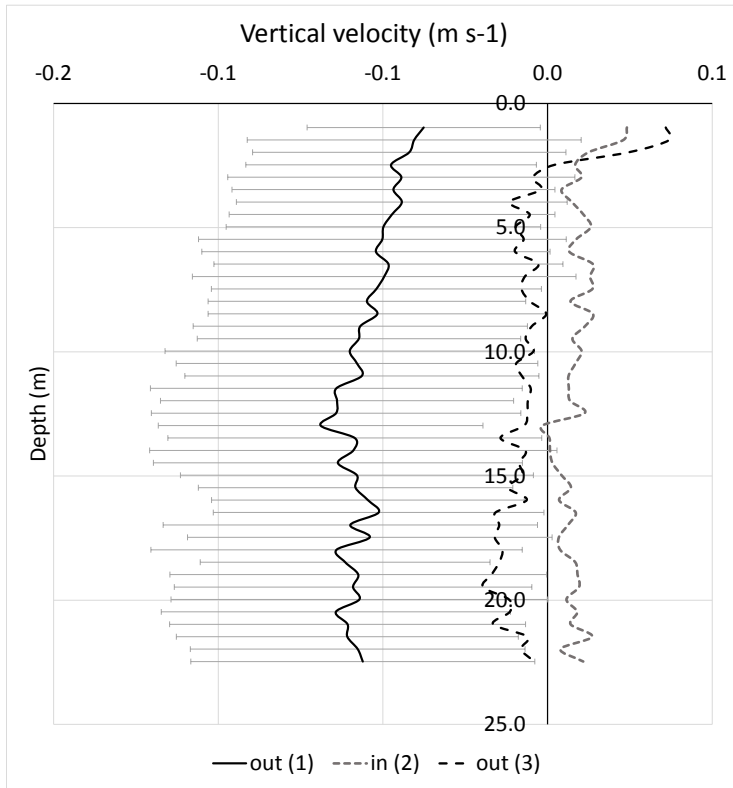


**Figure 41** Measurement of the vertical velocity component through the water column. Upper panel: vertical profiles before (1), during (2) and after (3) passage through the visible plume. Lower panel: time series of surface- and bottom-averaged vertical velocity during transect through the plume, marked by a spike in surface backscatter.

## 6. SYNTHESIS

The offshore wind energy industry in Europe is growing rapidly towards a predicted capacity by the year 2020 of ~ 24GW (Bloomberg New Energy Finance, July 2018). Extraction of energy from the marine system at this scale could affect atmospheric and oceanographic processes. The focus of the work presented here has been on the interaction of monopiles with their surrounding water, as opposed to turbine-monopile-air flow atmospheric effects. The presence of multiple large monopile-type structures in the water could affect current flows, turbulence and mixing, sediment transport and biological activity as evidenced by the range of academic papers published recently in this field (Table 1). The presence of turbid wakes associated with wind farms will attract attention, as they are obvious and persistent features visible at sea-level and from space. Impacts of the monopile wakes on the surrounding marine system are largely unknown. The occurrence of wakes at UK OWF sites was examined from satellite imagery: sites in the Thames area showed the highest prevalence. Results presented here for the Thanet OWF show that wakes are certainly present and are longer than the range of length scales predicted from scale models and numerical models, where estimates suggesting that the downstream effects have a length scale of approximately 8 to 10 multiples of the monopile diameter. Plume lengths of 1 km or more were regularly observed at Thanet (e.g. Figure 23), this would be equivalent to 200 or more monopile diameters.

The presence of turbid wakes at sites such as Thanet is persistent – very few satellite scenes show no evidence of wakes. Several potential environmental impacts of wake formation had been proposed prior to this study (van Hellefont and Ruddick, 2014; Rogan et al. 2016):

- A decrease in underwater light availability could affect primary production and the ability of sight-feeding predators to hunt their prey.
- Large-scale shifts in the patterns of suspended sediment could lead to changes in deposition or erosion patterns.
- Large offshore wind farms in areas of significant stratification close to the coast may experience altered thermal regimes due to changes in the distribution of heat throughout the water (Floeter et al. 2017).

A full analysis of these topics would require further ecological study, outside the parameters of this project. The focus of the work presented here was to establish the nature of surface wakes features, and their probable causes. To commence the analysis, the results generated during five days of sea surveys can be used to re-examine the original hypotheses.

**Hypothesis 1** stated that contrasts in colour between plumes and the surrounding water were due to differences in suspended sediment concentration and suspended sediment grain size.

Alternative hypothesis is that other factors such as bubble formation or resuspended plankton cause the visual manifestation of plumes.

The results clearly show evidence that the surface water within the plume was enriched by over 40% in the concentration of suspended material. The additional material present caused higher scattering, which was detectable by optical and acoustic instruments. Other optically-active constituents such as plankton (chlorophyll) or cDOM did not show significant enrichment within the plume. Hence, Hypothesis 1 is supported – the colour of turbid plumes was caused by increased suspended sediments.

**Hypothesis 2** presents three alternatives for the cause of increased sediments at the surface:

H2a) Plumes are caused by localised scouring of the seabed at the base of the monopile (as proposed by Vanhellemont & Ruddick (2014)).

H2b) Plumes are caused by the release of mud and organic material associated with epifauna colonising the monopile as proposed by Baeye & Fettweis (2015).

H2c) Plumes are caused by re-distribution of suspended sediment in the water column due to increased vertical mixing in the monopile wake.

Hypothesis 2a would have significant economic impacts, as extra scour protection could be necessary to prevent erosion at the base of the monopile. However, this study has shown that the total sediment concentration upstream of a monopile was similar to that in the wake, with the effect of turbulence in the wake being to re-distribute material from the lower to the upper water column. There was no evidence of localised scouring releasing additional sediment.

Evidence against H2b was the finding that the percentage of organic material in filtered seawater samples did not vary with depth or with sampling locations.

The evidence presented here strongly supports Hypothesis 2c. Not only can it be said with high confidence that suspended sediment concentration was higher at the surface, but initial evidence was found from both direct measurements and acoustic back-scatter that the near-bed concentration of sediment was actually lower within the plume. This indicates that a re-distribution of suspended material from the lower water column to the surface is caused by the increased turbulence within the wake. Although the waters of the outer Thames Estuary appeared to be very well-mixed, and do not display strong thermal stratification, there are noticeable vertical differences in the distribution of suspended sediments. This is driven by continuous upwards movement of sediment particles imparted by turbulence, and a tendency for particles to settle under gravity. Although direct acoustic measurements of water movements were inconclusive due to highly variable signals from vessel motion, there were indications of an alteration in the northwards-component of current velocity.

**Hypothesis 3** concerned the impact of plumes on OWF ecology and is only partly addressed by this scope of this study

H3) Formation of plumes may lead to changes in the ecology of waters around wind farms.

Firstly, the ecological impacts of locally-increased turbidity should be placed in a regional perspective. On the century time-scale, the southern North Sea has changed from a clear-water system in which sunlight penetrated to the sea-bed over large areas to a system with 50% reduced water clarity (Capuzzo et al. 2015). These changes have only recently been detected<sup>7</sup>, as turbidity or light attenuation measurements have not been part of national monitoring programmes. Reductions in water clarity have been reported for many other coastal seas and are likely to be caused by multiple factors. These can be categorised as:

Increased supply of light-attenuating materials from the land to the sea: Underwater light is absorbed or scattered by various materials such as sediment particles, dissolved organic matter, and phytoplankton. Increased sediment run-off from the land due to changing land use, and increased beach and cliff erosion are significant factors in increasing the supply of sediments to the North Sea. For example, Norwegian coastal waters have experienced an increased run-off of light-absorbing organic materials due to changes in land use, leading to 'coastal darkening' reported in that region and in the Baltic Sea.

Decreased sinks for light-attenuating materials in the sea. Destruction of naturally-occurring sediment sinks such as filter-feeding oyster reefs or sublittoral seagrass beds has prevented marine sediments from settling. Changes in benthic habitats may occur naturally due to storm events<sup>8</sup>, or may be caused by anthropogenic disturbance to the seabed. Once the protective, filtering layer of the seabed is lost, it becomes easier for waves and currents to re-suspend seabed sediments and increase sediment loading to the water column.

The observed long-term changes in water clarity in the North Sea are due to a combination of the impacts above, originating in changes to the terrestrial and marine environments as well as climate forcing (e.g. prevailing wind direction). From a societal point of view, a widely-held school of thought is that it is 'better' for the North Sea to be closer to the pre-industrial state (in this case, less turbid than at present). Increased light penetration will allow greater rates of carbon fixation by aquatic plants (phytoplankton, macroalgae and seagrasses), which would potentially support a larger and more diverse food-web. Alternatively, recent marine legislation such as the Marine Strategy Framework Directive (MSFD) does not specify a return to pristine conditions as necessary for "Good Environmental Status" (Rice et al. 2012)<sup>9</sup>.

However, the natural variability at the site is also of importance. Steep gradients in turbidity within a short distance of the OWF study site were observed in satellite images of the Thames region; these were caused by the river plume itself, and the interaction of waves and tides on the shallow seabed. Strong seasonal changes in turbidity were recorded in the satellite image time series, and also from SmartBuoys moored in the region. It is likely that the benthic species and habitats existing at sites such as Thanet were already adapted to an environment in which rapid changes in sediment deposition and erosion are a common feature. Smothering and burial are stress factors which would exclude some sensitive

---

<sup>7</sup> By synthesis of records from ship's logbooks.

<sup>8</sup> As evidenced by the severe storms of winter 2013-2014 which caused damage to intertidal and shallow subtidal habitat along the south-west coast of the UK.

<sup>9</sup> Rice et al. (2012) state "“Good Environmental Status” cannot be defined exclusively as "pristine Environmental Status", but rather status when impacts of all uses were sustainable. Uses are sustainable if two conditions are met: (1) the pressures associated with those uses do not hinder the ecosystem components to retain their natural diversity, productivity and dynamic ecological processes (2) recovery from perturbations is such that the attributes lie within their range of historical natural variation and must be rapid and secure".

species. Organisms in the water column would encounter periodically darker and more turbulent conditions on passage past a monopile, but these changes would be well within the range of variability encountered in any given two week period (e.g. neap-spring cycle). Hence, the additional turbidity added locally by monopile wakes would have limited ecological effects.

The economic impacts of turbid wake formation are not considered here, but may require an in-depth assessment once the scale of wake formation at all UK sites is known.

### **Recommendations and improvements**

In retrospect, the simplest measurements – collecting water samples in a bottle and filtering the contents – provided the strongest and most unequivocal evidence. A higher sampling density for gravimetric samples would be recommended. To avoid the costs associated with vessel charter, autonomous methods of acquiring water samples should be investigated. Remotely operated bottle water samplers are available, and could be tethered to a mooring and programmed to capture samples at regular intervals. The regular passage of crew transfer vessels to and from the OWF site may also provide an opportunity for sample collection at low cost.

Interpretation of results was complicated due to the vessel motion in relation to a slowly rotating plume (which was not always visible to the observer at sea level due to sun-glint and wave chop). Rather than the Lagrangian method of ‘chasing the plume’, an alternative Eulerian approach would be to use tethered instruments located at given distances from a chosen monopile. An upward-looking ADCP mooring together with high-resolution CTDs and optical sensors at different depths would allow plume passage to be recorded every 12 hours, and would allow investigation of between-day differences in turbulent intensity.

## 7. REFERENCES

- Baeye M, Fettweis M (2015) In situ observations of suspended particulate matter plumes at an offshore wind farm, southern North Sea. *Geo-Marine Lett* 35:247–255
- Baeye M, Quinn R, Deleu S, Fettweis M (2016) Detection of shipwrecks in ocean colour satellite imagery. *J Archaeol Sci* 66:1–6
- Bailey H, Senior B, Simmons D, Rusin J, Picken G, Thompson PM (2010) Assessing underwater noise levels during pile-driving at an offshore wind farm and its potential effects on marine mammals. *Mar Pollut Bull* 60:888–897
- Barnes BB, Hu C, Kovach C, Silverstein RN (2015) Sediment plumes induced by the Port of Miami dredging: Analysis and interpretation using Landsat and MODIS data. *Remote Sens Environ* 170:328–339
- Bergström L, Sundqvist F, Bergström U (2013) Effects of an offshore wind farm on temporal and spatial patterns in the demersal fish community. *Mar Ecol Prog Ser* 485:199–210
- Blauw AN, Benincà E, Laane RWPM, Greenwood N, Huisman J (2012) Dancing with the Tides: Fluctuations of Coastal Phytoplankton Orchestrated by Different Oscillatory Modes of the Tidal Cycle (M Krkosek, Ed.). *PLoS One* 7:e49319
- Capuzzo E, Stephens D, Silva T, Barry J, Forster RM (2015) Decrease in water clarity of the southern and central North Sea during the 20(th) -century. *Glob Chang Biol* 21:2206–2214
- Cazenave PW, Torres R, Allen JI (2016) Unstructured grid modelling of offshore wind farm impacts on seasonally stratified shelf seas. *Prog Oceanogr* 145:25–41
- Christiansen MB, Hasager CB (2005) Wake effects of large offshore wind farms identified from satellite SAR. *Remote Sens Environ* 98:251–268
- Davies-Colley RJ, Smith DG (2001) Turbidity, suspended sediment, and water clarity: A review. *J Am Water Resour Assoc* 37:1085–1101
- Eleveld MA, Pasterkamp R, Woerd HJ van der, Pietrzak JD (2008) Remotely sensed seasonality in the spatial distribution of sea-surface suspended particulate matter in the southern North Sea. *Estuar Coast Shelf Sci* 80:103–113
- Floeter J, Beusekom JEE van, Auch D, Callies U, Carpenter J, Dudeck T, Eberle S, Eckhardt A, Gloe D, Hänselmann K, Hufnagl M, Janßen S, Lenhart H, Möller KO, North RP, Pohlmann T, Riethmüller R, Schulz S, Spreizenbarth S, Temming A, Walter B, Zielinski O, Möllmann C (2017) Pelagic effects of offshore wind farm foundations in the stratified North Sea. *Prog Oceanogr* 156:154–173
- Franco A, Quintino V, Elliott M (2015) Benthic monitoring and sampling design and effort to detect spatial changes: A case study using data from offshore wind farm sites. *Ecol Indic* 57:298–304
- Gohin F, Loyer S, Lunven M, Labry C, Froidefond JM, Delmas D, Huret M, Herbland A (2005) Satellite-derived parameters for biological modelling in coastal waters: Illustration over the eastern continental shelf of the Bay of Biscay. *Remote Sens Environ* 95:29–46



- Grashorn S, Stanev E V. (2016) Kármán vortex and turbulent wake generation by wind park piles. *Ocean Dyn* 66:1543–1557
- Hasager C, Peña A, Christiansen M, Astrup P, Nielsen M, Monaldo F, Thompson D, Nielsen P (2008) Remote sensing observation used in offshore wind energy. *IEEE J Sel Top Appl EARTH Obs Remote Sens* 1:67–79
- Hasager C, Rasmussen L, Peña A, Jensen L, Réthoré P-E (2013) Wind Farm Wake: The Horns Rev Photo Case. *Energies* 6:696–716
- Heery EC, Bishop MJ, Critchley LP, Bugnot AB, Airoidi L, Mayer-Pinto M, Sheehan E V., Coleman RA, Loke LHL, Johnston EL, Komyakova V, Morris RL, Strain EMA, Naylor LA, Dafforn KA (2017) Identifying the consequences of ocean sprawl for sedimentary habitats. *J Exp Mar Bio Ecol*
- Li X, Chi L, Chen X, Ren Y, Lehner S (2014) SAR observation and numerical modeling of tidal current wakes at the East China Sea offshore wind farm. *J Geophys Res Ocean* 119:4958–4971
- Lindeboom HJ, Kouwenhoven HJ, Bergman MJN, Bouma S, Brasseur S, Daan R, Fijn RC, Haan D de, Dirksen S, Hal R van, Hille Ris Lambers R, Hofstede R ter, Krijgsveld KL, Leopold M, Scheidat M (2011) Short-term ecological effects of an offshore wind farm in the Dutch coastal zone; a compilation. *Environ Res Lett* 6:35101
- Lindeboom HJ, Veer HW van der, Philippart CJM, Salama MS, Kromkamp JC, Woerd HJ van der, Zuur AF, Cadée GC (2013) Four decades of variability in turbidity in the western Wadden Sea as derived from corrected Secchi disk readings. *J Sea Res* 82:67–79
- Mangi SC, Davis CE, Payne LA, Austen MC, Simmonds D, Beaumont NJ, Smyth T (2011) Valuing the regulatory services provided by marine ecosystems. *Environmetrics* 22:686–698
- Miles J, Martin T, Goddard L (2017) Current and wave effects around windfarm monopile foundations. *Coast Eng* 121:167–178
- Molen J van der, Smith HCM, Lepper P, Limpenny S, Rees J (2014) Predicting the large-scale consequences of offshore wind turbine array development on a North Sea ecosystem. *Cont Shelf Res* 85:60–72
- Raoux A, Tecchio S, Pezy J-P, Lassalle G, Degraer S, Wilhelmsson D, Cachera M, Ernande B, Guen C Le, Haraldsson M, Grangeré K, Loc'h F Le, Dauvin J-C, Niquil N (2017) Benthic and fish aggregation inside an offshore wind farm: Which effects on the trophic web functioning? *Ecol Indic* 72:33–46
- Reubens JT, Degraer S, Vincx M (2014) The ecology of benthopelagic fishes at offshore wind farms: a synthesis of 4 years of research. *Hydrobiologia* 727:121–136
- Rice J, Arvanitidis C, Borja A, Frid C, Hiddink JG, Krause J, Lorance P, Ragnarsson SA, Sköld M, Trabucco B, Enserink L, Norkko A (2012) Indicators for sea-floor integrity under the European marine strategy framework directive. *Ecol Indic* 12
- Rivier A, Bennis A-C, Pinon G, Magar V, Gross M (2016) Parameterization of wind turbine impacts on hydrodynamics and sediment transport. *Ocean Dyn* 66:1285–1299
- Rogan C, Miles J, Simmonds D, Iglesias G (2016) The turbulent wake of a monopile foundation. *Renew Energy* 93:180–187

Sterckx S, Knaeps S, Kratzer S, Ruddick K (2015) SIMilarity Environment Correction (SIMEC) applied to MERIS data over inland and coastal waters. *Remote Sens Environ* 157:96–110

Thiébot J, Bailly du Bois P, Guillou S (2015) Numerical modeling of the effect of tidal stream turbines on the hydrodynamics and the sediment transport – Application to the Alderney Race (Raz Blanchard), France. *Renew Energy* 75:356–365

Vanhellemont Q, Ruddick K (2014) Turbid wakes associated with offshore wind turbines observed with Landsat 8. *Remote Sens Environ* 145:105–115

Vanhellemont Q, Ruddick K (2016) ACOLITE FOR SENTINEL-2: AQUATIC APPLICATIONS OF MSI IMAGERY. *ESA Spec Publ*:9–13

Wilson JC, Elliott M (2009) The habitat-creation potential of offshore wind farms. *Wind Energy* 12:203–212

Wilson JC, Elliott M, Cutts ND, Mander L, Mendão V, Perez-Dominguez R, Phelps A (2010) Coastal and Offshore Wind Energy Generation: Is It Environmentally Benign? *Energies* 3:1383–1422

Yin Y, Moulinec C, Li M, Wolf J, Amoudry L, Walkington I, Taylor B (2016) Investigation of Turbid Wakes around London Array Offshore Wind Farm.

## 8. ACKNOWLEDGEMENTS

IECS would like to thank the management and crew of RV *Meriel D* for their assistance with the research cruises. IECS acknowledge the assistance of Vattenfall staff during project planning, and for allowing access to their Thanet site, and for comments on this report.

## APPENDIX

List of sampling events recorded at Thanet offshore windfarm during August 2016.

ID	datetime_GMT	Activity or event	in_plume	Comment	Additional comment	Rosette	optics_station	water_station
283	04/08/2016 07:52	Start of first upstream transect (northern edge of OWF)	0	Out of plumes	Flood tide on Northern edge: plumes easy to observed.			
284	04/08/2016 08:04	End of first upstream transect	0	Out of plumes	Flood tide on Northern edge: plumes easy to observed.			
285	04/08/2016 08:15	Start of second upstream transect	0	Out of plumes	Flood tide on Northern edge: plumes easy to observed.			
286	04/08/2016 08:26	End of second upstream transect	0	Out of plumes	Flood tide on Northern edge: plumes easy to observed.			
287	04/08/2016 08:51	Near E06		Near plume	Flood tide on Northern edge: plumes easy to observed.			
288	04/08/2016 08:55	In plume of E05	1	In plume	Flood tide on Northern edge: plumes easy to observed.			
289	04/08/2016 08:55	Out of plume of E05	0	Out of plumes	Flood tide on Northern edge: plumes easy to observed.			
290	04/08/2016 08:58	In plume of E04	1	In plume	Flood tide on Northern edge: plumes easy to observed.			
291	04/08/2016 08:59	Out of plume of E04	0	Out of plumes	Flood tide on Northern edge: plumes easy to observed.			
292	04/08/2016 09:02	In plume of E03	1	In plume	Flood tide on Northern edge: plumes easy to observed.			
293	04/08/2016 09:02	Out of plume of E03	0	Out of plumes	Flood tide on Northern edge: plumes easy to observed.			
294	04/08/2016 09:05	In plume of E02	1	In plume	Flood tide on Northern edge: plumes easy to observed.			
295	04/08/2016 09:05	Out of plume of E02	0	Out of plumes	Flood tide on Northern edge: plumes easy to observed.			
296	04/08/2016 09:10	In plume of E01		Near plume	Flood tide on Northern edge: plumes easy to observed.			
297	04/08/2016 09:10	Out of plume from E01	0	Out of plumes	Flood tide on Northern edge: plumes easy to observed.			
298	04/08/2016 09:13	Start of first downstream transect		Near plume	Flood tide on Northern edge: plumes easy to observed.			
299	04/08/2016 09:19	in plume	1	In plume	Flood tide on Northern edge: plumes easy to observed.			
300	04/08/2016 09:31	End of first upstream transect along Echo row		Near plume	Flood tide on Northern edge: plumes easy to observed.			
301	04/08/2016 09:34	Start of first downstream transect		Near plume	Flood tide on Northern edge: plumes easy to observed.			
302	04/08/2016 09:53	End of first upstream transect along Foxtrot row		Near plume	Flood tide on Northern edge: plumes easy to observed.			
303	04/08/2016 09:59	Start of long transit between rows F and G		Steaming south along line. No plumes obvious	Flood tide on Northern edge: plumes easy to observed.			
304	04/08/2016 10:56	End of long transit between rows F and G		Steaming south along line. No plumes obvious	Flood tide on Northern edge: plumes easy to observed.			
305	04/08/2016 11:46	Start of first upstream transect (southern edge of OWF)	0	Out of plumes	No ebb tide plumes visually observable. Nepheloid layer possibly pre-mixed over shoaling.			
306	04/08/2016 12:07	End of first upstream transect	0	Out of plumes	No ebb tide plumes visually observable. Nepheloid layer possibly pre-mixed over shoaling.			
307	04/08/2016 12:10	Start of second upstream transect (southern edge of OWF)	0	Out of plumes	No ebb tide plumes visually observable. Nepheloid layer possibly pre-mixed over shoaling.			
308	04/08/2016 12:36	End of second upstream transect	0	Out of plumes	No ebb tide plumes visually observable. Nepheloid layer possibly pre-mixed over shoaling.			
309	04/08/2016 12:40	Start of first downstream transect (southern edge of OWF)	0	Out of plumes	No ebb tide plumes visually observable. Nepheloid layer possibly pre-mixed over shoaling.			
310	04/08/2016 12:44	Near C15 plume		Near plume	No ebb tide plumes visually observable. Nepheloid layer possibly pre-mixed over shoaling.			
311	04/08/2016 12:55	Near B14 plume		Near plume	No ebb tide plumes visually observable. Nepheloid layer possibly pre-mixed over shoaling.			
312	04/08/2016 13:06	Near A12 plume		Near plume	No ebb tide plumes visually observable. Nepheloid layer possibly pre-mixed over shoaling.			
313	04/08/2016 13:12	End of first downstream transect (southern edge of OWF)	0	Out of plumes	No ebb tide plumes visually observable. Nepheloid layer possibly pre-mixed over shoaling.			
314	04/08/2016 13:16	Start of second downstream transect (southern edge of OWF)	0	Out of plumes	No ebb tide plumes visually observable. Nepheloid layer possibly pre-mixed over shoaling.			
315	04/08/2016 13:17	Near A11 plume		Near plume	No ebb tide plumes visually observable. Nepheloid layer possibly pre-mixed over shoaling.			

Investigation of offshore wind farm plume formation  
The Crown Estate

316	04/08/2016 13:26	Near B13 plume		Near plume	No ebb tide plumes visually observable. Nepheloid layer possibly pre-mixed over shoaling.		
317	04/08/2016 13:35	Near C14 plume		Near plume	No ebb tide plumes visually observable. Nepheloid layer possibly pre-mixed over shoaling.		
318	04/08/2016 13:42	End of second downstream transect (southern edge of OWF)	0	Out of plumes	No ebb tide plumes visually observable. Nepheloid layer possibly pre-mixed over shoaling.		
319	04/08/2016 13:43	Start of third downstream transect (southern edge of OWF)	0	Out of plumes	No ebb tide plumes visually observable. Nepheloid layer possibly pre-mixed over shoaling.		
320	04/08/2016 13:43	Near D14		Near plume	No ebb tide plumes visually observable. Nepheloid layer possibly pre-mixed over shoaling.		
321	04/08/2016 13:53	In plume from C13	1	In plume	No ebb tide plumes visually observable. Nepheloid layer possibly pre-mixed over shoaling.		
322	04/08/2016 14:09	Near B12		Near plume	No ebb tide plumes visually observable. Nepheloid layer possibly pre-mixed over shoaling.		
323	04/08/2016 14:12	End of third downstream transect (southern edge of OWF)	0	Out of plumes	No ebb tide plumes visually observable. Nepheloid layer possibly pre-mixed over shoaling.		
324	04/08/2016 14:14	Start of long transit transect to North in search of plumes	0	Out of plumes	No ebb tide plumes visually observable. Nepheloid layer possibly pre-mixed over shoaling.		
325	04/08/2016 14:35	End of long transit transect to North in search of plumes	0	Out of plumes	No ebb tide plumes visually observable. Nepheloid layer possibly pre-mixed over shoaling.		
326	04/08/2016 14:45	Starting approach to turbine	0	Out of plumes	No ebb tide plumes visually observable. Nepheloid layer possibly pre-mixed over shoaling.		
327	04/08/2016 14:50	Definitely in plume of turbine tower	1	In plume	No ebb tide plumes visually observable. Nepheloid layer possibly pre-mixed over shoaling.		
328	04/08/2016 14:52	Definitely to side of turbine (D05)	0	Out of plumes	No ebb tide plumes visually observable. Nepheloid layer possibly pre-mixed over shoaling.		
329	04/08/2016 14:53	upstream of turbine	0	Out of plumes	No ebb tide plumes visually observable. Nepheloid layer possibly pre-mixed over shoaling.		
330	04/08/2016 15:04	Slow approach to E05. hard to detect wake. Slow approach to downstream point. Out of gear and slow drift away from turbine.		Near plume	No ebb tide plumes visually observable. Nepheloid layer possibly pre-mixed over shoaling.		
331	04/08/2016 15:09	slow approach based on the drift pattern.	1	In plume	No ebb tide plumes visually observable. Nepheloid layer possibly pre-mixed over shoaling.		
332	04/08/2016 15:13	to side of turbine	0	Out of plumes	No ebb tide plumes visually observable. Nepheloid layer possibly pre-mixed over shoaling.		
333	04/08/2016 15:13	upstream of turbine	0	Out of plumes	No ebb tide plumes visually observable. Nepheloid layer possibly pre-mixed over shoaling.		
385		LISST in water	1	In plume			
334	04/08/2016 15:16	Weather poor - returning to port	0	Out of plumes			
335	05/08/2016 08:04	Slow steam into plume from E01	1	In plume			
336	05/08/2016 08:09	Passing monopile (1927)	1	In plume			
337	05/08/2016 08:09	Steaming upstream of E01	0	Out of plume			
338	05/08/2016 08:29	In transit to start position again	0	Out of plume			
339	05/08/2016 08:38	turned around and tested LISST	0	Out of plume			
340	05/08/2016 08:48	Drifting in plume	1	In plume			
341	05/08/2016 08:54	Slow steam into plume from E01	1	In plume			
342	05/08/2016 08:55	Out of gear and drifting with plume	1	In plume			
343	05/08/2016 08:56	LISST deployed and drifting in plume	1	In plume			
344	05/08/2016 09:12	Out of plume	0	Out of plume			
345	05/08/2016 09:17	Steaming to start position	0	Out of plume			
346	05/08/2016 09:28	Slow steam into plume from E01	1	In plume			
347	05/08/2016 09:38	Passing monopile (1927)	1	In plume			
348	05/08/2016 09:38	Passing monopile (1927)	0	Out of plume			
349	05/08/2016 09:38	Upstream of E01	0	Out of plume			
350	05/08/2016 09:39	LISST deployed	0	Out of plume			
351	05/08/2016 09:39	Water sample 1	0	Out of plume			E01_2
352	05/08/2016 09:40	Steaming to start position	0	Out of plume			
353	05/08/2016 09:41	LISST deployed	0	Out of plume			
354	05/08/2016 09:44	In plume and drifting	1	In plume			
355	05/08/2016 09:45	Water samples 2 and 3	1	In plume			E01_2
356	05/08/2016 09:49	Out of plume	0	Out of plume			
357	05/08/2016	Turned out of plume	0	Out of			

Investigation of offshore wind farm plume formation  
The Crown Estate

	09:51			plume	
358	05/08/2016 09:56	Slow steam into plume from E01	1	In plume	
359	05/08/2016 10:01	Passing monopile (1927)	1	In plume	
360	05/08/2016 10:01	Passing monopile (1927)	0	Out of plume	
361	05/08/2016 10:01	Upstream of E01	0	Out of plume	
362	05/08/2016 10:03	Drifting to tower but upstream	0	Out of plume	
363	05/08/2016 10:03	Rosette cage deployed upstream (may have passed through some turbid water)	0	Out of plume	
364	05/08/2016 10:16	Steaming to start position	0	Out of plume	
365	05/08/2016 10:46	Slow steam into plume from D03	1	In plume	
366	05/08/2016 10:46	Rosette cage deployed downstream - reached 10 m	1	in plume	
367	05/08/2016 10:48	Rosette surfaced	1	in plume	
368	05/08/2016 10:54	Passing monopile (1927)	0	Out of plume	
369	05/08/2016 10:55	Upstream of D03	0	Out of plume	
370	05/08/2016 10:56	Rosette deployed			
371	05/08/2016 10:59	Drifting to tower but upstream	0	Out of plume	
372	05/08/2016 11:05	Steaming to start position	0	Out of plume	
373	05/08/2016 11:10	Slow steam into plume from E01	1	In plume	
374	05/08/2016 11:17	Passing monopile (1927)	1	In plume	
375	05/08/2016 11:17	Passing monopile (1927)	0	Out of plume	
376	05/08/2016 11:17	Upstream of E01	0	Out of plume	
377	05/08/2016 11:21	Drifting to tower but upstream	0	Out of plume	
378	05/08/2016 11:23	LISST deployed upstream	0	Out of plume	
380	05/08/2016 11:24	Streaming to new upstream location	0	Out of plume	
379	05/08/2016 11:26	Water samples 4 and 5	0	Out of plume	E01_3
381	05/08/2016 11:26	Drifting to tower but upstream	0	Out of plume	
382	05/08/2016 11:32	Level with E01	0	Out of plume	
383	05/08/2016 11:33	Steaming to start position	0	Out of plume	
384	05/08/2016 11:59	Drifting across plume	1	In plume eventually	
386	05/08/2016 12:00	Water samples 6 and 8	1	In plume	E01_3
387	05/08/2016 12:03	End of drift - out of plume	0	Out of plume	
388	05/08/2016 12:07	Drifting across plume	1	In plume eventually	
389	05/08/2016 12:15	End of drift - out of plume	0	Out of plume	
390	05/08/2016 12:19	Drifting across plume	1	In plume eventually	
391	05/08/2016 12:29	Drifted to next turbine - plume merges along rows	1	In plume	
392	05/08/2016 12:31	Turn round D02	1	In plume	
393	05/08/2016 12:32	Steaming to start position	1	Mostly in plume	
394	05/08/2016 12:40	Slow steam into plume from E01	1	In plume	
395	05/08/2016 12:46	Passing monopile (1927)	1	In plume	
396	05/08/2016 12:46	Passing monopile (1927)	0	Out of plume	
397	05/08/2016 12:46	Upstream of E01	0	Out of plume	
398	05/08/2016 12:51	Drifting to tower but upstream	0	Out of plume	
399	05/08/2016 12:52	Water samples 9 and 10	0	Out of plume	E01_4
400	05/08/2016 13:03	End of upstream drift	0	Out of plume	
401	05/08/2016 13:06	Relocated to base of E01	0	Out of plume	

Investigation of offshore wind farm plume formation  
The Crown Estate

402	05/08/2016 13:06	Drifting downstream in plume	1	In plume		
403	05/08/2016 13:08	Water samples 11 and 12	1	In plume		E01_4
404	05/08/2016 13:19	End of drift - out of plume	0	Out of plume		
405	05/08/2016 13:21	Start of transect 1 across plume (60 m from tower)	1	Downstream and in plume for some of the transect		
406	05/08/2016 13:22	End of transect 1 across plume				
407	05/08/2016 13:23	Start of transect 2 across plume (130 m from tower)				
408	05/08/2016 13:24	End of transect 2 across plume				
409	05/08/2016 13:25	Start of transect 3 across plume (190 m from tower)				
410	05/08/2016 13:26	End of transect 3 across plume				
411	05/08/2016 13:27	Start of transect 4 across plume (265 m from tower)				
412	05/08/2016 13:28	End of transect 4 across plume				
413	05/08/2016 13:29	Start of transect 5 across plume (358 m from tower)				
414	05/08/2016 13:31	End of transect 5 across plume				
415	05/08/2016 13:32	Start of transect 6 across plume (358 m from tower)				
416	05/08/2016 13:34	End of transect 6 across plume				
417	05/08/2016 13:46	Start of transect 1 across plume (110 m from tower)				
418	05/08/2016 13:48	End of transect 1 across plume				
419	05/08/2016 13:49	Start of transect 2 across plume (180 m from tower)				
420	05/08/2016 13:51	End of transect 2 across plume				
421	05/08/2016 13:52	Start of transect 3 across plume (303 m from tower)				
422	05/08/2016 13:54	End of transect 3 across plume				
423	05/08/2016 13:55	Start of transect 4 across plume (426 m from tower)				
424	05/08/2016 13:57	End of transect 4 across plume				
425	05/08/2016 13:59	Start of transect 5 across plume (713 m from tower)				
426	05/08/2016 14:01	End of transect 5 across plume				
427	05/08/2016 14:02	Start of transect 6 across plume (911 m from tower)				
428	05/08/2016 14:04	End of transect 6 across plume				
1	17/08/2016 07:42	Start of transect	1	In plumes' transect	Broad scale mapping across multiple plumes on northern edge of OWF	
2	17/08/2016 07:44	Passing E05 at distance		Passing turbine - downstream		
3	17/08/2016 07:55	Passing E04 at distance		Passing turbine - downstream		
4	17/08/2016 07:59	Passing E03 at distance		Passing turbine - downstream		
5	17/08/2016 08:04	Passing E02 at distance		Passing turbine - downstream		
6	17/08/2016 08:08	Passing E01 at distance		Passing turbine - downstream		
7	17/08/2016 08:12	End of transect		In plumes' transect		
8	17/08/2016 08:20	Start of transect		In plumes' transect		
9	17/08/2016 08:21	Passing E02 at distance		Passing turbine - downstream		
10	17/08/2016 08:26	Passing F01 at distance		Passing turbine - downstream		
11	17/08/2016 08:30	Passing F02 at distance		Passing turbine -		

Investigation of offshore wind farm plume formation  
The Crown Estate

				downstream			
12	17/08/2016 08:35	Passing F03 at distance		Passing turbine - downstream			
13	17/08/2016 08:37	End of transect		In plumes' transect			
14	17/08/2016 08:40	Start of transect		In plumes' transect			
15	17/08/2016 08:41	Passing F04 close to turbine		Passing turbine - downstream			
16	17/08/2016 08:46	Passing F03 close to turbine		Passing turbine - downstream			
17	17/08/2016 08:52	Passing F02 close to turbine		Passing turbine - downstream			
18	17/08/2016 08:56	Passing F01 close to turbine		Passing turbine - downstream			
19	17/08/2016 09:03	End of transect		In plumes' transect			
20	17/08/2016 09:06	Start of transect	0	Upstream - out of plumes			
21	17/08/2016 09:23	End of transect	0	Upstream - out of plumes			
22	17/08/2016 09:28	Start of transect	0	Upstream - out of plumes			
23	17/08/2016 09:36	End of transect	0	Upstream - out of plumes			
24	17/08/2016 12:27	Start of transect	1	In plumes	All turbines slight to moderate plume		
25	17/08/2016 12:30	Passing close to A11 - slight to moderate plume		Passing turbine - downstream			
27	17/08/2016 12:44	Passing close to C14 - slight to moderate plume		Passing turbine - downstream			
28	17/08/2016 12:51	Passing close to D16 - slight to moderate plume		Passing turbine - downstream			
29	17/08/2016 12:52	End of transect	1	In plumes	All turbines slight to moderate plume		
30	17/08/2016 12:56	Start of transect	1	In plumes	Turbines A12, B14, C15, D17 moderate plume		
31	17/08/2016 12:58	Passing close to D16 upstream	0	Upstream - out of plumes			
32	17/08/2016 13:01	Passing close to C15 - slight to moderate plume		Passing turbine - downstream			
33	17/08/2016 13:09	Passing close to B14 - slight to moderate plume		Passing turbine - downstream			
34	17/08/2016 13:17	Passing close to A12 - slight to moderate plume		Passing turbine - downstream			
35	17/08/2016 13:22	End of transect	1	In plumes	Turbines A12, B14, C15, D17 moderate plume		
36	17/08/2016 13:26	Start of transect	0	Upstream - out of plumes	Clear water into OWF		
26	17/08/2016 13:37	Passing close to B13 - slight to moderate plume		Passing turbine - downstream			
37	17/08/2016 13:44	End of transect	0	Upstream - out of plumes	Clear water into OWF		
38	17/08/2016 13:54	Passing through plume of E16		Passing turbine - downstream			
39	17/08/2016 14:03	Steaming into plume from E16					
40	17/08/2016 14:07	Out of plume from E16					
41	17/08/2016 14:10	Steaming into plume from D17	1	In plume			
42	17/08/2016 14:13	Out of plume from D17	0	Upstream - out of plumes			
44	17/08/2016 14:25	Passing F14 - moderate/strong plume	1	In plume			
43	17/08/2016 14:25	Start of long transect (NNW)					



Investigation of offshore wind farm plume formation  
The Crown Estate

45	17/08/2016 14:30	Passing F13 - moderate/strong plume	1	In plume				
46	17/08/2016 14:34	Passing close to F12 - moderate/strong plume	1	In plume				
47	17/08/2016 14:38	Passing close to F11 - slight plume	1	In plume				
48	17/08/2016 14:42	Passing close to F10 - no obvious plume		Passing turbine - downstream	Tidal energy diminishing			
49	17/08/2016 14:46	Passing close to F09 - no obvious plume		Passing turbine - downstream	Tidal energy diminishing			
50	17/08/2016 14:49	Passing close to F08 - no obvious plume		Passing turbine - downstream	Tidal energy diminishing			
51	17/08/2016 14:53	Passing close to F07 - no obvious plume		Passing turbine - downstream	Tidal energy diminishing			
52	17/08/2016 14:56	Passing close to F06 - slight plume		In plume	Tidal energy diminishing			
53	17/08/2016 14:59	Passing close to F05 - no obvious plume		Passing turbine - downstream	Tidal energy diminishing			
54	17/08/2016 15:03	Passing close to F04		Passing turbine - downstream	Tidal energy diminishing			
55	17/08/2016 15:07	Passing close to F03 - slight plume		In plume	Tidal energy diminishing			
56	17/08/2016 15:11	Passing close to F02 - no obvious plume		Passing turbine - downstream	Tidal energy diminishing			
57	17/08/2016 15:14	Passing close to F01 - no obvious plume		Passing turbine - downstream	Tidal energy diminishing			
58	17/08/2016 15:14	End of long transect (NNW)		Low water	Tidal energy diminishing			
59	17/08/2016 15:20	End of day						
60	18/08/2016 08:26	Start of small-scale transects						
61	18/08/2016 08:26	Start of transect 1 - 50 m		Passing E1 - downstream	Strong plume in centre of transects			
62	18/08/2016 08:30	End of transect 1 - 50 m						
63	18/08/2016 08:30	Start of transect 2 - 50 m		Passing E1 - downstream	Strong plume in centre of transects			
64	18/08/2016 08:33	End of transect 2 - 50 m						
65	18/08/2016 08:33	Start of transect 3 - 50 m		Passing E1 - downstream	Strong plume in centre of transects			
66	18/08/2016 08:34	End of transect 3 - 50 m						
67	18/08/2016 08:35	Start of transect 4 - 50 m		Passing E1 - downstream	Strong plume in centre of transects			
68	18/08/2016 08:36	End of transect 4 - 50 m						
69	18/08/2016 08:37	Start of transect 5 - 50 m		Passing E1 - downstream	Strong plume in centre of transects			
70	18/08/2016 08:39	End of transect 5 - 50 m						
71	18/08/2016 08:40	Start of transect 6 - 50 m		Passing E1 - downstream	Strong plume in centre of transects			
72	18/08/2016 08:42	End of transect 6 - 50 m						
73	18/08/2016 08:43	Start of transect 1 - 100 m		Passing E1 - downstream	Strong plume in centre of transects			
74	18/08/2016 08:47	End of transect 1 - 100 m						
75	18/08/2016 08:48	Start of transect 2 - 100 m		Passing E1 - downstream	Strong plume in centre of transects			
76	18/08/2016 08:50	End of transect 2 - 100 m						
77	18/08/2016 08:50	Start of transect 3 - 100 m		Passing E1 - downstream	Strong plume in centre of transects			
78	18/08/2016 08:53	End of transect 3 - 100 m						
79	18/08/2016 08:54	Start of transect 4 - 100 m		Passing E1 - downstream	Strong plume in centre of transects			
80	18/08/2016 08:56	End of transect 4 - 100 m						
81	18/08/2016 08:56	Start of transect 5 - 100 m		Passing E1 - downstream	Strong plume in centre of transects			
82	18/08/2016 08:59	End of transect 5 - 100 m						
83	18/08/2016 09:00	Start of transect 6 - 100 m		Passing E1 - downstream	Strong plume in centre of transects			
84	18/08/2016	End of transect 6 - 100 m						

Investigation of offshore wind farm plume formation  
The Crown Estate

	09:02					
85	18/08/2016 09:03	Start of transect 1 - 150 m		Passing E1 - downstream	Strong plume in centre of transects	
86	18/08/2016 09:06	End of transect 1 - 150 m				
87	18/08/2016 09:06	Start of transect 2 - 150 m		Passing E1 - downstream	Strong plume in centre of transects	
88	18/08/2016 09:08	End of transect 2 - 150 m				
89	18/08/2016 09:08	Start of transect 3 - 150 m		Passing E1 - downstream	Strong plume in centre of transects	
90	18/08/2016 09:11	End of transect 3 - 150 m				
91	18/08/2016 09:11	Start of transect 4 - 150 m		Passing E1 - downstream	Strong plume in centre of transects	
92	18/08/2016 09:13	End of transect 4 - 150 m				
93	18/08/2016 09:14	Start of transect 5 - 150 m		Passing E1 - downstream	Strong plume in centre of transects	
94	18/08/2016 09:17	End of transect 5 - 150 m				
95	18/08/2016 09:17	Start of transect - 150 m		Passing E1 - downstream	Strong plume in centre of transects	
96	18/08/2016 09:19	End of transect 6 - 150 m				
97	18/08/2016 09:20	Start of transect 7 - 150 m		Passing E1 - downstream	Strong plume in centre of transects	
98	18/08/2016 09:23	End of transect 7 - 150 m				
99	18/08/2016 09:24	Start of transect 1 - 200 m		Passing E1 - downstream	Strong plume in centre of transects	
100	18/08/2016 09:26	End of transect 1 - 200 m				
101	18/08/2016 09:27	Start of transect 2 - 200 m		Passing E1 - downstream	Strong plume in centre of transects	
102	18/08/2016 09:29	End of transect 2 - 200 m				
103	18/08/2016 09:30	Start of transect 3 - 200 m		Passing E1 - downstream	Strong plume in centre of transects	
104	18/08/2016 09:32	End of transect 3 - 200 m				
105	18/08/2016 09:32	Start of transect 4 - 200 m		Passing E1 - downstream	Strong plume in centre of transects	
106	18/08/2016 09:36	End of transect 4 - 200 m				
107	18/08/2016 09:36	Start of transect 5 - 200 m		Passing E1 - downstream	Strong plume in centre of transects	
108	18/08/2016 09:38	End of transect 5 - 200 m				
109	18/08/2016 09:39	Start of transect - 200 m		Passing E1 - downstream	Strong plume in centre of transects	
110	18/08/2016 09:43	End of transect 6 - 200 m				
111	18/08/2016 09:44	Start of transect 1 - 300 m		Passing E1 - downstream	Strong plume in centre of transects	
112	18/08/2016 09:46	End of transect 1 - 300 m				
113	18/08/2016 09:47	Start of transect 2 - 300 m		Passing E1 - downstream	Strong plume in centre of transects	
114	18/08/2016 09:51	End of transect 2 - 300 m				
115	18/08/2016 09:51	Start of transect 3 - 300 m		Passing E1 - downstream	Strong plume in centre of transects	
116	18/08/2016 09:53	End of transect 3 - 300 m		Stopped halfway through due to time		
117	18/08/2016 10:08	Start of transect 1 - 50 m		Passing E1 - upstream		
118	18/08/2016 10:10	End of transect 1 - 50 m				
119	18/08/2016 10:11	Start of transect 2 - 50 m		Passing E1 - upstream		
120	18/08/2016 10:13	End of transect 2 - 50 m				
121	18/08/2016 10:13	Start of transect 3 - 50 m		Passing E1 - upstream		
122	18/08/2016 10:15	End of transect 3 - 50 m				
123	18/08/2016 10:16	Start of transect 4 - 50 m		Passing E1 - upstream		
124	18/08/2016 10:17	End of transect 4 - 50 m				
125	18/08/2016 10:18	Start of transect 5 - 50 m		Passing E1 - upstream		

Investigation of offshore wind farm plume formation  
The Crown Estate

126	18/08/2016 10:21	End of transect 5 - 50 m						
127	18/08/2016 10:22	Start of transect 2 - 50 m		Passing E1 - upstream				
128	18/08/2016 10:23	End of transect 3 - 50 m						
129	18/08/2016 10:24	Start of transect 3 - 50 m		Passing E1 - upstream				
130	18/08/2016 10:26	End of transect 4 - 50 m						
131	18/08/2016 10:27	Start of transect 3 - 50 m		Passing E1 - upstream				
132	18/08/2016 10:29	End of transect 4 - 50 m						
133	18/08/2016 10:30	Start of transect 3 - 50 m		Passing E1 - upstream				
134	18/08/2016 10:33	End of transect 4 - 50 m						
135	18/08/2016 10:53	Start of transect		Long transit transect				
136	18/08/2016 10:56	Passing close to F03 - no obvious surface plume	0	Passing turbine - downstream				
137	18/08/2016 11:00	Passing close to F04 - no obvious surface plume	0	Passing turbine - downstream				
138	18/08/2016 11:05	Passing close to F05 - no obvious surface plume	0	Passing turbine - downstream				
139	18/08/2016 11:10	Passing close to F06 - no obvious surface plume	0	Passing turbine - downstream				
140	18/08/2016 11:15	Passing close to F07 - no obvious surface plume	0	Passing turbine - downstream				
141	18/08/2016 11:20	Passing close to F08 - no obvious surface plume	0	Passing turbine - downstream				
142	18/08/2016 11:24	Passing close to F09 - no obvious surface plume	0	Passing turbine - downstream				
143	18/08/2016 11:29	Passing close to F10 - no obvious surface plume	0	Passing turbine - downstream				
144	18/08/2016 11:33	Passing close to F11 - no obvious surface plume	0	Passing turbine - downstream				
145	18/08/2016 11:38	Passing close to F12 - no obvious surface plume	0	Passing turbine - downstream				
146	18/08/2016 11:43	Passing close to F13 - no obvious surface plume	0	Passing turbine - downstream				
147	18/08/2016 11:50	Passing close to F14 - slight surface plume	1	Passing turbine - downstream				
148	18/08/2016 12:01	Passing close to E17 - slight surface plume	1	Passing turbine - upstream				
149	18/08/2016 12:09	Passing close to D16 - slight surface plume	1	Passing turbine - upstream				
150	18/08/2016 12:11	End of transit transect						
151	18/08/2016 12:19	Steaming into the plume of C15 to establish heading	1	In plume				
152	18/08/2016 12:23	Steam complete - at base of C15	1	In plume				
153	18/08/2016 12:28	Passive drift in plume from C15	1	In plume				
154	18/08/2016 12:37	End of drift in plume from C15	1	In plume				
155	18/08/2016 12:40	Start of transect 1 - 300 m		Passing C15 - downstream	Patchy, moderate plume in centre of transects			
156	18/08/2016 12:42	End of transect 1 - 300 m						
157	18/08/2016 12:42	Start of transect 2 - 300 m		Passing C15 - downstream	Patchy, moderate plume in centre of transects			
158	18/08/2016 12:44	End of transect 2 - 300 m						
159	18/08/2016 12:45	Start of transect 3 - 300 m		Passing C15 - downstream	Patchy, moderate plume in centre of transects			
160	18/08/2016 12:47	End of transect 3 - 300 m						

Investigation of offshore wind farm plume formation  
The Crown Estate

161	18/08/2016 12:48	Start of transect 4 - 300 m		Passing C15 - downstream	Patchy, moderate plume in centre of transects		
162	18/08/2016 12:50	End of transect 4 - 300 m					
163	18/08/2016 12:50	Start of transect 5 - 300 m		Passing C15 - downstream	Patchy, moderate plume in centre of transects		
164	18/08/2016 12:53	End of transect 5 - 300 m					
165	18/08/2016 12:55	Start of transect 1 - 300 m		Passing C15 - downstream	Patchy, moderate plume in centre of transects		
166	18/08/2016 12:57	End of transect 1 - 300 m					
167	18/08/2016 12:58	Start of transect 2 - 300 m		Passing C15 - downstream	Patchy, moderate plume in centre of transects		
168	18/08/2016 13:01	End of transect 2 - 300 m					
169	18/08/2016 13:01	Start of transect 3 - 300 m		Passing C15 - downstream	Patchy, moderate plume in centre of transects		
170	18/08/2016 13:03	End of transect 3 - 300 m					
171	18/08/2016 13:04	Start of transect 4 - 300 m		Passing C15 - downstream	Patchy, moderate plume in centre of transects		
172	18/08/2016 13:06	End of transect 4 - 300 m					
173	18/08/2016 13:07	Start of transect 5 - 300 m		Passing C15 - downstream	Patchy, moderate plume in centre of transects		
174	18/08/2016 13:10	End of transect 5 - 300 m					
175	18/08/2016 13:11	Start of transect 6 - 300 m		Passing C15 - downstream	Patchy, moderate plume in centre of transects		
176	18/08/2016 13:13	End of transect 6 - 300 m					
177	18/08/2016 13:13	Start of transect 1 - 200 m		Passing C15 - downstream	Patchy, moderate plume in centre of transects		
178	18/08/2016 13:15	End of transect 1 - 200 m					
179	18/08/2016 13:16	Start of transect 2 - 200 m		Passing C15 - downstream	Patchy, moderate plume in centre of transects		
180	18/08/2016 13:18	End of transect 2 - 200 m					
181	18/08/2016 13:19	Start of transect 3 - 200 m		Passing C15 - downstream	Patchy, moderate plume in centre of transects		
182	18/08/2016 13:22	End of transect 3 - 200 m					
183	18/08/2016 13:22	Start of transect 4 - 200 m		Passing C15 - downstream	Patchy, moderate plume in centre of transects		
184	18/08/2016 13:25	End of transect 4 - 200 m					
185	18/08/2016 13:25	Start of transect 5 - 200 m		Passing C15 - downstream	Patchy, moderate plume in centre of transects		
186	18/08/2016 13:28	End of transect 5 - 200 m					
187	18/08/2016 13:29	Start of transect 1 - 100 m		Passing C15 - downstream	Patchy, moderate plume in centre of transects		
188	18/08/2016 13:31	End of transect 1 - 100 m					
189	18/08/2016 13:32	Start of transect 2 - 100 m		Passing C15 - downstream	Patchy, moderate plume in centre of transects		
190	18/08/2016 13:34	End of transect 2 - 100 m					
191	18/08/2016 13:35	Start of transect 3 - 100 m		Passing C15 - downstream	Patchy, moderate plume in centre of transects		
192	18/08/2016 13:37	End of transect 3 - 100 m					
193	18/08/2016 13:37	Start of transect 4 - 100 m		Passing C15 - downstream	Patchy, moderate plume in centre of transects		
194	18/08/2016 13:39	End of transect 4 - 100 m					
195	18/08/2016 13:40	Start of transect 5 - 100 m		Passing C15 - downstream	Patchy, moderate plume in centre of transects		
196	18/08/2016	End of transect 5 - 100 m					

Investigation of offshore wind farm plume formation  
The Crown Estate

	13:42							
198	18/08/2016 13:43	End of transect 1 - 50 m						
197	18/08/2016 13:43	Start of transect 1 - 50 m		Passing C15 - downstream	Patchy, moderate plume in centre of transects			
199	18/08/2016 13:45	Start of transect 2 - 50 m		Passing C15 - downstream	Patchy, moderate plume in centre of transects			
200	18/08/2016 13:47	End of transect 2 - 50 m						
201	18/08/2016 13:47	Start of transect 3 - 50 m		Passing C15 - downstream	Patchy, moderate plume in centre of transects			
202	18/08/2016 13:49	End of transect 3 - 50 m						
203	18/08/2016 13:50	Start of transect 4 - 50 m		Passing C15 - downstream	Patchy, moderate plume in centre of transects			
204	18/08/2016 13:51	End of transect 4 - 50 m						
205	18/08/2016 13:51	Start of transect 5 - 50 m		Passing C15 - downstream	Patchy, moderate plume in centre of transects			
206	18/08/2016 13:53	End of transect 5 - 50 m						
207	18/08/2016 13:55	Start of transect 1 - 100 m		Passing C15 - upstream				
208	18/08/2016 13:56	End of transect 1 - 100 m						
209	18/08/2016 13:57	Start of transect 2 - 100 m		Passing C15 - upstream				
210	18/08/2016 13:59	End of transect 2 - 100 m						
211	18/08/2016 14:01	Start of transect 3 - 100 m		Passing C15 - upstream				
212	18/08/2016 14:03	End of transect 3 - 100 m						
213	18/08/2016 14:03	Start of transect 4 - 100 m		Passing C15 - upstream				
214	18/08/2016 14:05	End of transect 4 - 100 m						
215	18/08/2016 14:05	Start of transect 5 - 100 m		Passing C15 - upstream				
216	18/08/2016 14:06	End of transect 5 - 100 m						
217	18/08/2016 14:07	Start of transect 6 - 100 m		Passing C15 - upstream				
218	18/08/2016 14:08	End of transect 6 - 100 m						
219	19/08/2016 08:14	Steaming into plume (towards E1)	1	In plume	Trial run to set heading of plume			
220	19/08/2016 08:16	Turing out of plume from E1	1	In plume	Trial run to set heading of plume			
221	19/08/2016 08:16	Passinr round e1	0	Out of plume	Trial run to set heading of plume			
222	19/08/2016 08:17	Upstream of E1	0	Out of plume				
223	19/08/2016 08:21	Upstream of E1	0	Out of plume				
224	19/08/2016 08:25	Water sampling E1_1 surface	0	Upstream - out of plume				E1_1
225	19/08/2016 08:30	Water sampling E1_1 bottom	0	Upstream - out of plume				E1_1
226	19/08/2016 08:55	Rosette in water at 5 m	0	Upstream - out of plume	Rosette dip 1	1	ST01	
227	19/08/2016 09:06	Water sampling E1_1 mid-water	0	Upstream - out of plume				E1_1
228	19/08/2016 09:14	Steaming into plume (towards E1)	1	In plume				
229	19/08/2016 09:16	Still in plume (at base on E1)	1	In plume				
230	19/08/2016 09:17	Attaching to tower - heavy wash	1	In plume				
231	19/08/2016 09:27	Moored to tower	1	In plume				
232	19/08/2016 09:28	Water sampling E1_2 surface (1m)	1	In plume		1	ST02	E1_2
233	19/08/2016 09:31	Water sampling E1_2 mid-water (10 m)	1	In plume				E1_2
234	19/08/2016 09:34	Water sampling E1_2 bottom (20 m)	1	In plume				E1_2
235	19/08/2016 09:39	LISST in water	1	In plume				

Investigation of offshore wind farm plume formation  
The Crown Estate

236	19/08/2016 10:01	Detached from tower	1	In plume				
237	19/08/2016 10:02	Rosette in water at 2.5 m	1	In plume		1	ST03	
238	19/08/2016 10:05	Detected from tower and out of plume	0	Out of plume				
239	19/08/2016 10:28	Out of plume	0	Out of plume				
240	19/08/2016 10:28	Rosette in water at 2.5 m	0	Out of plume		1	ST05 _1	
241	19/08/2016 10:35	Rosette in water at 2.5 m	1	In plume		1	ST05 _2	
242	19/08/2016 10:36	Water sampling E1_3 surface (1m)	1	In plume				E1_3
243	19/08/2016 10:41	Out of plume	0	Out of plume				
244	19/08/2016 10:42	Water sampling E1_2 surface (1m)	0	Out of plume				E1_3
245	19/08/2016 10:52	In plume note	1	In plume				
246	19/08/2016 10:53	Out of plume note	0	Out of plume				
247	19/08/2016 10:55	Transit south on turn of the tide	0	Out of plume	Plumes running along lines of turbines			
248	19/08/2016 11:23	In plume note	1	In plume				
249	19/08/2016 11:24	Out of plume note	0	Out of plume				
250	19/08/2016 11:36	In plume note - plume very weak now	1	In plume				
251	19/08/2016 11:37	Out of plume note	0	Out of plume				
252	19/08/2016 12:12	Steaming into plume (towards C15)	1	In plume	Trial run to set heading of plume			
253	19/08/2016 12:16	Turned out of plume	0	Out of plume				
254	19/08/2016 12:37	Steaming into plume (towards C15)	1	In plume				
255	19/08/2016 12:38	In plume note (C15)	1	In plume				
256	19/08/2016 12:42	Turing out of plume (going round the side of the tower)	1	In plume				
257	19/08/2016 12:43	Upstream of C15	0	Upstream - out of plume				
258	19/08/2016 12:53	LISST in water	0	Upstream - out of plume				
259	19/08/2016 12:54	Water sampling C15_1 surface (1m)	0	Upstream - out of plume				C15_1
260	19/08/2016 12:56	Water sampling C15_1 mid-water (10 m)	0	Upstream - out of plume				C15_1
261	19/08/2016 12:59	Water sampling C15_1 bottom (20 m)	0	Upstream - out of plume				C15_1
262	19/08/2016 13:22	Rosette in water at 2.5 m	0	Upstream - out of plume		1	ST06	
263	19/08/2016 13:24	Water sampling C15_1 surface (1m)	0	Upstream - out of plume		1	ST06	C15_2
264	19/08/2016 13:26	Water sampling C15_1 mid-water (13 m)	0	Upstream - out of plume		1	ST06	C15_2
265	19/08/2016 13:35	Rosette out of water	0	Upstream - out of plume				
266	19/08/2016 13:47	Attaching to turbine tower - heavy wash	1	In plume				
267	19/08/2016 13:53	Water sampling C15_1 surface (1m)	1	In plume				C15_3
268	19/08/2016 13:55	Water sampling C15_1 mid-water (10 m)	1	In plume				C15_3
269	19/08/2016 13:58	Water sampling C15_1 bottom (20 m)	1	In plume				C15_3
270	19/08/2016 14:10	Rosette in water at 1.3 m	1	In plume		1	ST07	
271	19/08/2016 14:12	Water sampling C15_1 surface (1.3 m)	1	In plume		1	ST07	C15_4
272	19/08/2016 14:13	Rosette in water at 1.3 m	1	In plume		1	ST07	
273	19/08/2016 14:20	Out of plume	0	Out of plume				
274	19/08/2016 14:27	Steaming into plume (towards C15)	1	In plume				
275	19/08/2016 14:29	Drifting in plume	1	In plume				

Investigation of offshore wind farm plume formation  
The Crown Estate

276	19/08/2016 14:35	Water sampling C15_1 mid-water (11 m)	1	In plume			C15_4
277	19/08/2016 14:54	Steaming into plume (towards C15)	1	In plume			
278	19/08/2016 14:57	Drifting in plume	1	In plume			
279	19/08/2016 14:58	Water sampling C15_1 surface (1m)	1	In plume			C15_5
280	19/08/2016 14:59	Water sampling C15_1 mid-water (10 m)	1	In plume			C15_5
281	19/08/2016 15:02	Water sampling C15_1 bottom (20 m)	1	In plume			C15_5
282	19/08/2016 15:05	End of day					

ISBN 978-1-906410-77-3

---

**London**

The Crown Estate  
1 St James's Market  
London  
SW1Y 4AH  
T 020 7851 5000

---

**[www.thecrownestate.co.uk](http://www.thecrownestate.co.uk)**

 [@TheCrownEstate](https://twitter.com/TheCrownEstate)

November 2018